

(NASA-CR-105602) THE STRUCTURE OF THE
ALKALINE-EARTH METAL DIFFUSION FLAME H.F.
Sullivan (Princeton Univ.) May 1969 196 p

N72-75431

00/99 Unclas
42968

FF No. 602 (D)	<u>196</u> (ACCESSION NUMBER)	<u>2-D</u> (THRU)
	<u>196</u> (PAGES)	<u>33</u> (CODE)
	<u>CR-105602</u> (NASA CR OR TMX OR AD NUMBER)	<u>33</u> (CATEGORY)
	AVAILABLE TO U.S. GOVERNMENT AGENCIES AND CONTRACTORS ONLY	

PRINCETON UNIVERSITY
DEPARTMENT OF
AEROSPACE AND MECHANICAL SCIENCES

PRICES SUBJECT TO CHANGE

N72-75431

THE STRUCTURE OF THE ALKALINE-EARTH
METAL DIFFUSION FLAME


by

Henry F. Sullivan

Technical Report No. 865

Department of Aerospace
and Mechanical Sciences

Directed and
Approved by:



I. Glassman
Professor of Aerospace
Sciences

This research was supported by the National
Aeronautics and Space Administration under
NASA Grant NGR 31-001-129.

Guggenheim Laboratories for the Aerospace Propulsion Sciences
Department of Aerospace and Mechanical Sciences
PRINCETON UNIVERSITY
Princeton, New Jersey

May, 1969

i . .

1962

ACKNOWLEDGMENTS

The author would like to express his sincere appreciation to his thesis advisor, Prof. Irvin Glassman. The guidance, understanding and encouragement which he provided throughout the author's graduate studies at Princeton are acknowledged with thanks.

Numerous helpful discussions were held, as well, with Prof. Arthur M. Mellor, Mr. Frederick C. Gouldin, and Dr. James G. Hansel. The significant interest the author's associates had in the development of the model outlined in this report is sincerely appreciated.

Correspondence and personal communication with Dr. Alvin S. Gordon (NWC), Prof. Leo Brewer and Dr. David Green (U of C, Berkeley), and Prof. Robert Hauge (Rice), also contributed to the development of the present investigation. Mr. Robert Brown assisted with the final phases of the experimental work and his help is acknowledged with thanks.

The construction and maintenance of the apparatus used in the experimental studies is the important contribution of Mr. Anthony Bozowski.

The completion of this investigation was made possible by research funds under NASA Grant No. NGR 31-001-129. The support of the Propulsion Branch, Applied Materials and Physics Division, of the Langley Research Center was particularly appreciated.

TABLE OF CONTENTS

Title Page	i
Acknowledgments	ii
Table of Contents	iv
List of Tables	vii
List of Figures	viii
I. Introduction	1
II. Flame Models	11
1. Finite Reaction Zone Model Due to Coffin	12
2. Liquid Oxide Bubble Model Due to Fassell and Co-Workers	14
3. Collapsed Reaction Zone Model Due to Brzustowski and Glassman	17
4. Extensions of the Brzustowski - Glassman Model Due to Knipe	21
5. Heterogeneous Reaction Model Due to Markstein	25
III. Discussion of Spectroscopic Data	30
1. Energy Levels, Known Transitions and Other Band Systems Attributed to the Alkaline-Earth Oxides	31
a. Beryllium Oxide	32
b. Magnesium Oxide	35
c. Calcium Oxide	39
d. Strontium Oxide	40
e. Barium Oxide	44
2. Ground Electronic States and the Possibility of Low-Lying Triplet States for the Alkaline-Earth Oxides	46
a. Beryllium Oxide	47
b. Magnesium Oxide	48
c. Calcium Oxide	50
d. Strontium Oxide	52
e. Barium Oxide	52
Summary	53

3.	Energy Level Diagrams for the Alkaline-Earth Metals and Atomic Oxygen	53
IV.	Experimental Apparatus and Procedure	61
1.	Materials	
a.	Gases	61
b.	Metal Samples	63
2.	Wire-burning Apparatus	
a.	Apparatus Description	64
b.	Procedure	70
c.	Associated Diagnostic Equipment	71
3.	Two-Dimensional Diffusion Flame Burner	
a.	Apparatus Description	72
b.	Associated Diagnostic Equipment	80
c.	Procedure	80
V.	Experimental Observations for the Combustion of Magnesium, Calcium and Strontium	82
1.	Wire Experiments	82
a.	Calcium Wire Experiments	83
(i)	Visual and Photographic Observations	83
(ii)	Photographs through Narrow Band Interference Filters at Selected Wavelengths	85
(iii)	Space-Resolved Spectroscopic Observations	86
b.	Strontium Wire Experiments	96
(i)	Visual and Photographic Observations	96
(ii)	Space-Resolved Spectroscopic Observations	97
c.	Magnesium Wire Experiments	
(i)	Visual and Photographic Observations	103
(ii)	Spectroscopic Observations	104
d.	Wire Experiments - Effect of Water Vapor	106
2.	Two-Dimensional Diffusion Flame Burner Experiments	109
a.	Magnesium Burner Experiments	109
(i)	Visual Observations	113
(ii)	Space-Resolved Spectroscopic Observations	114
b.	Calcium Burner Experiments	119
(i)	Visual Observations	119
(ii)	Space-Resolved Spectroscopic Observations	120

c.	Strontium Burner Experiments	124
(i)	Visual Observations	124
(ii)	Space-Resolved Spectroscopic Observations	125
VI.	Discussion and Interpretation of Experimental Observations	130
1.	Comments on the Spectroscopic Observations	130
2.	Wire Burning Experiments	
a.	Calcium	133
b.	Strontium	136
c.	Magnesium	137
3.	Effect of Water Vapor	137
4.	Two-Dimensional Diffusion Flame Burner Experiments	139
VII.	Discussion of a New Flame Structure Model	141
1.	Zone of Reaction	142
2.	Thermal or Chemiluminescent Excitation	143
a.	Experimental Observations	144
b.	Supporting Evidence for Thermal Excitation - Temperature Measurements in Metal Flames	146
3.	Relative Temperatures in the Two Flame Zones	149
4.	Location of Condensed Oxide Particles in the Flame	150
5.	Oxide Particle Sizes	152
6.	Particle Movement in the Flame	153
7.	Homogeneous versus Heterogeneous Reaction	156
8.	Possible Reaction Steps for the Production of Oxide Vapor	158
a.	Reaction Steps Involving the Alkaline-Earth Peroxide	159
b.	Reaction Steps Involving the Alkaline-Earth Metal Dimer	162
(i)	Evidence for the Existence of the Alkaline-Earth Metal Dimer	162
VIII.	Summary of Flame Model	168
	List of References	172
	Appendix A - Vaporization of the Alkaline-Earth Oxides	180
	Abstract	185

LIST OF TABLES

<u>Table Number</u>	<u>Title</u>	<u>Page Number</u>
1.	Melting and boiling points @ 1 atm for the alkaline-earth metals and their oxides	9
2.	Band systems of beryllium oxide	33
3.	Band systems of magnesium oxide	37
4.	Band systems of calcium oxide	40
5.	Band systems of strontium oxide	42
6.	Band systems of barium oxide	44
7.	Dissociation energies of the alkaline- earth oxides	47
8.	Typical gas analyses	62
9.	Spectral lines observed in the calcium flames (wire experiments)	94
10.	Spectral lines observed in the strontium flames (wire experiments)	101
11.	Spectral features observed in the magnesium flames (wire experiments) Ref. Brzustowski (16, 54)	108
12.	Mole fraction of dimer versus tempera- ture	164
13.	Sublimation of the monoxides in vacuo	181

LIST OF FIGURES

<u>Figure Number</u>	<u>Title</u>	<u>Page Number</u>
1	Droplet burning theory model	4
2	Cross-section of cylindrical stagnant-film model with finite reaction zone	13
3	Model for combustion with metal evaporation and expansion of the liquid oxide shell	16
4	A model of aluminum particle combustion	24
5	Schematic representation of vapor phase burning	26
6	Heterogeneous reaction model	29
7	Energy level diagram for BeO	34
8	Energy level diagram for MgO	38
9	Energy level diagram for CaO	41
10	Energy level diagram for SrO	43
11	Energy level diagram for BaO	45
12	Energy level diagram for Be	55
13	Energy level diagram for Mg	56
14	Energy level diagram for Ca	57
15	Energy level diagram for Sr	58
16	Energy level diagram for Ba	59
17	Energy level diagram for O	60
18	Wire-burning apparatus	66
19	Wire-burning apparatus schematic	67
20	Electrical schematic (Wire-burning apparatus)	68
21	Combustion chamber interior (Wire-burning apparatus)	69
22	Schematic of end view of 2-dimensional diffusion flame burner	73

LIST OF FIGURES (Cont'd.)

<u>Figure Number</u>	<u>Title</u>	<u>Page Number</u>
23	2-dimensional diffusion flame burner	74
24	Combustion chamber and optical arrangement (burner apparatus)	77
25	Low pressure two-dimensional diffusion flame burner - flow schematic	78
26	Overall view of burner apparatus	79
27	Calcium wire burning in 20% O ₂ , 80% Ar at 50 torr total pressure	84
28	Calcium flame in 20% O ₂ , 80% Ar at 50 torr total pressure photographed through an inter- ference filter passing the radiation due to CaO band emission plus continuum. (nominal wavelength 6250 Å)	87
29	Calcium flame in 20% O ₂ , 80% Ar at 50 torr total pressure photographed through an interference filter passing the radiation due to continuum only, i.e., no CaO band emission or Ca line emission. (nominal wavelength 4990 Å)	88
30	Calcium flame in 20% O ₂ , 80% Ar at 50 torr total pressure photographed through an inter- ference filter passing the radiation due to Ca line emission plus continuum (nominal wavelength 4200 Å)	89
31	Calcium flame in 20% O ₂ , 80% Ar at 50 torr total pressure photographed through an inter- ference filter passing the radiation due to Ca line emission plus continuum (nominal wave- length 4231 Å)	90
32	Space-resolved flame spectrum of calcium at 50 torr, 20% O ₂ , 80% Ar	92
33	Principle features of the Ca - O ₂ flame spectrum (wire experiments)	93
34	Strontium wire-burning in 20% O ₂ , 80% Ar at 50 torr total pressure	98

LIST OF FIGURES (Cont'd.)

<u>Figure Number</u>	<u>Title</u>	<u>Page Number</u>
35	Space-resolved flame spectrum of strontium at 50 torr, 20% O ₂ , 80% Ar	99
36	Principal features of the Sr - O ₂ flame spectrum (wire experiments)	100
37	Magnesium ribbon burning in 20% O ₂ , 80% Ar at 50 torr total pressure	105
38	UV band systems of the Mg -O ₂ flame spectrum (wire experiments)	107
39	Effect of water vapor. Magnesium wire experiment.	110
40	Effect of water vapor. Calcium wire experiment.	111
41	Effect of water vapor. Strontium wire experiment.	112
42	Spectrum of magnesium 2-D diffusion flame. Total pressure 200 torr. Oxidizer mixture 10% O ₂ - 90% Ar.	115
43	Spectrum of magnesium 2-D diffusion flame. Total pressure 200 torr. Oxidizer mixture 10% O ₂ - 90% Ar. (Enlargements of Figure 42)	116
44	Spectrum of magnesium 2-D diffusion flame. Total pressure 200 torr. Oxidizer mixture 10% O ₂ - 90% Ar. (Enlargements of Figure 42)	117
45	Spectrum of calcium 2-D diffusion flame. Total pressure 200 torr. Oxidizer mixture 10% O ₂ - 90% Ar.	121
46	Spectrum of calcium 2-D diffusion flame. Total pressure 200 torr. Oxidizer mixture 10% O ₂ - 90% Ar (Enlargements of Figure 45)	122
47	Spectrum of calcium 2-D diffusion flame. Total pressure 200 torr. Oxidizer mixture 10% O ₂ - 90% Ar (Enlargements of Figure 45)	123

LIST OF FIGURES (Cont'd.)

<u>Figure Number</u>	<u>Title</u>	<u>Page</u>
48	Spectrum of strontium 2-D diffusion flame. Total pressure 200 torr. Oxidizer mixture 10% O ₂ - 90% Ar	126
49	Spectrum of strontium 2-D diffusion flame. Total pressure 200 torr. Oxidizer mixture 10% O ₂ - 90% Ar (Enlargements of Figure 48)	127
50	Spectrum of strontium 2-D diffusion flame. Total pressure 200 torr. Oxidizer mixture 10% O ₂ - 90% Ar (Enlargements of Figure 48)	128
51	Schematic representation of flame structure	167

CHAPTER I - INTRODUCTION

Although the first experiments on the combustion of metals date back almost two hundred years (1) to the work of van IngennHauz in 1782, the current, strong interest in this field stems from the use of metals in propellants. Although the use of metal additives results in undesirable high molecular weight, condensed phase oxide products, the high heat of combustion of metals (per unit weight of fuel and oxidizer) overcomes these disadvantages to give a net increase in performance (i.e., higher specific impulse). In other rocket applications, where loading density becomes the paramount consideration, the use of metals is even more attractive.

Additional impetus for a fundamental study of metal combustion derives from such diverse areas as abort re-entry of orbiting reactors, nuclear reactor fires, photoflash applications, tracer bullets and general illumination devices such as flares.

The desired knowledge of the details of the combustion process differs widely in these varied applications. In propellant considerations one is concerned primarily with obtaining efficient combustion, or more specifically, complete combustion of the metal component within the short residence times available in rocket motors. Here, one must know first of all whether the metal reacts efficiently in the vapor phase or whether possibly slow surface reaction on the surface

of the metal particle is to be expected. Also, factors affecting the ease of ignition and the length of ignition delay times must be obtained. In addition, because the condensed reaction products can contribute to performance inefficiencies due to both thermal lag and velocity lag as the gases are expanded through the nozzle, it is important to know the range of particle sizes to be expected. Thus, one desires a knowledge of the nucleation, growth and agglomeration steps for the oxide particles. Accurate size determination of these particles is also important if one wishes to explain the role played by the metal oxide smoke in damping pressure oscillations within the rocket motor. Metal combustion may in itself couple with or give rise to such pressure disturbances.

In the applications utilizing the intense light output of metal flames, the interest is in the fundamental radiation characteristics. The radiation may be thermal or chemiluminescent in character. If the radiation is chemiluminescent, there is the possibility of tailoring the light output to suit specific applications such as controlling the color temperature of a flash bulb. Here, too, a knowledge of the particulars concerning the condensed particles is important, since the continuum radiation emitted by these high temperature condensed species may, under certain conditions, be the dominant radiation overshadowing the discrete line and band radiation of the excited atomic and molecular species.

In 1959, Glassman (2) published a paper in which several basic hypotheses were presented. These hypotheses were a consequence of fundamental reasoning concerning the thermodynamic behavior of the metals and their oxides. The points presented in this paper can be conveniently summarized as is done below:

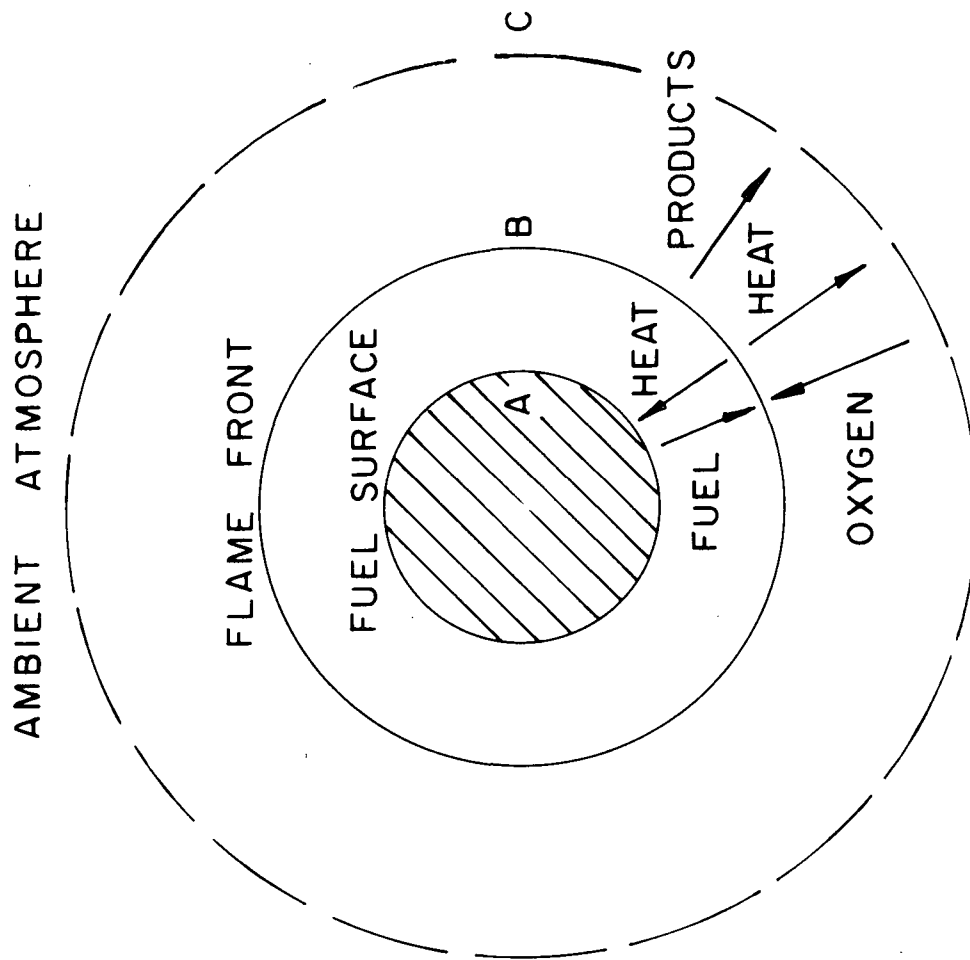
- (1) The upper limit for the flame temperature is a value equal to the boiling point of the metal oxide.

The limiting of the flame temperature to the boiling point of the oxide is a direct result of the fact that for most metals the heat of vaporization of their oxide is greater than the heat available in the reaction forming the oxide. Note that since a great number of the oxides also dissociate upon vaporization (3), this is a further energy barrier at the boiling point temperature of the oxide.

This hypothesis assumes realistic initial temperatures for the reactants, since initial temperatures could be chosen sufficiently high that the flame temperature could exceed the boiling point of the oxide.

- (2) If the boiling point of the metal oxide is greater than the boiling point of the metal, "steady-state" combustion takes place in the vapor phase. For the opposite situation in which the boiling point of the metal exceeds the boiling point of the metal oxide, a surface combustion process is expected.

This criterion for vapor phase or surface reaction is readily understood on the basis of the idealized model used for hydrocarbon droplet burning, which is shown in Figure 1.



DROPLET BURNING THEORY MODEL

For vapor phase reaction to occur, the flame temperature at some distance from the droplet surface must be greater than the droplet temperature so that heat feedback from the detached reaction zone provides the energy to vaporize the fuel. Since the flame temperature is limited to the boiling point of the oxide as pointed out above, and since the droplet temperature will not exceed the boiling point of the metal, the necessary condition for vapor phase burning is that the boiling point of the oxide be greater than the boiling point of the metal.

It was later pointed out (4) that statement (2) was a necessary but not a sufficient condition for vapor phase combustion. The reason is that heat losses could lower the flame temperature to a value less than the boiling point of the oxide.

- (3) Radiation plays an important part in metal combustion.

Because of the high temperatures occurring in metal flames and because of possibly large concentrations of condensed products in a high temperature region, it was felt that radiation both to the surroundings and from the reaction zone to the droplet surface could be important.

- (4) Ignition phenomena could be entirely different from the controlling steady combustion phenomena.

Statement (4) recognizes that although the "steady state" combustion could take place by a vapor phase mechanism,

the pre-ignition reactions were generally surface reactions and thus there was no reason to anticipate that the same type of behavior would govern both cases.

The experimental work which this thesis describes was undertaken in large part to verify and provide further substantiation of some of these hypotheses. A recent extensive investigation by Mellor (5) has examined the problem of metal ignition and has presented a model for metal ignition along with experimental evidence to support the ignition model.

In order to determine whether calcium and strontium would burn in the vapor phase, as would be predicted by the criterion for vapor phase combustion, an experimental investigation of the combustion behavior of these metals was undertaken. Some of the early experimental observations with calcium indicated that existing models of the flame structure, which were based in large part on the collapsed flame zone model of hydrocarbon droplet theory (suitably modified for metal fuels), were not correct. A decision was made to attempt to determine more precisely the flame structure of metal vapor-phase diffusion flames, in particular the flames of the alkaline-earth metals Mg, Ca and Sr.

The present investigation, described in the following chapters, is primarily experimental in nature. In order to

present a general model free from the peculiarities of a particular metal and a particular experiment, several metals were used in two different combustion configurations. Magnesium, calcium, and strontium were studied, some in much more detail than others. The two different combustion configurations employed were the following:

- (1) Metal samples in the form of wires or strands were heated by resistive methods until ignition occurred. Controlled atmospheres of oxygen and argon were used at various sub-atmospheric pressures. Diagnostic techniques included photography, observation of radiation of selected wavelengths (isolated by narrow band pass interference filters), and space-resolved spectroscopy.
- (2) A two-dimensional metal-oxygen diffusion flame was obtained by adapting for metal combustion studies, a special burner previously used by Wolfhard and Parker (6) for the spectroscopic investigation of hydrocarbon flames. The main diagnostic technique applied to this two-dimensional flame was space-resolved spectroscopy.

It is hoped that some aspects of the model will also be applicable to the flames of both barium and beryllium since these metals and their oxides are iso-electronic with the metals and oxides studied in the present investigation.

Table 1 lists the relative melting points and boiling points of the metal and the oxide for the group IIA elements for which the flame structure model is expected to hold. It is immediately obvious from an examination of this table, that the vapor-phase criterion is easily satisfied despite the uncertainty which surrounds most of these high temperature thermochemical values. Thus, all five of these

metals are predicted to burn in the vapor phase.

The present investigation confirms the predicted vapor phase combustion for Mg, Ca, and Sr as supported by visual, photographic and spectroscopic observations.

In summary, the present investigation of the flame structure of vapor phase flames for the group IIA metals seeks to contribute additional evidence which may eventually result in answers to the following as yet unanswered questions:

- (1) The radiation from the flames may be thermal or chemiluminescent in nature. If it is indeed chemiluminescent, is there a logical series of kinetic steps to account for the energies involved in the excitation?
- (2) Does the flame temperature approach its limiting value of the boiling point of the oxide?
- (3) What range of particle sizes can be expected in metal combustion reactions? What control can be exercised over the processes of nucleation, growth, and agglomeration in the condensation of the oxide products?
- (4) Is a significant portion of the reaction proceeding by a heterogeneous mechanism on the surface of condensed oxide particles?

Chapter II will review existing flame models and the basis for their support. Chapter III is a literature survey of the current spectroscopic data for the alkaline-earth oxides. Energy level diagrams for the metals as well as the oxides are presented in this chapter. Chapter IV describes the experimental apparatus and procedure used in the present investigation. Chapter V contains the experi-

TABLE 1

Atomic Number	Metal	Predominant Metal Oxide	Melting Points °C		Boiling Points °C @ 1 atm		Vapor Phase Criterion Satisfied
			T _{MP} ^M	T _{MP} ^{MO}	T _{BP} ^M	T _{BP} ^{MO}	
4	Be	BeO	1283 (7) ¹	2547 (7)	2484 (7)	3787 (7)	✓
12	Mg	MgO	649 (7)	2800 (8)	1105 (7)	3600 (8)	✓
20	Ca	CaO	848 (8)	2580 (8)	1240 (8)	2850 (8)	✓
38	Sr	SrO	774 (8)	2430 (8)	1366 (8)	3000 (8)	✓
56	Ba	BaO	850 (8)	1923 (8)	1527 (8)	2000 (8)	✓

¹Numbers in parentheses refer to references listed at the end of this report.

mental observations and Chapter VI is a discussion of these observations. Chapter VII presents the details of the proposed model for the flame structure, including a comparison with features of flame models of other investigators. Chapter VIII is a summary. Appendix A is a literature survey of vaporization data for the alkaline-earth oxides.

CHAPTER II - FLAME MODELS

In this chapter the various models that have been presented in the literature to represent the flame structure of metal-oxygen diffusion flames will be reviewed.

The evidence to support these proposed models varies significantly. In some cases visual observation alone is the sole criterion suggesting a flame model. Burning rate calculations performed under the guidelines of this postulated model are then compared with experimentally determined burning rates to judge the validity of the model. Other models result from more complete experimental determinations including such diagnostic measurements as optical spectroscopy, electron microscopy and x-ray diffraction studies of the combustion products, quench studies of metal particles in all stages of combustion, and determination of kinetic rate constants.

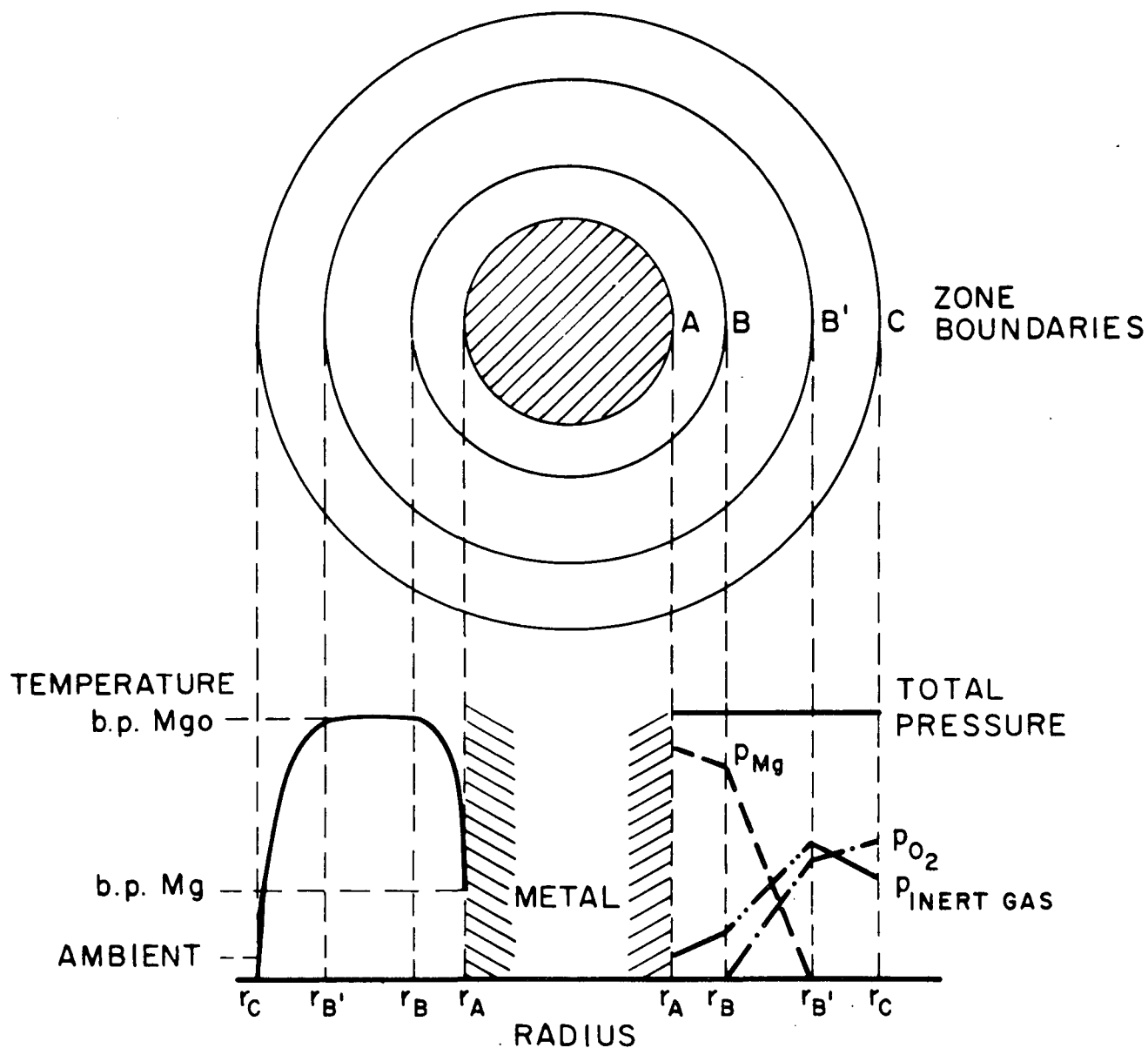
It should be pointed out that unknown or uncertain high temperature values for many of the parameters required in order to be able to perform an analytical calculation of a burning rate, preclude the possibility of definitely establishing one flame model as correct on the basis of comparing calculated and measured burning rates. In the same manner it has not been possible to assess critically the various assumptions that have been made in all of these admittedly idealized and simplified models.

1. Finite Reaction Zone Model Due to Coffin

The earliest of these models is due to Coffin (9). In his experiments Coffin studied the burning of magnesium ribbons in various mixtures of oxygen with argon, nitrogen, helium and argon-water vapor. His evidence indicated a vapor phase reaction for magnesium combustion bearing some analogy to the combustion of liquid fuel drops. However, the model generally used for liquid fuel droplets, Figure 1, was not used by Coffin. Instead of this "collapsed flame front" model, a finite thickness for the reaction zone was adopted. Coffin's model is illustrated in Figure 2.

In this cylindrical model, there are three concentric zones. The inner zone AB contains only the metal vapor and the inert diluent. Metal, which is vaporized at the fuel surface by the heat conducted back from the reaction zone, diffuses from the ribbon surface at A, where it is at a temperature close to the boiling point of the metal, to the reaction zone which starts at B. The reaction zone was considered to be at the boiling point of the magnesium oxide, as had been suggested by experimental flame temperature measurements (10, 11). It was also believed that the oxide dissociated almost completely upon vaporization (12).

The reaction zone BB' thus consisted of a mixture of magnesium vapor, oxygen and condensed oxide at the boiling point of the metal oxide in a stagnant film of inert gas.



CROSS SECTION OF CYLINDRICAL
STAGNANT - FILM MODEL WITH FINITE
REACTION ZONE; p , PARTIAL PRESSURE.

REF: COFFIN, K.P. NACA TN 3332 DEC. 1954

It was assumed that chemical equilibrium existed among the species in this zone.

The third zone B'C is the zone through which oxidizer diffuses from the surroundings to the constant temperature reaction zone. The oxygen is heated from the ambient temperature of the surroundings to the flame temperature as it diffuses inward. The condensed oxide from the reaction zone cools as it moves outward from the reaction zone through the zone B'C.

Idealized assumptions which were made for this model were as follows: free convection was ignored; the pressure was considered to be 1 atmosphere throughout the system; the inert gas was considered as a stagnant film throughout the system.

2. Liquid Oxide Bubble Model Due To Fassell and Co-Workers

A second model for the combustion of metal particles has been proposed by Fassell and co-workers (13, 14). Although these authors indicated that the gas phase spherical diffusion flame theory adequately accounted for the combustion of magnesium, they suggested that higher boiling metals did not burn in conformity with this model. A particular case of this latter category of metals was aluminum. In the experiments of Fassell et al, aluminum and various aluminum-magnesium alloy particles were burned in two different types of torches in either methane-oxygen mixtures, or a combination

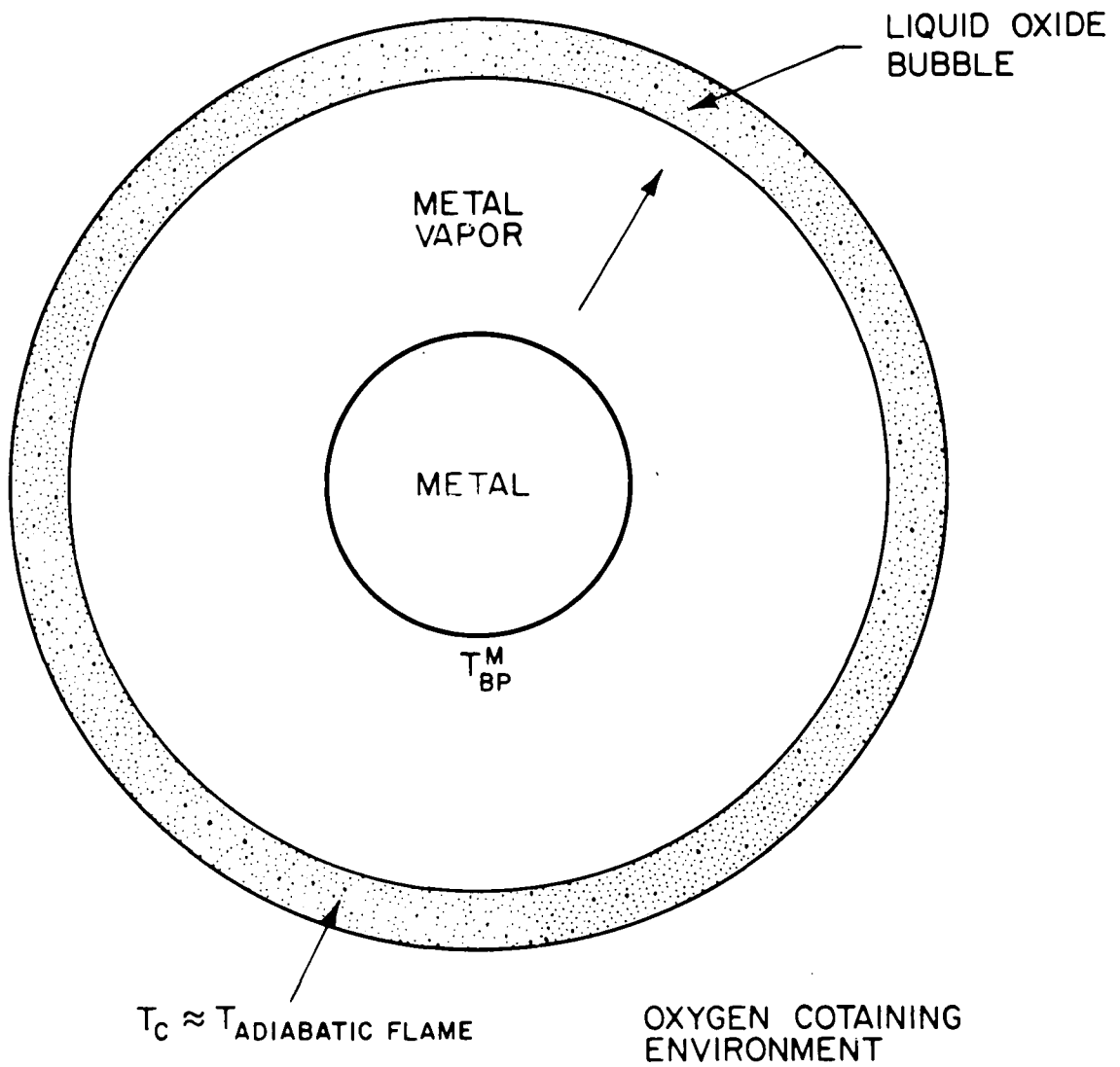
of methane, oxygen and air.

Visual observations, high speed photographic measurements and detailed observations including x-ray diffraction of the combustion products suggested to these workers that the diffusion flame model which had apparently been successfully applied to the combustion of magnesium, did not in fact represent the case of aluminum combustion. Based largely on the appearance of the combustion products, Fassell et al proposed the model which is depicted schematically in Figure 3.

A continuous layer of molten oxide covers the metal droplet. The evaporating metal from the droplet, which is considered to be at its boiling point, causes the molten oxide layer to form a bubble. The limiting step to further reaction is considered to be diffusion, through this molten oxide layer, of either metal vapor diffusing outward, or oxygen diffusing inward. Reaction is considered to take place at the liquid oxide interface. The authors considered the possibility of the molten oxide bubble exceeding a critical size and bursting, thus scattering fragments of both oxide and freshly exposed metal.

It was thought that this model provided the explanation of the numerous hollow oxide spheres present in the combustion products. It also satisfied one of the difficulties which arose from the x-ray diffraction studies, namely the appearance of species such as MgAl_2O_4 which would

(16)



REF. : FASSELL ET AL. COMBUSTION AND FLAME 7,227-34 (1963)

MODEL FOR COMBUSTION WITH METAL
EVAPORATION AND EXPANSION OF THE
LIQUID OXIDE SHELL

FIGURE 3

not be thought likely to occur in a vapor phase diffusion flame.

3. Collapsed Reaction Zone Model Due to Brzustowski and Glassman

The first model due to Coffin subsequently came under criticism by Brzustowski and Glassman (15). In addition to certain facets which they felt had to be included in the analytical model (thermal radiation from the flame front to the surroundings and to the droplet surface; diffusion of oxygen toward the flame front being affected by the condensed product), they stated that the thick reaction zone used by Coffin predicted a flame structure "notably different" from observed flames. Coffin's contribution was felt to be the comparison of the diffusion flames of metals and of hydrocarbons. This comparison was the basis on which Brzustowski and Glassman proceeded to develop a flame model which is outlined below.

The analysis was based on the theory developed to describe the combustion of hydrocarbon droplets, namely the collapsed flame front model depicted in Figure 1, but was modified to account for specific characteristics pertaining to metal combustion. These particular features are presented below:

- (1) The flame temperature will be fixed at the boiling point of the oxide. Some oxide will always form in the condensed state. (Coffin's model was a particular case of this general statement. His model was specifically for magnesium.)

- (2) The presence of the condensed oxide products will affect the diffusion of oxygen to the reaction zone. Movement of these solid or liquid products must occur due to bulk motion of gaseous species since they cannot diffuse.
- (3) Thermal radiation will probably be an important consideration because of the existence of these condensed species in the high temperature regions of the flame. It can possibly result in higher evaporation rates for the fuel due to an increased heat feedback, but it can also lead to significant losses to the surroundings.
- (4) In the case of metal combustion, evaporation rates of the fuel may not be fast compared to diffusional processes.

With the above considerations in mind, the collapsed flame zone model of Figure 1 becomes the metal combustion model proposed by Brzustowski and Glassman. Heat feedback (due to both conduction and radiation) from the thin flame front B, evaporates metal from the fuel surface at A. This metal vapor, at a temperature which may be several hundred degrees lower than the metal boiling point, diffuses through the stagnant film AB toward the high temperature flame front at B.

Oxidizer from the surroundings diffuses toward the flame front through the film BC. This diffusion of the oxidizer is opposed by the outward movement of combustion products which were formed in the thin flame front at B. Heat is conducted and radiated to the surroundings through this film BC.

As in the case of the earlier model of Coffin, idealizations considered in this model include uniform

pressures throughout the system, and a system steady in time. It was assumed that combustion products did not diffuse back to the fuel surface through the film AB, but that all products diffused through the film BC to the surroundings. This last assumption was justified in part by the observation of Brzustowski that although oxide was observed on the wire surface (probably from back diffusion of the products) it did not appear to have an appreciable effect on the observed burning mechanism. As will be pointed out later in this chapter, more recent experimental work of other investigators does not support this assumption of no back diffusion of the combustion products.

An important feature of the Brzustowski-Glassman model is the attention paid to the condensed oxide products. Condensed oxide particles can be transported out of the flame zone only if a bulk outward gas velocity exists in the zone BC. The diffusion equation for this zone gives the conditions under which such a bulk velocity can be achieved.

A parameter α is defined as the fraction of the condensed oxide product that is vaporized. This parameter is a function of the flame radius when there is dissociation in the flame zone and subsequent recombination in the zone BC. The result, derived analytically by Brzustowski, illustrates that an outward bulk velocity in the zone BC occurs when more than one mole of gaseous products is formed

for every mole of oxidizer participating in the reaction.

In the reaction zone itself, the degree of dissociation of the oxide varies according to the balance between heat liberated in the reaction and heat radiated or conducted to the surroundings. If heat losses are large enough, it would be expected that condensed oxide deposits would appear in the flame front itself.

It has sometimes been incorrectly stated in the literature that a collapsed reaction zone assumption would define zero concentrations for the reacting species at the flame front. Brzustowski (16) points out the correct definition of a collapsed flame front as follows: ". . . . to a desired degree of accuracy, the dimensions of the reaction zone and the changes in reactant concentrations through it are small with respect to the dimensions and concentration differences involved in the diffusion processes."

Brzustowski found Coffin's thick flame zone model unacceptable because, firstly, it assumed that no gaseous oxide was present because of complete dissociation, whereas spectroscopic observations showed significant oxide vapor radiation and secondly, Brzustowski's interpretation of his flame photographs showed an entirely different structure. Over a large pressure range from 50 torr to 12 atmospheres the bright flame zone thickness was small in comparison with the dimension between the metal surface and the flame front.

4. Extensions of the Brzustowski-Glassman Model Due to Knipe

In a survey paper on aluminum particle combustion by Christensen, Knipe and Gordon (17), a critical discussion of aluminum particle combustion models was presented. The two models discussed were the models due to Fassell et al and the Brzustowski-Glassman model discussed in the previous two sections of this chapter.

One of the criticisms of the model of Fassell and co-workers is that the postulated rate-controlling step of diffusion through the oxide shell must be accepted with some caution because of considerable uncertainty about the magnitude of this diffusion rate. This model does take into account the normal metal oxide coating which exists on the metal particle prior to ignition, but the bubble of oxide which is proposed may be unstable.

A criticism of the Brzustowski-Glassman model is that it does not explain the fate of the normal oxide coating which exists on the metal surface. A suggestion is that the oxide may accumulate in one area giving rise to a metal sphere with an agglomerated oxide cap. The basis for this suggestion comes from observations of such metal-oxide configurations in quench studies. However, this is then a considerable departure from the idealized one-dimensional, spherically symmetric model of Brzustowski and Glassman.

Another criticism of this model is the treatment of

dissociation fragments in the reaction zone. Allowing for the fact that their precise nature is not known, aluminum and oxygen atoms are the major fragments of dissociation of the oxide. Since the reaction zone is at a high temperature, it is expected that a heterogeneous reaction will be more likely than vapor-phase reaction to gaseous oxides, and as a consequence the conditions favorable to the nucleation of the condensed oxide may play some role in determining the location of the reaction zone.

Christensen et al conclude from this survey of combustion models that the Brzustowski-Glassman model does describe the gross features of aluminum particle combustion but that there are significant features not contained in the idealized model. As a consequence, Knipe (18) sought to extend the Brzustowski-Glassman model as is indicated below.

The Brzustowski-Glassman model does indicate the conditions under which condensed oxide may build up in the reaction zone. Knipe suggests that this fact should raise strong questions about the applicability of a steady state approximation especially in view of the many statements in the literature suggesting that, because of the condensed nature of the products, radiation will be an important heat transfer mechanism in metal flames. As pointed out previously, Knipe also proposes that the principle reaction path will be via heterogeneous processes on the condensed oxide within the reaction zone. It is also stated that the zone of con-

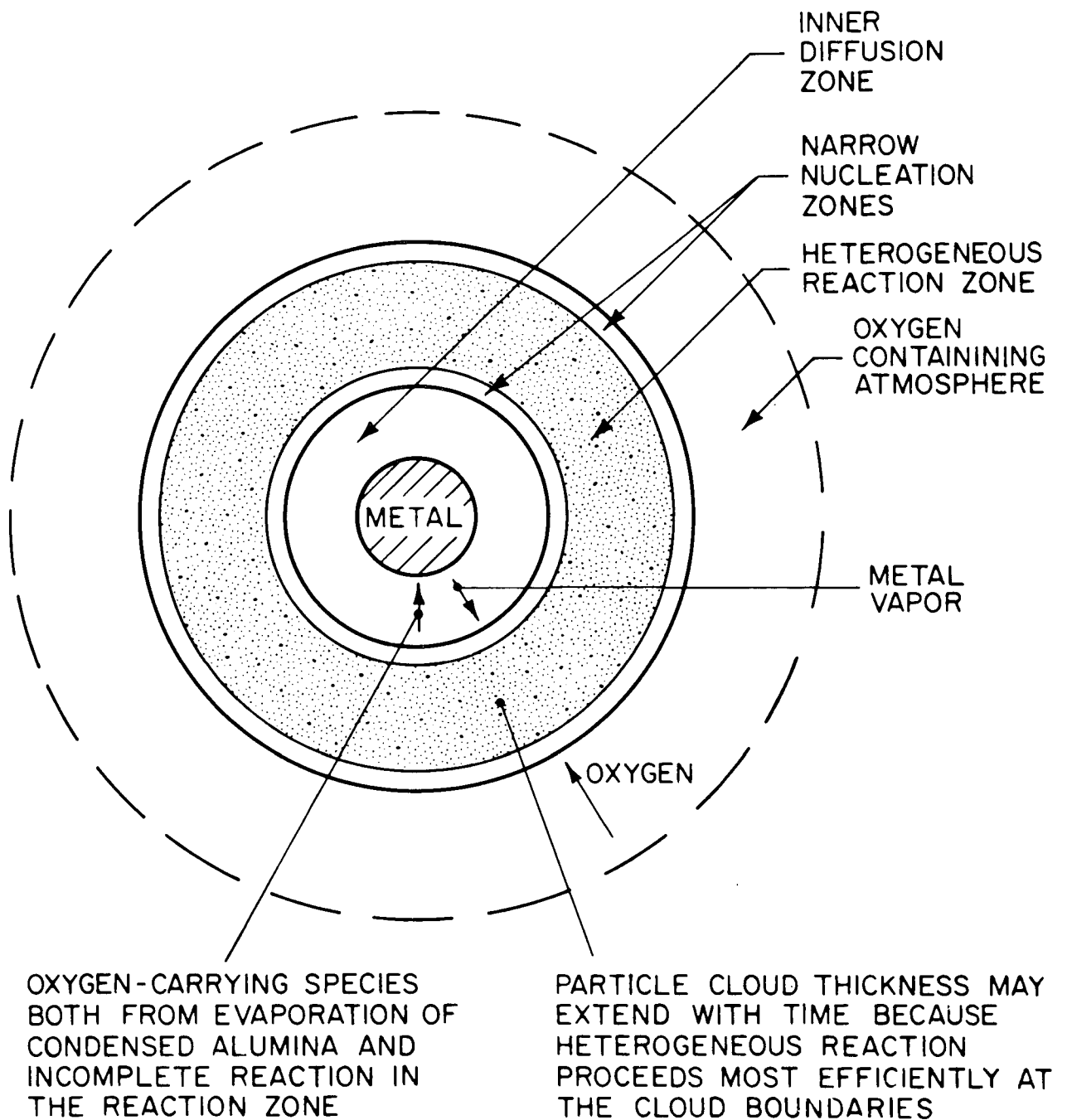
densified oxide particles has been observed experimentally to possess considerable thickness. This is a plausible observation for such a proposed heterogeneous reaction zone since dissipation of heat, which occurs most efficiently at the edges of this thick zone, significantly affects the progress of the reaction.

In the Brzustowski-Glassman model, back-diffusion of the gaseous combustion products to the metal surface was assumed not to take place. However, experimental observations of Prentice (18) showed that significant amounts of oxide did build up on the metal surface during combustion, indicating that oxygen-containing species were present in the region between the metal particle and the flame front.

Figure 4 is an attempt to represent schematically the model which Knipe proposes.

This model is characterized by a heterogeneous reaction zone of appreciable thickness which probably extends in both directions with time as mentioned previously. A narrow nucleation zone is expected to exist between the reaction zone and a position where the inward-diffusing oxygen-containing species (both evaporation products and partially reacted species) make up a saturated vapor relative to condensation. A second nucleation zone is proposed on the oxidizer side of the reaction zone.

Note that the importance of recognizing the back diffusion of gaseous combustion products is of more signifi-



REF. : R.H. KNIPE
 NOTS TP 3916 APRIL 1966
 TECHNICAL PROGRESS REPORT 415

A MODEL OF ALUMINUM PARTICLE COMBUSTION

cance than merely explaining some of the features attributed to a non-symmetrical burning configuration (e.g. particle spinning). Condensation of oxide on the metal surface would be an appreciable heat transfer mechanism operating between the reaction zone and the particle surface since much of the heat of reaction is in the heat of condensation.

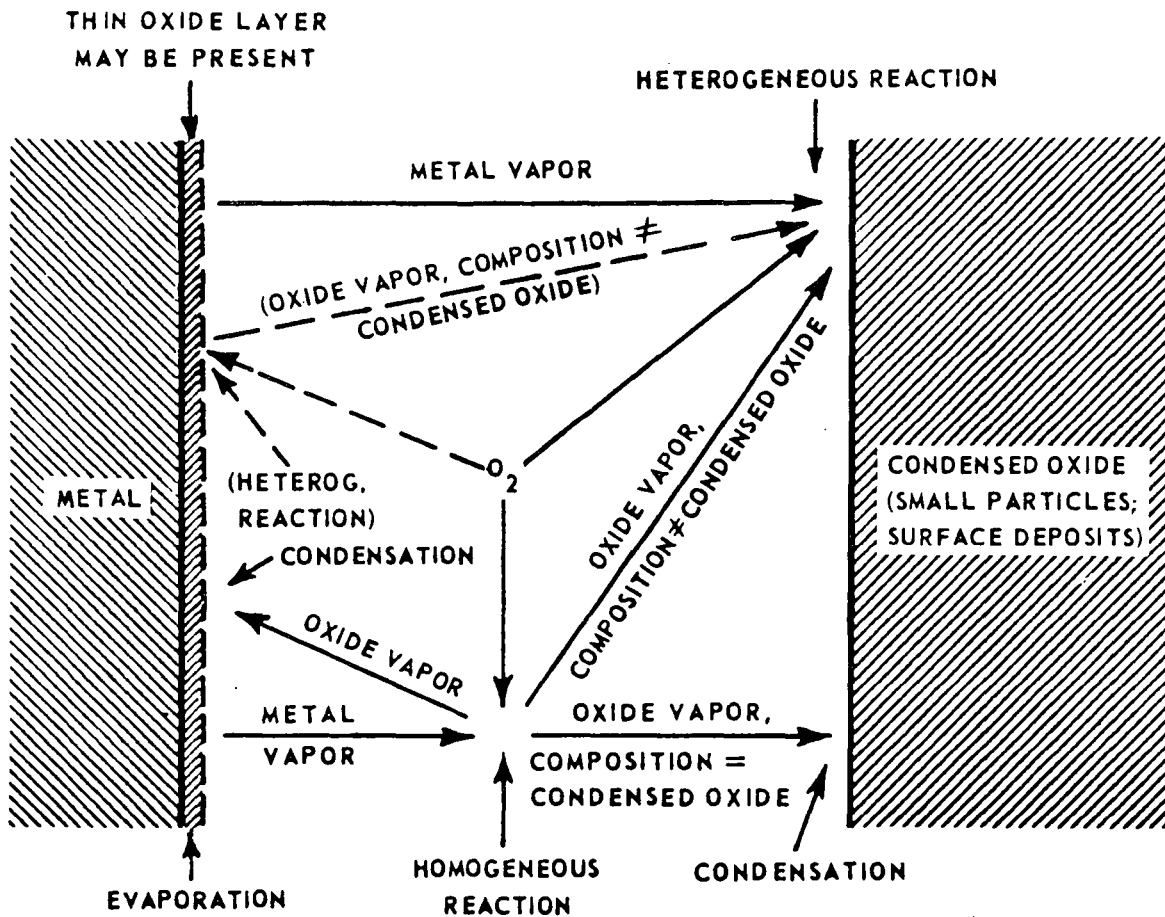
5. Heterogeneous Reaction Model Due to Markstein

Markstein (19), although he has not set out a specific flame model, has discussed vapor-phase burning of metals and has contributed significantly to the problem of whether or not heterogeneous reaction or homogeneous reaction dominate metal combustion, in particular in the case of magnesium.

Figure 5 is reproduced from Markstein's paper (19) and represents a schematic representation of most of the processes that might possibly play a role in vapor-phase combustion.

Markstein states that heterogeneous reaction on the metal surface is not likely a significant process once the vapor phase flame is fully developed. This statement is reflected in the schematic by the dashed lines used to depict this process.

Back diffusion of oxide vapor is also expected to be significant as evidenced by a consideration of the experimental evidence of Macek (20).



REF. MARKSTEIN, G.H. II TH SYMPOSIUM (INTERNATIONAL) ON
COMBUSTION Pg 219-234 THE COMBUSTION INSTITUTE,
PITTSBURGH, PENNA.

SCHEMATIC REPRESENTATION OF VAPOR-PHASE BURNING

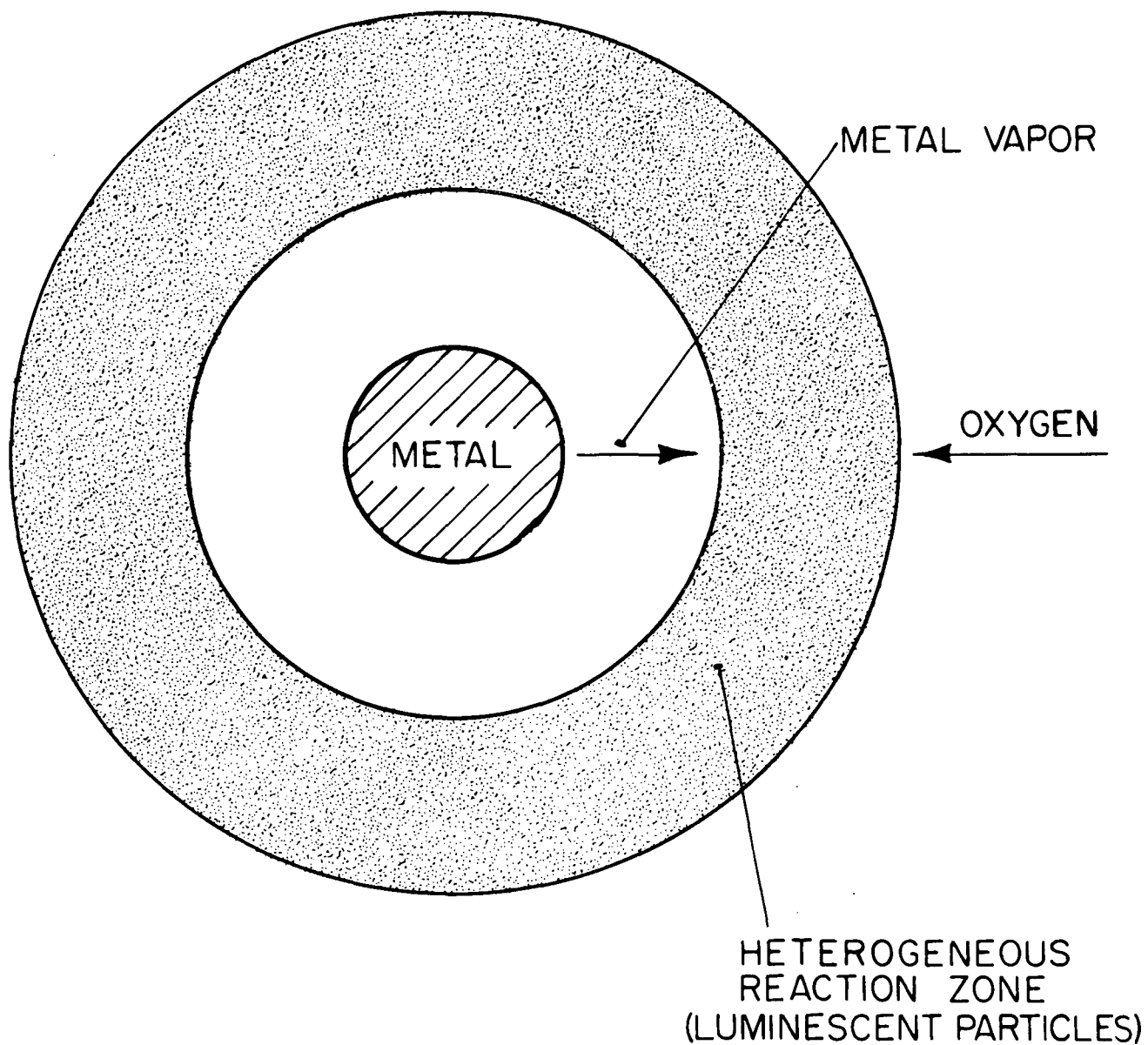
Markstein agrees that the question of heterogeneous versus homogeneous reaction is far from settled and thus far has been an area of speculation and controversy. In an earlier work (21) Markstein seems to have demonstrated the strong role played by heterogeneous reactions in low pressure dilute magnesium-oxygen flames. In these experiments magnesium vapor was carried in an inert carrier gas (Argon). The mixture of magnesium and argon carrier gas entered the stagnant oxygen-argon atmosphere of the combustion chamber through an orifice. Total pressures ranged from about 2 to 10 torr. The spectra of the resulting flame showed no line and band radiation at all, but instead consisted of continuum radiation with several maxima. In addition, it was observed that oxide growths were present near the orifice. The luminescence of these oxide growths was also characterized by a broad maximum in the blue closely resembling that of the dilute flame spectrum. Markstein suggested that the reaction path was following a heterogeneous route. Recent work of Markstein (19, 22, 23) has been an attempt to determine rate constants for this proposed heterogeneous reaction and to obtain further experimental evidence to elucidate details of the mechanism.

Markstein is cautious about the interpretation of emission spectra by other authors as being an indication of homogeneous reaction, suggesting that the high electronic energies of the states observed in spectra may be difficult

to explain on the basis of kinetic steps that are probably not highly exothermic.

If one were to postulate the structure of a combustion model which would fit the particular conditions of Markstein's experiments, namely low pressure highly-diluted flames, it would appear schematically as indicated in Figure 6.

Note that nucleation zones are not specifically defined. Markstein stated (21) that some homogeneous reaction may be required initially to furnish sites for the ensuing heterogeneous reaction but that in the fully developed reaction it would be expected that homogeneous reaction would not be significant. Since oxide vapor is not present due to the lack of homogeneous reaction, it would also be likely that not much oxide would appear on the metal surfaces. This statement is based on two facts. Firstly, most evaporation products dissociate, and thus, very little oxide vapor for back diffusion could be expected from this process. Secondly, it was pointed out earlier that Markstein felt that heterogeneous reaction on the metal surface was unimportant when fully developed reaction had been established. Thus the schematic in Figure 6 indicates no back diffusion of oxide vapor to the metal surface.



HETEROGENEOUS REACTION MODEL

FIGURE 6

CHAPTER III - DISCUSSION OF SPECTROSCOPIC DATA

It was pointed out in Chapter I that Glassman (2) was able to suggest significant hypotheses about the nature of metal combustion strictly on the basis of fundamental reasoning concerning thermochemical data for the metals and their oxides. The importance of knowing the proper values of these thermochemical data in attempting to define and interpret flame models cannot be underestimated. Since many of these thermochemical values are based on spectroscopically determined constants, an accurate knowledge of the electronic states of the metals and their oxides is a prime requisite. In addition, since the primary diagnostic technique used in the experiments reported in later chapters is spectroscopy, the reliance upon spectroscopic data is of dual importance. A survey of the spectroscopic literature for the alkaline-earth oxides shows that a great deal of uncertainty, confusion and speculation still exists despite a significant amount of research in this area in recent years.

In view of the importance of spectroscopic and thermochemical data in the problem of flame structure determination, it was considered essential to include the following critical analysis as an integral part of this thesis.

1. Energy Levels, Known Transitions and Other Band Systems Attributed to the Alkaline-Earth Oxides

Several band systems in the visible part of the spectrum have been analyzed for each of the alkaline-earth metal oxides and have been assigned to transitions between singlet states of the diatomic oxide, e.g., CaO.

As reported in a survey paper by Schofield (24), other oxides (Be_2O , Sr_2O , Ba_2O , $(\text{BeO})_n$ $n = 1, 2, \dots, 6$ and $(\text{BaO})_2$) have been identified in the gas phase by techniques such as mass spectrometry. This author is, however, presently unaware of any spectroscopic evidence with the exception of the hypotheses of some authors that the complex and as yet unresolved band systems due to the oxides may be due to polymeric emitters. For example, Gaydon (25) has suggested that the green and orange band systems of calcium oxide are much too complex to be the result of a transition between singlet states, that a transition between triplet states is possible, but, also, that a polyatomic emitter such as Ca_2O_2 is favored.

As pointed out above, all of the band systems that have been analyzed for these oxides, correspond to transitions between singlet states. There are reasons, however, for expecting triplet states to exist. These reasons are two-fold. The lowest lying singlet states $X'\Sigma$ do not correlate with ground state atoms, M (1S) and O (3P). The Wigner-Witmer rule indicates that only $^3\Pi$ or $^3\Sigma$ molecular states correlate

with the 1S and 3P states of the metal and oxygen atoms respectively (26).

The second reason for expecting triplet states is that molecular orbital calculations such as performed by Brewer and Trajmar (27) and Richards, Verhaegen and Moser (28) suggest low-lying triplet states, and even the possibility of a triplet for the ground state of MgO .

Additional confusion in the spectra of alkaline-earth oxides has arisen in the past because of the existence of alkaline-earth hydroxide bands in the same spectral regions (in several cases completely overlapping regions) as those of the oxides. The recent experimental activity in this field has resolved much of this confusion by isotope substitution experiments.

In the following sections the spectroscopic data for each of the metal oxides will be dealt with separately.

The reference for the following data, except where specifically noted otherwise, is Pearse and Gaydon (29,30).

a. Beryllium Oxide

All of the band systems thought to be due to beryllium oxide have been ascribed to the diatomic oxide BeO and, although all of the systems for which states are given correspond to transitions between singlet states, the complex structure of the UV bands suggests that two or more singlet systems and a triplet system may be overlapping in this spectral region

(29). Contrary to what is suggested for other complex oxide bands (i.e. for magnesium, calcium, strontium and barium) it is not suggested that the complexity may be due to a polyatomic or polymeric emitter. This is the case even though the polyatomic specie Be_2O and polymeric species $(\text{BeO})_n$ $n = 1, 2, \dots, 6$ have been identified (24).

The notation for the states of BeO as reported in Ref. 29 has recently been revised (30) to conform to that of Herzberg (31).

The observed systems, the transitions and the wavelengths of the (0,0) bands of these systems are summarized in Table 2.

An energy level diagram illustrating the transitions is provided in Figure 7.

TABLE 2

BAND SYSTEMS OF BERYLLIUM OXIDE

<u>BeO</u>		<u>$\lambda_{(0,0)} \text{ \AA}^\circ$</u>
Blue-Green System	$B'\Sigma \rightarrow X''\Sigma$	4,708.6
Red System	$A'\pi \rightarrow X''\Sigma$	10,826.6
Bengtsson's U. V. System	$D'\pi \rightarrow A'\pi$	3,134.0
Harvey and Bell's U. V. System	$C'\Sigma \rightarrow A'\pi$	3,363.7
Lagervist's System	$B'\Sigma \rightarrow A'\pi$	8,358.

Note that there are additional bands in the UV which are not specifically mentioned in the systems of either Bengtsson or Harvey and Bell, both of which are considered to be somewhat doubtful groupings.

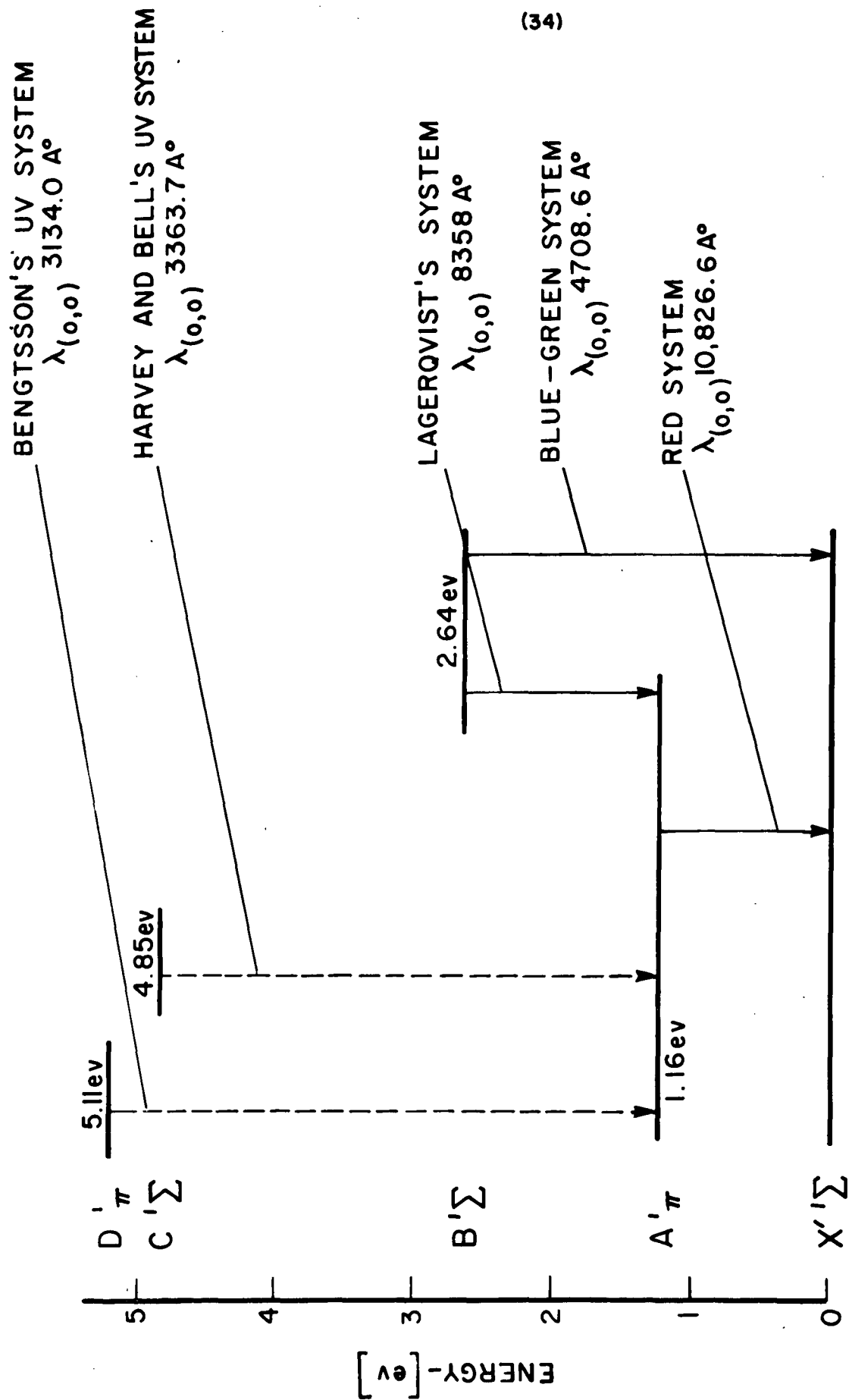


FIGURE 7

b. Magnesium Oxide

Until a few years ago there were only two band systems of magnesium oxide which had been analyzed. These were the red and green systems, both of which have been assigned to transitions between singlet states of the diatomic oxide MgO.

Other bands in the UV were ascribed to an oxide of magnesium, but the complexity of these bands was taken as an indication that they were due either to transitions between triplet states of the diatomic oxide or that the emitter was either polyatomic or polymeric.

Brewer and Trajmar (27) and Brewer, Trajmar and Berg (32) showed that some of these UV bands belonged to a system which they assigned to a transition between singlet states of the diatomic oxide, i.e., $C'\Sigma \rightarrow A'\pi$ for MgO. They also presented evidence (27) that the emitter of the UV bands was not polyatomic. Based on mass action measurements they concluded "that no substantial portion of either the oxide or hydroxide bands can be due to a polyatomic molecule with more than one magnesium or one oxygen per molecule." Additional evidence of only one oxygen atom in the oxide is provided by the oxygen isotope substitution experiments of Pesic (33).

Still another band system in the UV assigned to transitions between singlet states of the diatomic oxide ($D'\Delta \rightarrow A'\pi$) was found by Trajmar and Ewing (34,35).

These two new systems accounted for some but not all of the UV bands ascribed to the oxide.

The possibility that these two new systems are not really due to transitions between singlet states has been proposed recently by Green (36). Based on the near equality of spectroscopic constants, there is the possibility that the $C'\Sigma^-$ and $D'\Delta$ states are not singlets, but might be components of a triplet. Green presents considerable discussion about this point and experimental attempts to answer the difficulty. The question is not fully resolved.

Brewer and Trajmar (27) have made estimates of the energies of the unknown levels of MgO. They indicate that any triplet transitions would occur either in the infrared or in the UV at wavelengths shorter than 4000 \AA° with the possible exception of a $^3\Pi \rightarrow ^3\Sigma^-$ transition, whose position is uncertain, but which might possibly occur in the visible.

In view of the prediction of low-lying triplet states for MgO (27,28), Green (36) searched the near UV and visible regions of the spectrum ($2400 \rightarrow 6500 \text{ \AA}^\circ$) for other bands due to the oxide. His results, and suggested emitters, are as summarized below:

A band system in the region from 3672 to 3688 \AA° is proposed to be due to MgO.

A second weaker band system in the region from 3637 to 3647 \AA° is probably due to an emitter other than MgO.

The strong band heads at 3720.6 , 3721.0 and 3721.4 \AA° are thought to be due to MgO. Pesic's work (33) indicates that the emitter contains one oxygen atom.

There is an additional series of bands which are present in the region from 2600 to 2800 \AA . It is not certain which emitter is responsible for these bands.

The analyzed spectroscopic states, the transitions and the wavelength of the (0,0) band for the systems of MgO, as well as the bands attributed to a magnesium oxide specie, are summarized in Table 3.

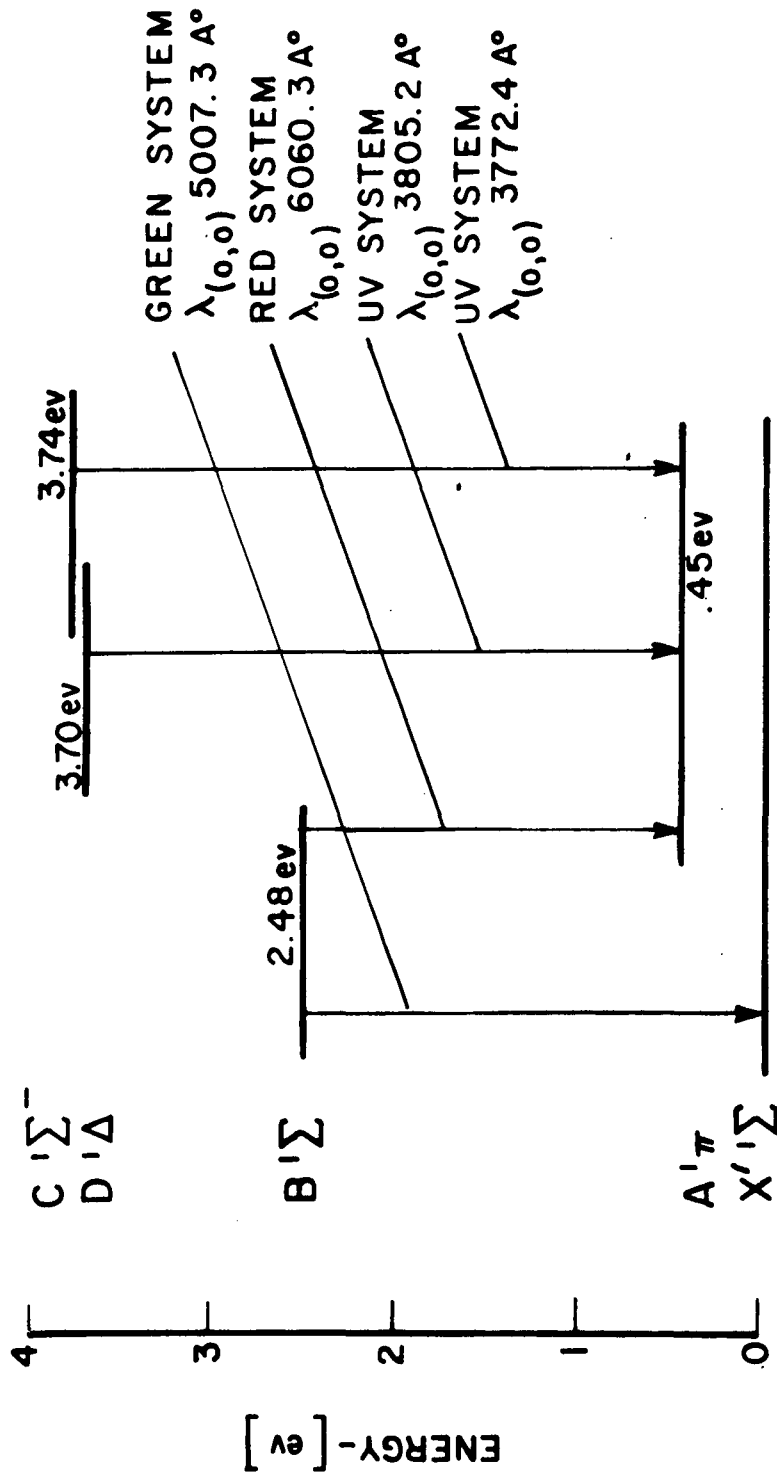
An energy level diagram illustrating the transitions is provided in Figure 8.

TABLE 3
BAND SYSTEMS OF MAGNESIUM OXIDE

<u>MgO</u>		<u>$\lambda(0,0) \text{ \AA}$</u>
Red System	$B'\Sigma \rightarrow A'\pi$	6060.3
Green System	$B'\Sigma \rightarrow X'\Sigma$	5007.3
UV System	$C'\Sigma^- \rightarrow A'\pi$	3773.5
UV System	$D'\Delta \rightarrow A'\pi$	3806.3

<u>Other Bands</u>	<u>Emitter</u>
System at 3672 to 3688 \AA	probably MgO
System at 3637 to 3647 \AA	probably not MgO
Bands at 3720.6, 3721.0, 3721.4 \AA	probably MgO
Bands from 2600 to 2800 \AA	emitter uncertain

Note that there are still weak features in the complex UV part of the spectrum that are unassigned. The complicating effects of MgOH bands in this region increase the problems of analysis.



ENERGY LEVEL DIAGRAM FOR MgO

FIGURE 8

c. Calcium Oxide

There are three band systems in the visible and near UV regions of the spectrum that have been assigned to the diatomic oxide CaO . These systems are the extreme red, blue and UV systems and all correspond to transitions between singlet states. It was recently shown by Hauge (37) that the additional bands in the near infra-red are a part of the extreme red system mentioned above and do not constitute a fourth band system.

In addition to these analyzed band systems there are also strong band systems in the green and orange regions of the spectrum that have been shown to be due to the oxide (25), (although other bands in the same region belong to the hydroxide CaOH) but have not been analyzed because of their complexity. It is suggested (29, 30) that the complexity may be due to a polyatomic oxide such as Ca_2O_2 . Recent oxygen isotope substitution experiments by Hauge (37) on green and orange band systems observed in an arc between calcium electrodes have not resolved the confusion. The emitter of the green bands which Hauge observed, very likely contains only one oxygen per molecule but there is the possibility that CaOH was the emitter in these experiments since extensive efforts were not taken to eliminate water. The wavelengths of the band heads observed by Hauge correspond to the wavelengths attributed to CaOH by Gaydon (25) in his hydrogen-deuterium substitution experiments. Hauge observed the presence of CaH bands, which indicate that some hydrogen was present in his experiments.

In the case of the orange band system, Hauge did not observe an isotopic shift, thus it was either too small to be measured or oxygen is not contained in the emitter.

It is obvious that the identity of the emitter of the orange and green band systems attributed to calcium oxide is still largely unresolved.

The known states of CaO, the transitions that have been analyzed and the wavelength of the (0,0) band for each transition is summarized in Table 4. An energy level diagram illustrating the known states and transitions is provided in Figure 9.

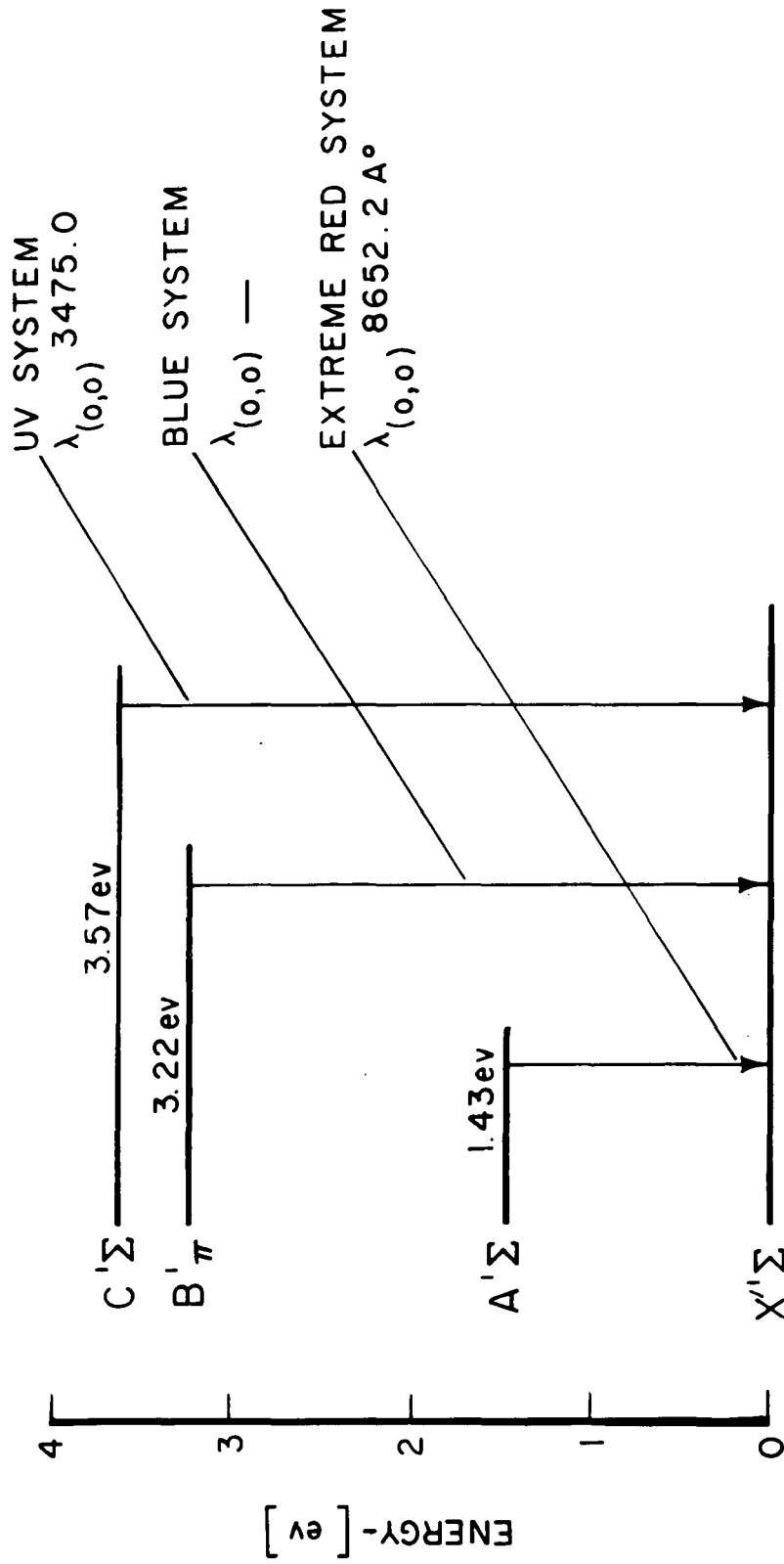
TABLE 4
BAND SYSTEMS OF CALCIUM OXIDE

<u>CaO</u>		<u>$\lambda(0,0)$ [A°]</u>
Extreme Red System	$A'\Sigma \rightarrow X'\Sigma$	8652.2
Blue System	$B'\Pi \rightarrow X'\Sigma$?
UV System	$C'\Sigma \rightarrow X'\Sigma$	3475.0
<u>Other Bands</u>		

The green and orange band systems that have been assigned to calcium oxide (other bands in these same regions belong to the hydroxide) have not been analyzed because of their complexity. It is possible that they correspond to transitions between triplet states of the diatomic oxide, or that the emitter is polyatomic or polymeric.

d. Strontium Oxide

The three band systems that have been analyzed have all been assigned to transitions between singlet states

ENERGY LEVEL DIAGRAM FOR CaO

of the diatomic oxide, SrO.

In addition there are bands located in the orange and red regions of the spectrum near 5950 \AA° and 6050 \AA° and in the region between 6400 and 6850 \AA° that have not been analyzed. It has been suggested that a polyatomic oxide may be the emitter of these bands.

Isotope substitution experiments and other techniques often used to identify the nature of the emitter have apparently not been applied to these band systems as was done for both magnesium and calcium oxides.

The known states of SrO, the transitions that have been analyzed and the wavelength of the (0,0) band for these systems have been summarized in Table 5.

Figure 10 is an energy level diagram for SrO.

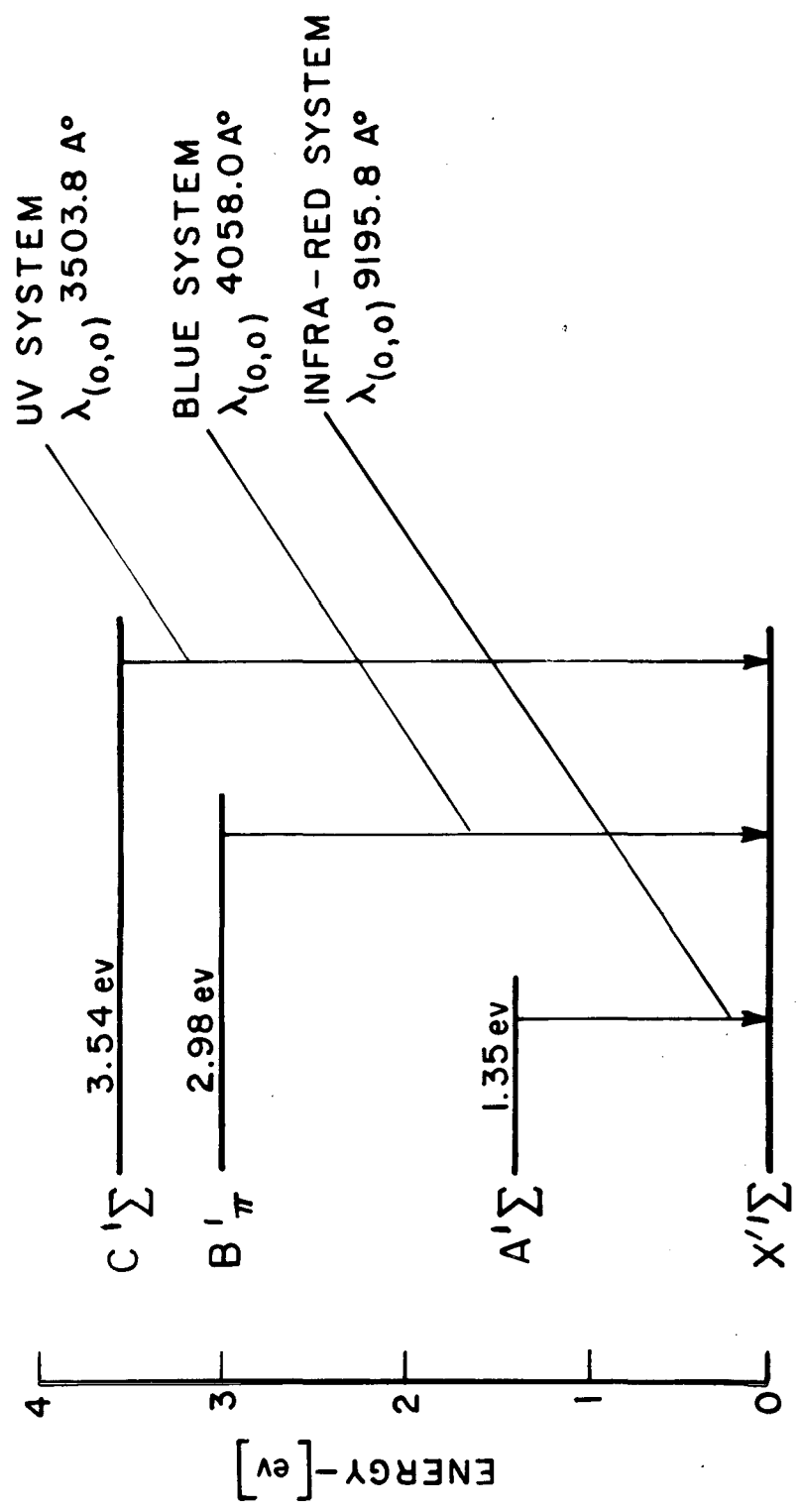
TABLE 5

BAND SYSTEMS OF STRONTIUM OXIDE

<u>SrO</u>		<u>$\lambda (0,0) [\text{\AA}^\circ]$</u>
Infra-Red System	$A' \Sigma \rightarrow X' \Sigma$	9195.8
Blue System	$B' \pi \rightarrow X' \Sigma$	4058.0
UV System	$C' \Sigma \rightarrow X' \Sigma$	3503.8

Other Bands

Other unanalyzed bands attributed to the oxide occur near 5950 \AA° and 6050 \AA° and between 6400 and 6850 \AA° . These bands may be due to a polyatomic oxide. Note that there are also hydroxide bands (SrOH) in most of the spectral regions in which these unanalyzed bands are formed.



ENERGY LEVEL DIAGRAM FOR SrO

FIGURE 10

e. Barium Oxide

There is one extensive band system in the visible region of the spectrum that has been assigned to a transition between singlet states of the diatomic oxide, BaO. The recent work of Wharton, Kaufman and Klemperer (38) and Wharton and Klemperer (39) in molecular-beam studies has shown that the lower state ($X'^1\Sigma$) involved in this analyzed band system is the ground state of BaO and that there are no other states within 4000 cm^{-1} of this state.

Other more complex bands attributed to the oxide near 4800, 5020, 5500 \AA° and in the infra-red have not been analyzed and may be due to a polyatomic oxide. Once again, isotope substitution experiments have apparently not been used for these bands as was the case for magnesium oxide and calcium oxide.

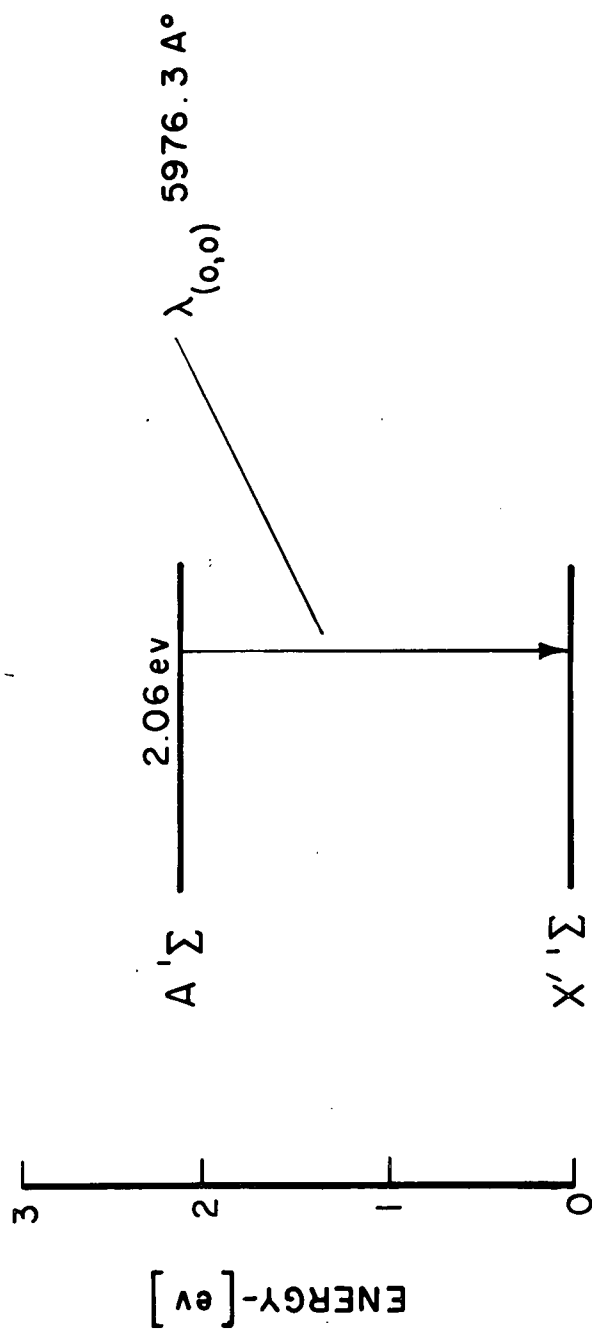
Table 6 summarizes the spectral data for barium oxide and Figure 11 is an energy level diagram for the known system of BaO.

TABLE 6BAND SYSTEMS OF BARIUM OXIDE

<u>BaO</u>		<u>$\lambda(0,0) [\text{\AA}^\circ]$</u>
Extensive System in the Visible	$A'\Sigma \rightarrow X'^1\Sigma$	5976.3

Other Bands

Other bands attributed to the oxide are found near 4800, 5020, 5550 \AA° and in the infra-red. The emitter may be a polyatomic oxide. Note that bands due to the hydroxide are found in the same spectral regions as these unanalyzed oxide bands.



ENERGY LEVEL DIAGRAM FOR BaO

2. Ground Electronic States and the Possibility of Low-Lying Triplet States for the Alkaline-Earth Oxides

In the previous section of this chapter it was pointed out that in many cases the lowest observed electronic level may not be the ground state for the alkaline-earth oxide molecules. (To indicate this uncertainty a prime will be used in the spectroscopic notation, e.g. $X'\Sigma$ rather than $X'\Sigma$.) A knowledge of the nature of the ground state and also of other low-lying states is a requisite if one intends to calculate thermochemical data for these species or analyze presently unknown band systems. In the case of the oxides of interest, the existence of a triplet ground state or of low-lying triplet states would strongly influence the calculations due to the statistical weight of these triplet states in the partition function. Whereas, the lowest observed $^1\Sigma$ states have a statistical weight of 1, a $^3\Sigma$ or $^3\Pi$ state would have a statistical weight of 3 or 6 respectively. The presence of low-lying $^3\Sigma$ and $^3\Pi$ states is predicted for these alkaline-earth oxides, but as stated in the earlier section of this chapter, no triplet states have yet been observed experimentally for any of these oxides.

In general, if the ground state of a diatomic molecule is known, it is possible to obtain the dissociation energy directly by means of a Birge-Sponer extrapolation. However, for the case of the diatomic alkaline-earth oxides a Birge-Sponer extrapolation is probably not suitable since these molecules exhibit a high degree of ionic bonding (24). Table 7 illustrates the wide discrepancy between Birge-Sponer extrapolations for the lowest observed electronic levels and a recommended value

for the dissociation energy taking into account spectroscopic, thermochemical cycle, and direct experimental values (24).

TABLE 7

DISSOCIATION ENERGIES OF THE ALKALINE-EARTH OXIDES

	Birge-Sponer Extrapolation		Recommended Values Ref (24)	
BeO	111	(kcal/mole)	101.5 $^1\Sigma$	(kcal/mole)
			96.7 $^3\Sigma$	(kcal/mole)
MgO	39	(kcal/mole)	82 $^3\Sigma$	(kcal/mole)
CaO	37	(kcal/mole)	87 $^3\Sigma$	(kcal/mole)
SrO	35	(kcal/mole)	95 $^3\Sigma$	(kcal/mole)
BaO	127	(kcal/mole)	125.0 $^3\Pi$	(kcal/mole)

a. Beryllium Oxide

For BeO it appears that the ground state is $X'^1\Sigma$. The Birge-Sponer extrapolation for the dissociation energy agrees reasonably well with the value determined from thermal studies. The recent calculations of Verhaegen and Richards (40) indicate a $^1\Sigma$ ground state. They also show that the lowest lying excited state, a $^3\Pi$, lies sufficiently high above the $^1\Sigma$ state so that there is very little contribution from the $^3\Pi$ state to the electronic partition function. The conclusion of Verhaegen and Richards is not in agreement with the statements of Brewer and Trajmar (27) who indicate that the $^3\Pi$ state for BeO should be the major contributor to the thermodynamic functions at high temperatures. The statement by Brewer and Trajmar is based on a semi-empirical method,

the application of molecular orbital correlations to predict the low-lying electronic states (41). The approximate spacing of the energy levels in BeO is obtained by a comparison with the spacing in C_2 . On this basis it is expected that the $^3\Pi$ state would lie slightly above the $X'\Sigma$ state for BeO, but that for the purposes of high-temperature thermodynamic properties one should assume a $^3\Pi$ ground state.

Kaufman (26) also suggests that the $X''\Sigma$ state is the ground state for BeO, pointing out that in addition to the agreement found between the dissociation energies determined by spectroscopic and thermal studies, there have been no perturbations observed in the lower vibrational energies of $X'\Sigma$.

b. Magnesium Oxide

Of all the alkaline-earth oxides, it appears that if a triplet state is the ground state, it will be so for the case of magnesium oxide. The previous section illustrated that for BeO most of the evidence pointed to an $X'\Sigma$ ground state. As will be shown in the following sections, the strong experimental evidence of Wharton et al (38) and Kaufman et al (26) for BaO and SrO respectively, indicate that $X'\Sigma$ is almost certainly the ground state. Since the energy levels of CaO and SrO are almost identical, Kaufman et al (26) indicate that $X'\Sigma$ should also be the ground state for CaO. This leaves only MgO as a likely possibility for a triplet ground state.

The molecular orbital correlations of Brewer and Trajmar (27) indicate that the $^3\Pi$ state for MgO would lie slightly below the $X'\Sigma$ state for MgO, whereas for BeO they had predicted the $^3\Pi$ state would be slightly higher than the $X'\Sigma$. In any case they state that for the purpose of calculating thermodynamic properties at high temperature, one should assume a $^3\Pi$ ground state.

The calculations of Richards, Verhaegen and Moser (28) for MgO, similar to those performed by Verhaegen and Richards (40) for BeO, do not agree with Brewer and Trajmar's indication of a $^3\Pi$ ground state for MgO, although it is pointed out that the triplet levels lie close enough to $X'\Sigma$ to influence the partition function. The calculations (28) indicate a $^1\Sigma$ ground state with $^3\Pi$ and $^3\Sigma$ levels as close as 0.3 eV to the ground state. The effect of these low-lying triplet levels changes the partition function by almost a factor of three. The correction to the dissociation energy reported by Drowart et al (42) amounts to a decrease in the value by 4.5 kcal/mole.

Kaufman et al (26) report that the three studies (43, 44, 45) which show that $X'\Sigma$ is not the ground state are of doubtful value for the following reasons: part of the emission in the experiments of Brewer and Porter (43) was later shown to be due MgOH; Bulewicz and Sugden (44) "somewhat arbitrarily used only the high-temperature limit of their data"; the thermochemistry of the system used by Thrush (45) was not well known, and "the spectra were not actually

identified with a triplet system as Thrush claims". The transpiration study of MgO by Alexander, Ogden and Levy (46) concludes that $X'\Sigma$ is the ground state. Thus, Kaufman et al (26) conclude that the question of the ground state is still unanswered.

Schofield (24) considers that the ground state is probably a triplet, and that $X''\Sigma$ lies about 20 or 30 kcal above this unknown ground state, rather than the 50 kcal suggested in other work (43, 44).

c. Calcium Oxide

The known states of CaO are very similar to those of SrO and the evidence presented to show that $X'\Sigma$ is not the ground state is almost exactly the same in both cases. On the basis of their strong evidence that $X'\Sigma$ is the ground state for SrO, Kaufman et al (26) suggest that it is likely that CaO has $X'\Sigma$ as a ground state also. They indicate that the flame studies of Huldt and Lagerqvist (47) are subject to question because of the possibility of such species as SrOH and CaOH in the flames. These flame studies (47) would place $X''\Sigma$ $18,000\text{ cm}^{-1}$ (2.2eV) above the ground state.

Schofield (24) indicates that the dihydroxides, e.g. $\text{Ca}(\text{OH})_2$, must also be considered and, in fact, except at very high temperatures and in flames of very low water vapor content, the dihydroxide will be more important than the hydroxide (48).

However, for $\text{Ca}(\text{OH})_2$, no thermodynamic data are available and the flame results cannot be corrected. The result is that the dissociation energy determined from hydrogen

containing flames is an upper limit value only (24).

Hollander et al (49, 50) attempted to verify the importance of small amounts of water vapor by performing their flame studies in both "dry" and "moist" flames. Their conclusion was that the dissociation energy was not measurably influenced by the presence of hydrogen.

On the other hand, Schofield (24) indicates that the methods used by Hollander et al are "very susceptible" to the formation of small amounts of dihydroxide, and that in the case of BaO (for which the data for $\text{Ba}(\text{OH})_2$ can be applied) one should find a difference of 9 kcal/mole in the dry and moist flames. Although this was the situation in one case, it did not appear that CaO and SrO results showed any effect. The implication that the dihydroxide formation in the flames of these last two metals is less important, is not in agreement with the conclusions reached by Schofield (24) from two other flame studies (51, 48).

As was reported in the earlier sections for BeO and MgO, Brewer and Trajmar (27) estimated the position of the unknown but expected low-lying triplet level $^3\Pi$ from a knowledge of the energy level of the $^1\Pi$ state which results from the same molecular configuration. The splitting between the $^1\Pi$ and $^3\Pi$ states was expected to vary little in going from C_2 to BeO and MgO and in this way, the approximate position of the $^3\Pi$ state could be located. In the case of CaO the low-lying $^1\Pi$ level has not been experimentally determined. Hauge (37) presents some evidence which gives a lower limit

for the spacing between the $X'\Sigma$ and the ${}^1\Pi$ states. Since no perturbations were found in the $X'\Sigma$ up to $v''=8$, (and it is expected that the $X'\Sigma$ and ${}^1\Pi$ state would perturb one another) the ${}^1\Pi$ state may lie higher than 5500 cm^{-1} (.68eV) above the $X'\Sigma$. Hauge indicates that this conclusion should be accepted with some reservation.

d. Strontium Oxide

Kaufman et al (26) indicate that the $X'\Sigma$ state is "almost certainly the ground electronic state of SrO ". Their molecular-beam magnetic deflection experimental results lead to the conclusion that the $X'\Sigma$ state is certainly not $13,000\text{ cm}^{-1}$ (1.6eV) above the ground state as is indicated by flame studies (47).

The discussion of the flame studies of Huldt and Lagerqvist (47) and of Hollander et al (49, 50) would lead to the same conclusions as reached in the previous section for CaO , namely that the possible formation of the hydroxide and dihydroxide could seriously alter the results.

e. Barium Oxide

For BaO it appears that the ground state is $X'\Sigma$ based on the experimental evidence of Wharton et al (38). This molecular-beam experiment indicates that the lowest observed electronic level " $X'\Sigma$ " is the ground state of BaO and that there are no other states within 4000 cm^{-1} (.495eV) of this state" (26).

Also for BaO , the dissociation energy determined from Birge-Sponer extrapolations agrees well with that de-

terminated from thermal studies (26).

Schofield (24) indicates that the results of molecular-beam experiments referred to above along with the fact that rotational perturbations are not observed in the $X'\Sigma$ state tended to confirm this state as the ground state. He points out however that the recent experiments of Newbury (52) required an electronic statistical weight of 10 rather than 1 ($^1\Sigma$) to remove discrepancies in the data.

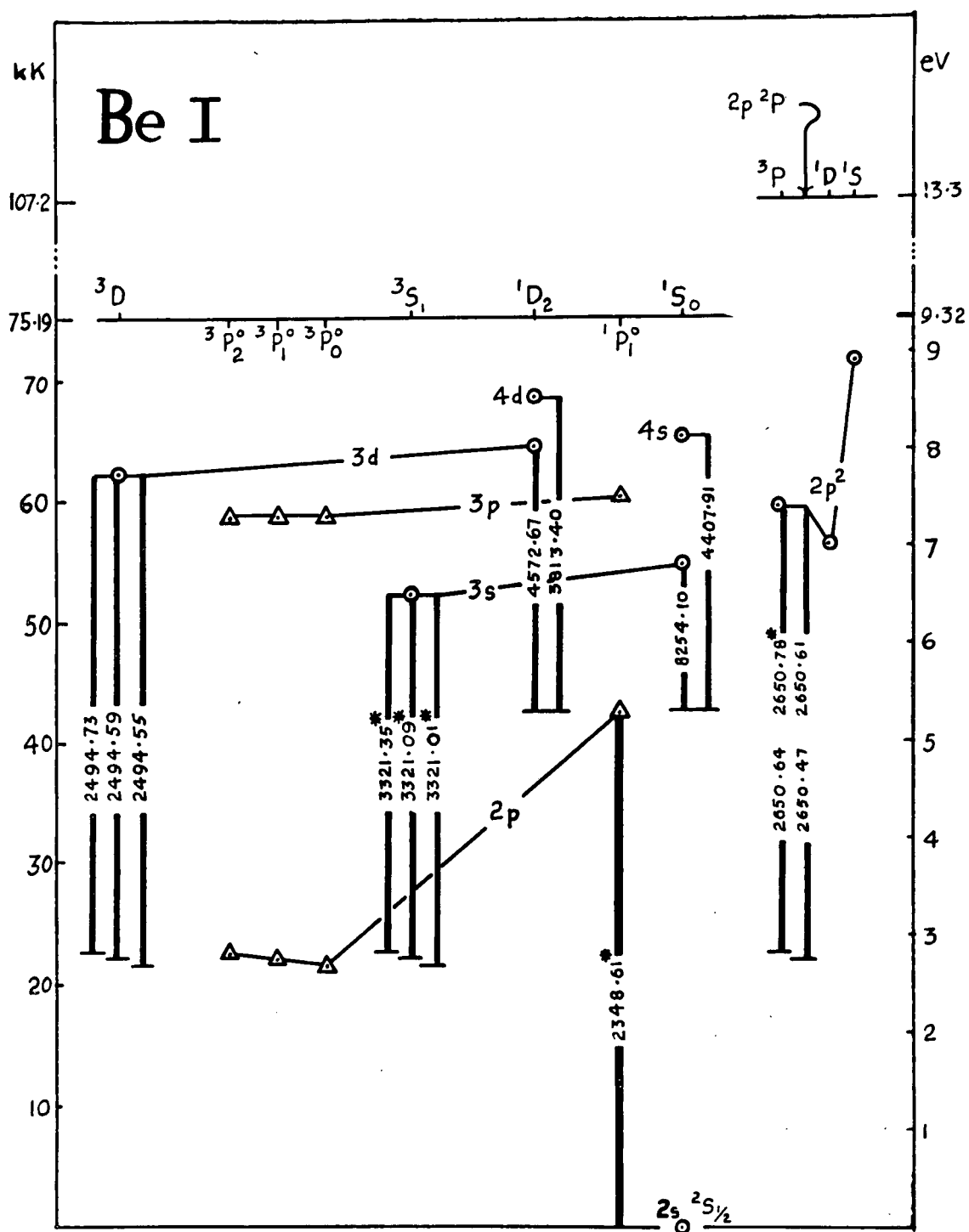
Summary

Considering all the evidence regarding the identity of the electronic ground state for the alkaline-earth oxides, it is clear that the issue is not fully resolved. In the case of BeO and MgO, although the ground states may indeed be the $X'\Sigma$ states, triplet states are expected to lie very close to the ground state. The conclusions of Kaufman et al (26), that $X'\Sigma$ is the ground state for BaO and SrO, are supported by convincing experimental evidence. The strong similarities between the energy level diagrams of CaO and SrO indicate the likelihood that $X'\Sigma$ is the ground state for CaO also.

3. Energy Level Diagrams for the Alkaline-Earth Metals and Atomic Oxygen

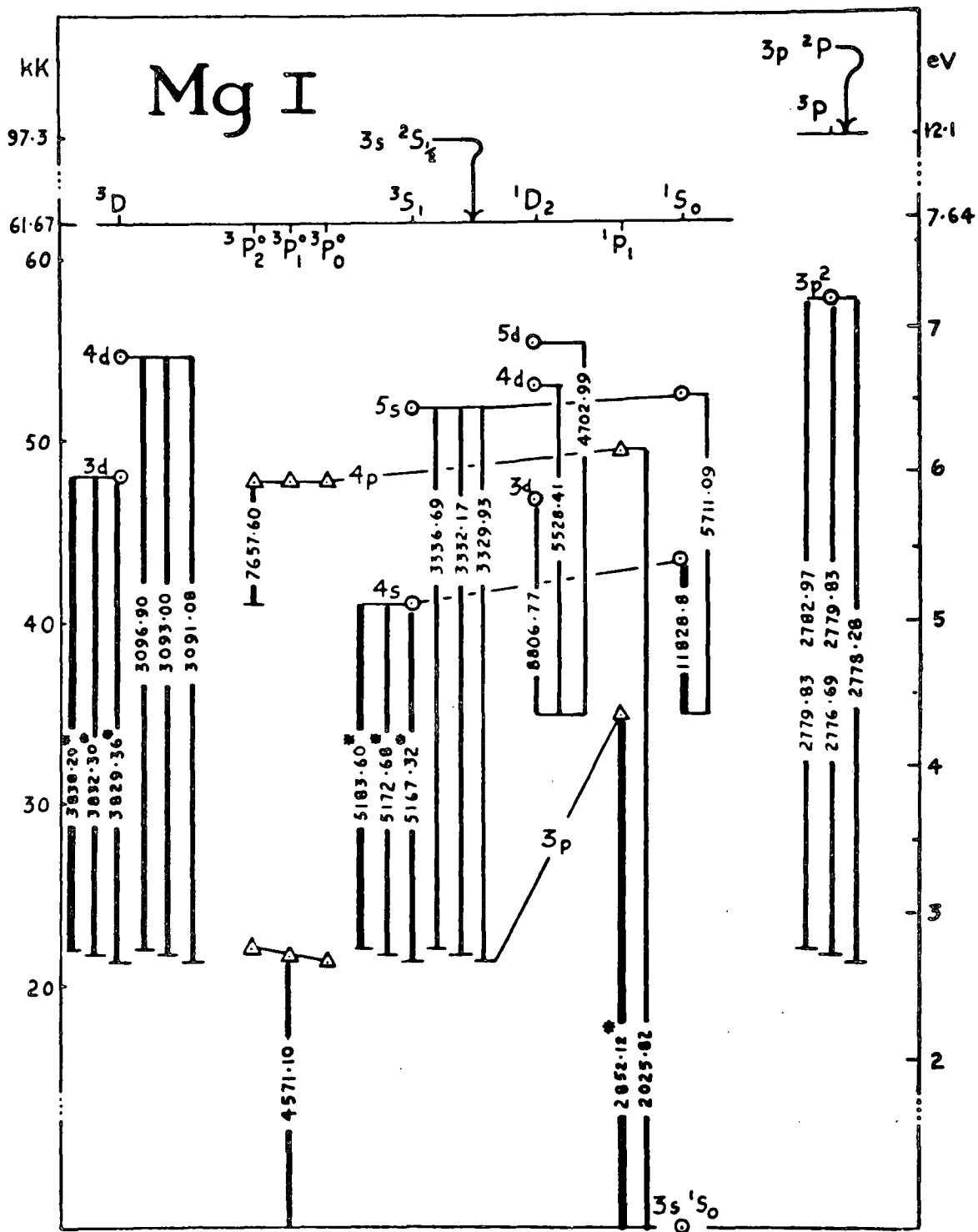
To complete the spectroscopic data presented in this chapter, energy level diagrams of the alkaline-earth metals and of atomic oxygen are reproduced in Figures 12 - 17. The information contained in these figures will be required in

the discussion of the spectroscopic observations reported in Chapter V, but for convenience, the figures have been placed in this chapter with the spectroscopic data for the oxides.



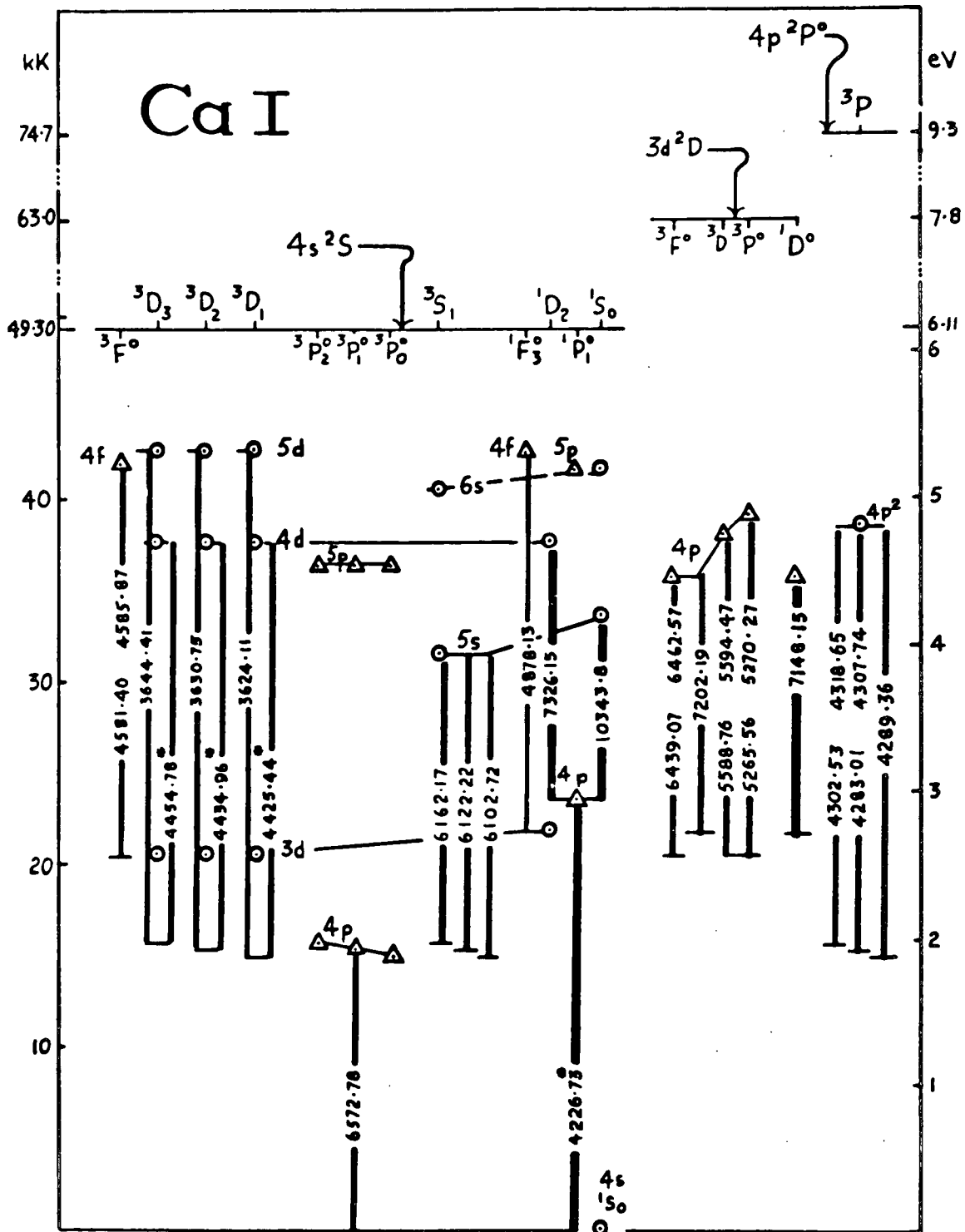
From Candler's ATOMIC SPECTRA AND THE VECTOR MODEL
 Copyright 1964, D. Van Nostrand Company, Inc.
 Princeton, New Jersey 08540

FIGURE 12



From Candler's ATOMIC SPECTRA AND THE VECTOR MODEL
Copyright 1964, D. Van Nostrand Company, Inc.
Princeton, New Jersey 08540

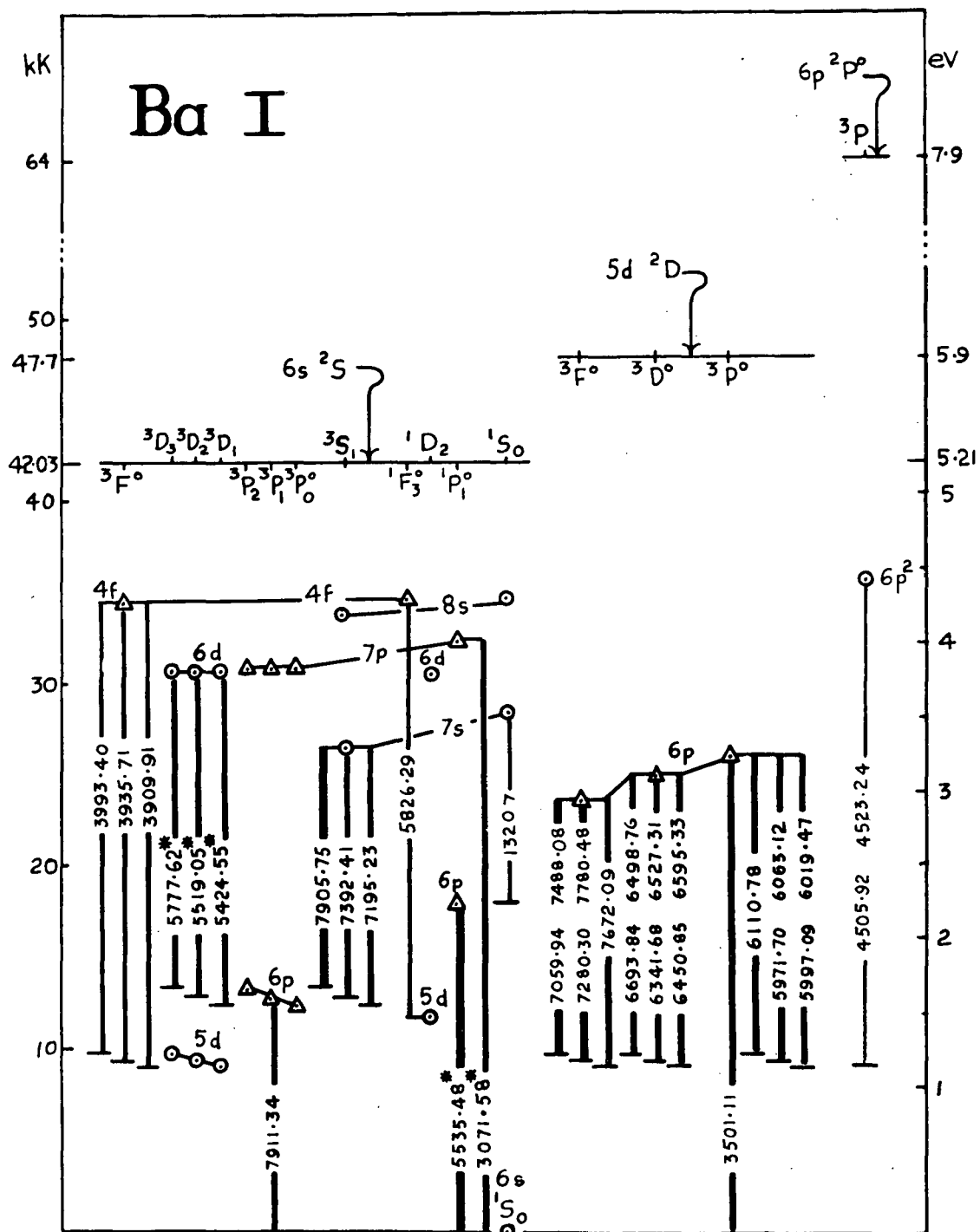
FIGURE 13



From Candler's ATOMIC SPECTRA AND THE VECTOR MODEL
Copyright 1964, D. Van Nostrand Company, Inc.
Princeton, New Jersey 08540

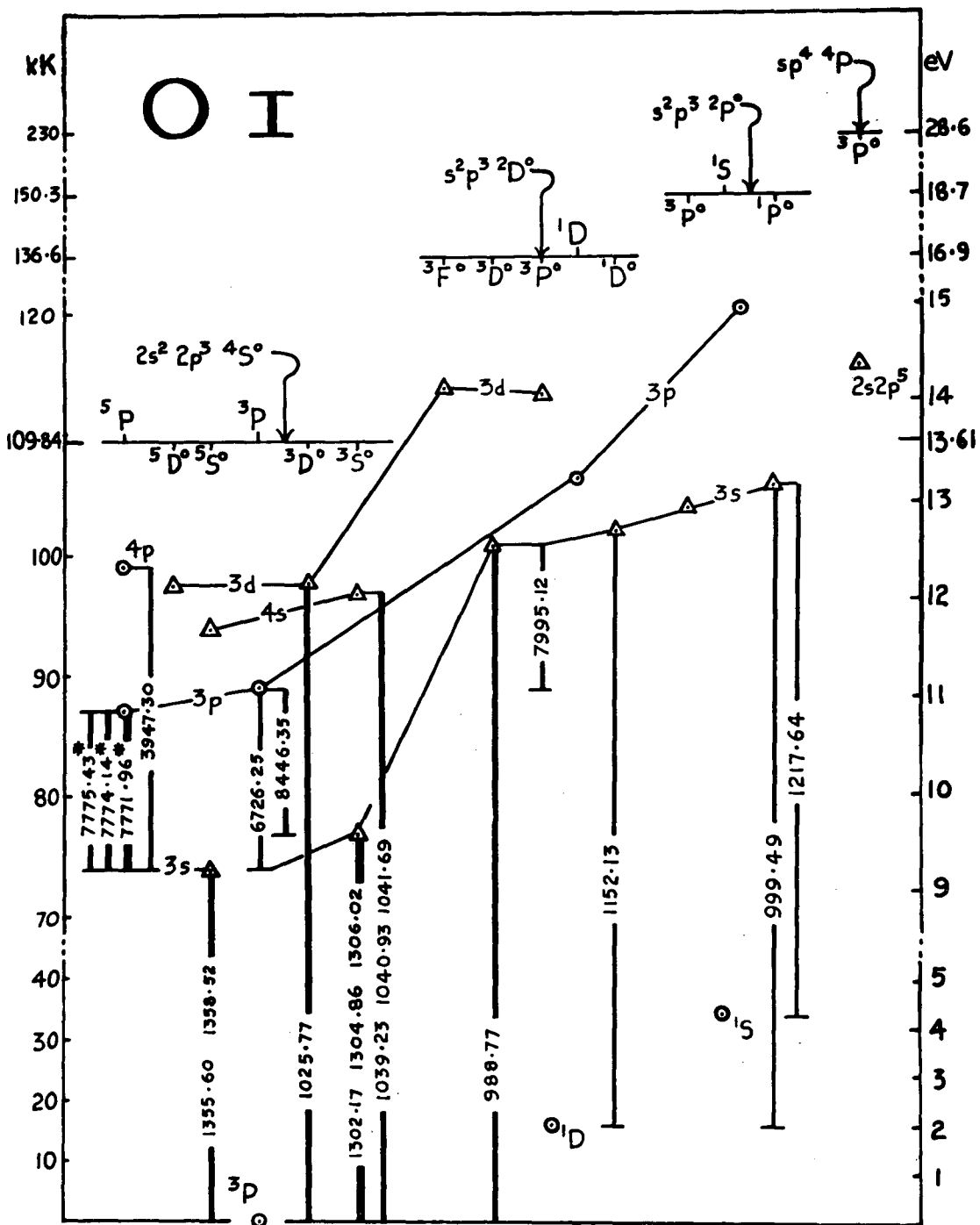
FIGURE 14

FIGURE 15



From Candler's ATOMIC SPECTRA AND THE VECTOR MODEL
 Copyright 1964, D. Van Nostrand Company, Inc.
 Princeton, New Jersey 08540

FIGURE 16



From Candler's ATOMIC SPECTRA AND THE VECTOR MODEL
Copyright 1964, D. Van Nostrand Company, Inc.
Princeton, New Jersey 08540

FIGURE 17

CHAPTER IV - EXPERIMENTAL APPARATUS AND PROCEDURE

In the experiments performed to determine the flame structure of the alkaline-earth metal-oxygen flames, two different experiments were performed. The present chapter is a description of the apparatus and procedure for these two experiments, namely, the wire-burning experiments and the two-dimensional diffusion flame burner experiments.

The first part of this chapter outlines the materials used in these studies. The following section contains a description of the wire-burning apparatus, the procedure used in the wire-burning studies and the associated diagnostic equipment. The last part of the chapter describes the two-dimensional diffusion flame burner which was originally designed for spectroscopic studies of hydrocarbon flames (6, 53), but which has been adapted to metal combustion studies in this work.

1. Materials

a. Gases

All of the experiments to be described in the following chapter were performed in atmospheres of oxygen and argon, with the exception of the few tests performed to assess the effects of water vapor. Gases were obtained from the Liquid Carbonic Division of General Dynamics. The gases used were of commercial purity. Typical analyses for these gases are listed in Table 8.

TABLE 8
TYPICAL GAS ANALYSES

Argon	99.998%
N_2	less than 10 ppm
O_2	less than 10 ppm
H_2	less than 5 ppm
Oxygen	99.5%
$N_2 + H_2$	less than 5000 ppm
H_2O	less than 11 ppm

In all of the wire burning experiments and in about half of the burner experiments, the desired mixture of oxygen and argon was prepared for one day's experiments in a mixing chamber charged to a total pressure of 2 atmospheres. Mixing was by diffusion.

In other burner experiments the oxygen-argon mixture was a commercially prepared mixture supplied by The Matheson Company, Inc. The oxygen used in these mixtures was ultra-high purity grade. The oxygen purity for this grade is 99.95% minimum. The argon in these mixtures was high purity grade with a purity of 99.995% minimum.

All of the experiments were carried out at sub-atmospheric pressures. Most of the wire experiments were performed at 50 torr with a few experiments carried out over the range from about 1 torr to 760 torr. Most of the experiments performed in the two-dimensional diffusion flame burner

were performed at 200 torr.

b. Metal Samples

In the wire-burning experiments the desired sample size was a wire of about 1 mm diameter with a length of about 11 mm. For the metals used in the present investigation the desired sample dimensions were not readily available from suppliers.

Magnesium wire is available in only one size, 0.76 mm dia. In all of the experiments performed by Brzustowski (16, 54), and in some of the experiments performed in the present investigation, magnesium in ribbon form was used. The ribbon, with typical dimensions of 2.9 mm in width and 0.0016 mm. in thickness, was obtained from Baker and Adamson (Code 1901).

Calcium is not available in wire form. Strands of calcium were obtained by cutting narrow strips from a thin sheet of the material. It was possible to obtain strands with quite uniform dimensions, typically 1.0 mm x 1.0 mm x 12 cm. The calcium was obtained from A. D. MacKay Inc. The stated purity of the calcium sheet was 99.0% with the balance largely CaCl_2 . The calcium was shipped and stored in mineral oil. This oil was removed before an experiment either by washing the sample in hexane or in a vapor degreaser using Freon 113 as the fluid. The experiments showed no difference between the two cleaning methods.

Strontium is not available in wire form or in sheet form. Strands of strontium were prepared by pressing rods of

strontium 15.9 mm in diameter to a sheet of approximate thickness 1.25 mm which was then cut into narrow strips to yield strontium strands of approximately square cross-section.

Typical strand dimensions were 1.25 mm x 1.25 mm x 12 cm.

The strontium rods were obtained from A. D. MacKay Inc. The stated purity was 99.0% with Mg, Ca and Ba as the main impurities. The storage in mineral oil and treatment prior to test were the same for strontium as reported above for calcium.

In the burner experiments the sample dimensions were less critical since the metal was vaporized and carried in an inert carrier gas in the experiment. The calcium and strontium burner experiments were performed with the samples as outlined above for the wire-burning experiments. Two or three strands were cut into shorter lengths, typically 2.5 cm., for one burner experiment. The magnesium for the burner experiments was obtained from A. D. MacKay Inc. in the form of rods 3.2 mm. in diameter. These rods were cut into 2.5 cm. lengths. About 10 such lengths of magnesium were used in each experiment. The stated purity of the magnesium was 99.9% +.

2. Wire-burning Apparatus

a. Apparatus Description

The essential features of the wire-burning apparatus used in these experiments are the same as used initially by Brzustowski (16, 54) and more recently by Mellor (5). All of the experiments were performed at sub-atmospheric pressures

and the experiments were carried out in either a bell jar or the combustion chamber pictured in Figure 18. The details of the apparatus are essentially the same for either the bell jar or the combustion chamber.

Figure 19 is a schematic representation of the system showing all parts of the apparatus with the exception of the circuit used to obtain ignition of the wire samples. A schematic of this circuit is shown in Figure 20.

The combustion chamber itself was a vessel designed to operate at pressures up to 20 atmospheres. The dimensions of the vessel were 25 cm. dia., 30 cm. long yielding a volume of 14.7 litres. Quartz observation windows 2.54 cm. in diameter were located in the front and rear sections of the chamber as well as on the horizontal and vertical axes passing through the center of the chamber as pictured in Figure 18. Visual, photographic and spectroscopic observations were made through these quartz windows.

The drying chamber which was used when filling either the mixing chamber or the combustion chamber was a Matheson Model 460 Purifier with a type R cartridge. Dew points of -100°F can be achieved with these cartridges.

The metal samples were mounted between large brass electrodes as indicated in Figure 21. Most of the samples were mounted vertically, as indicated in the photograph, although some of the initial experiments were performed with the sample mounted horizontally. The vertical configuration was found to be more suitable for the space-resolved spectro-

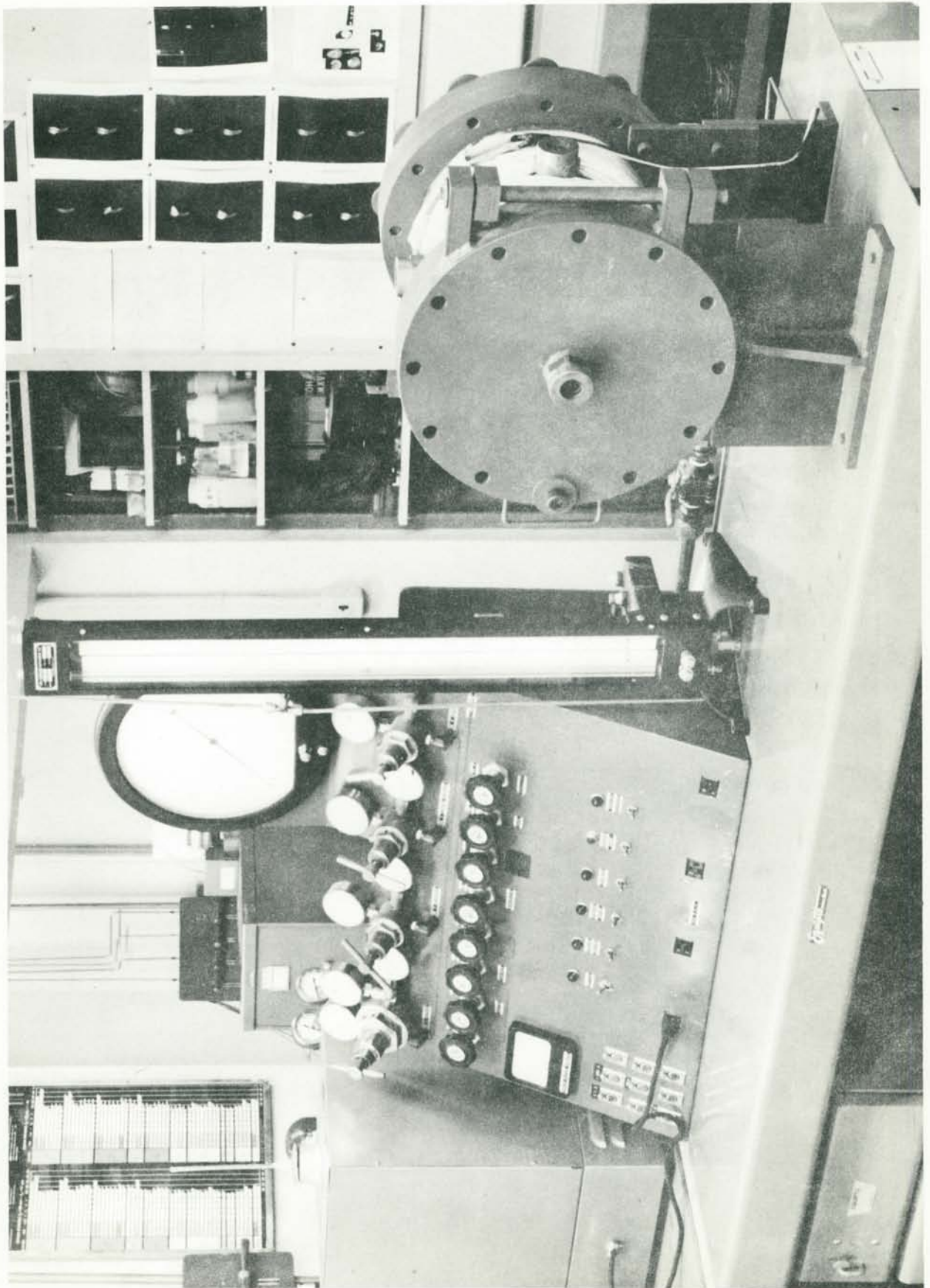
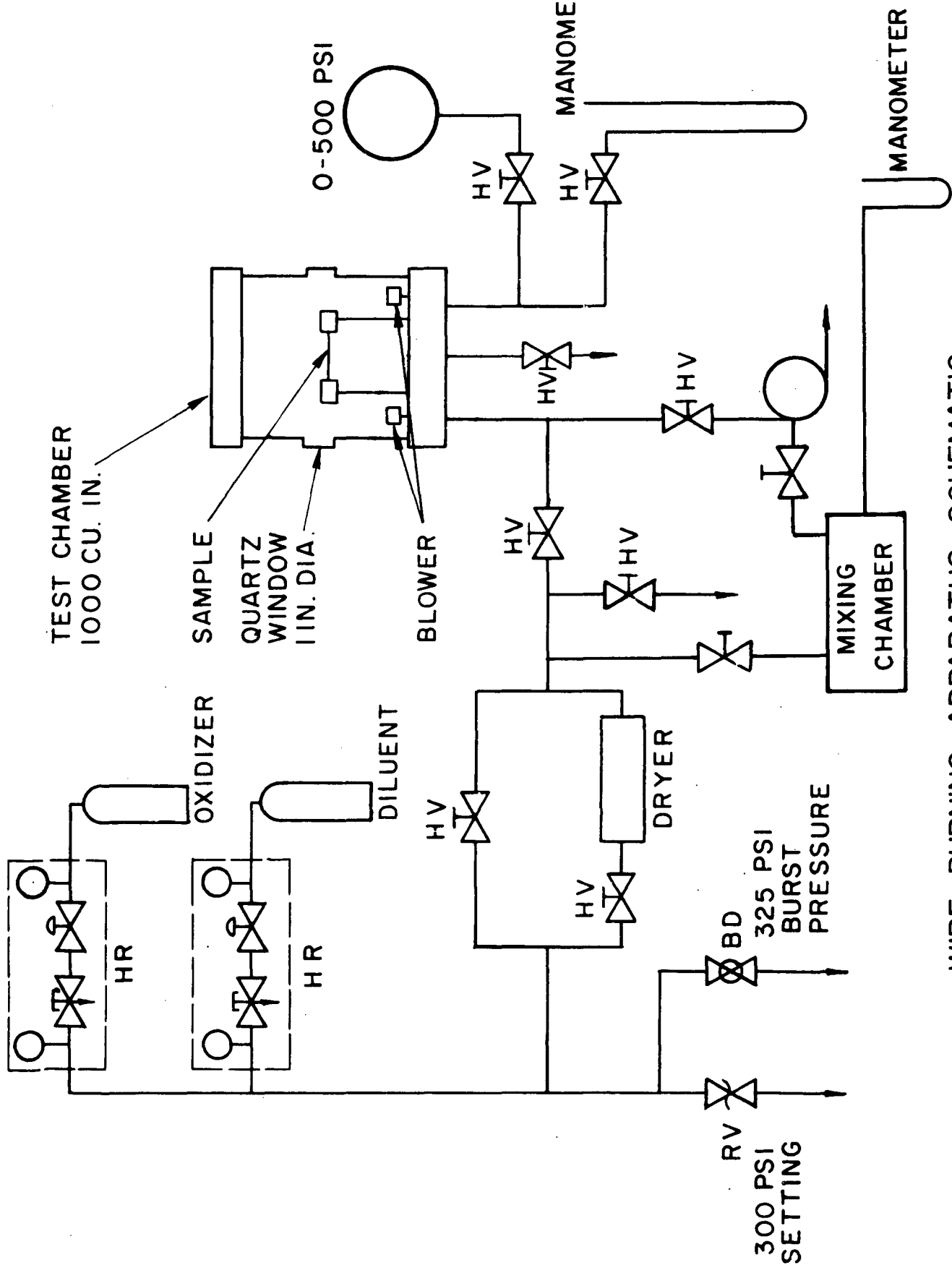


FIGURE 18

(67)

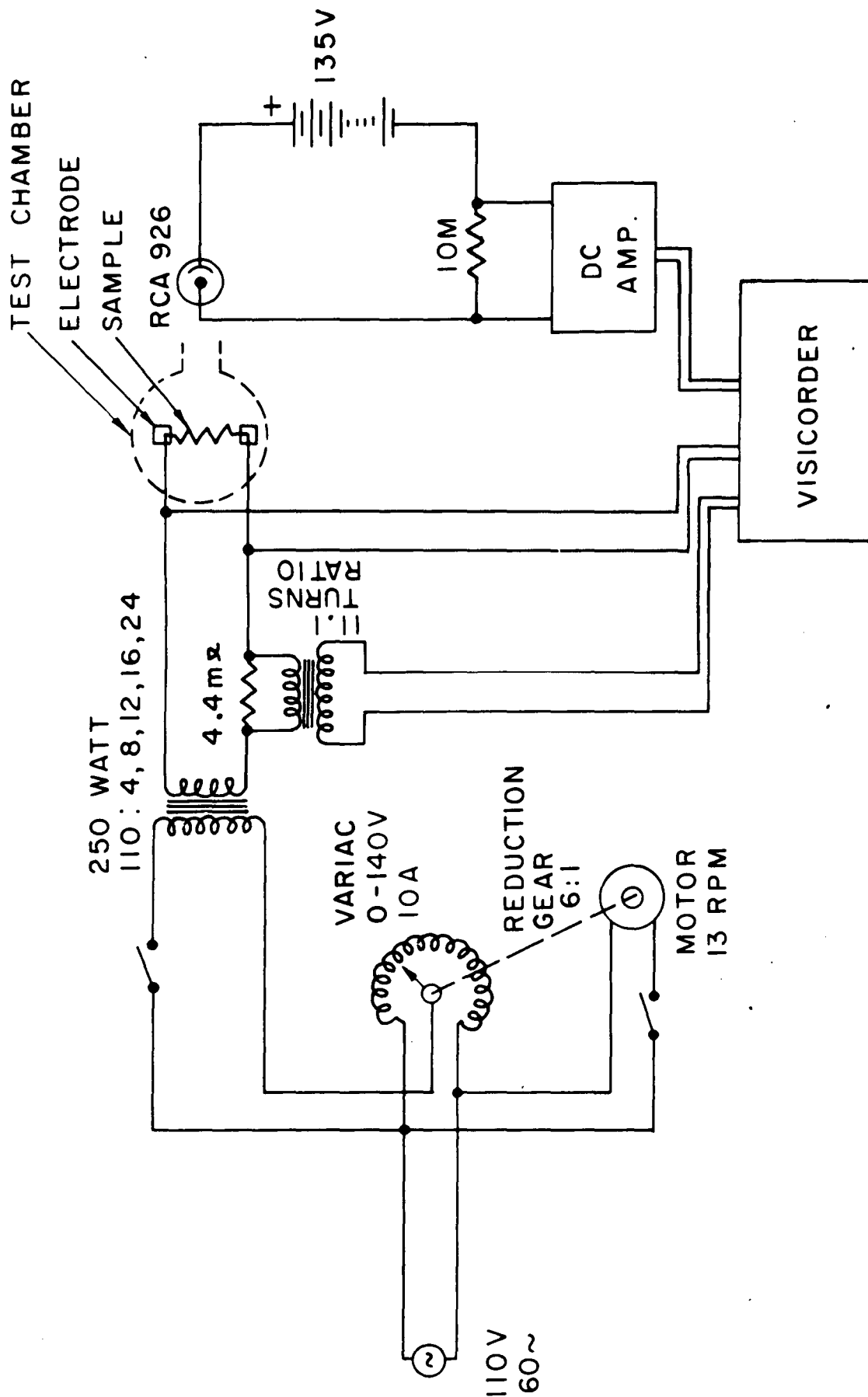


WIRE-BURNING APPARATUS SCHEMATIC

FIGURE 19

JPR 1479c

(68)



ELECTRICAL SCHEMATIC
(WIRE - BURNING APPARATUS)

FIGURE 20

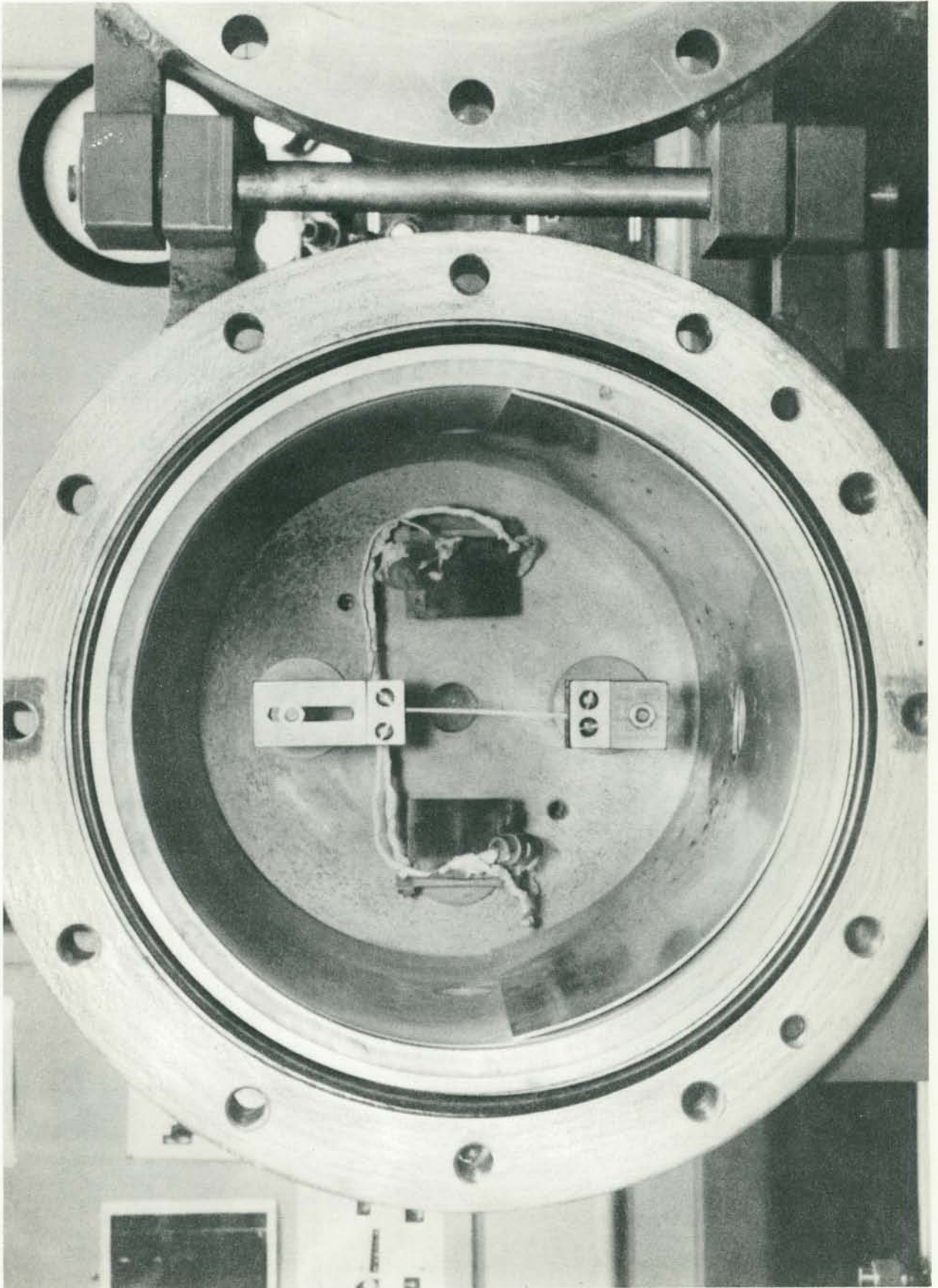


FIGURE 21

scopic experiments.

The wire sample was heated to the point of ignition by applying a voltage to the electrodes that increased linearly with time. This was accomplished by using a motor and reducing gears to rotate the brush on a Variac. Brzustowski (16, 54) reports more details on this method of igniting wire samples.

Although the heating current to the electrodes was not terminated when the sample ignited (unless of course the sample broke at the time of ignition) it was determined by separate tests that this did not appear to affect the flame. Pictures of the flame when the metal sample was still intact showed the same structure as those in which the metal sample had broken and continued to burn at both electrodes.

The voltage, current and light output were all recorded on a Honeywell Model 1206 Visicorder.

b. Procedure

A metal sample of Mg, Ca or Sr (the Ca and Sr samples were cleaned as noted earlier to remove the oil under which they were stored) was mounted between the large brass electrodes as pictured in Figure 21. The chamber was then closed and evacuated to a total pressure of about 100μ . The chamber was then filled with argon and again evacuated to a pressure of about 100μ . This flushing procedure was performed at least once and in many cases twice. The desired atmosphere of oxygen and argon was then admitted to

the chamber either from the mixing chamber, or by mixing in the combustion chamber itself using the component gases argon and oxygen from the gas storage bottles. The blowers mounted in the chamber, which can be seen in Figure 21, were used to aid mixing.

When the desired atmosphere at the specified total pressure for the experiment was in the chamber, the power to the Variac and to the motor to drive the Variac was then turned on. The voltage across the metal sample thus increased linearly with time. The current passing through the sample caused it to heat to the point of ignition. It should be noted that this requirement that the metal sample retain structural integrity until the point of ignition was not a problem in either the calcium or strontium experiments and that only in the low-pressure magnesium experiments does one experience breaking of the metal sample without ignition and combustion. Brzustowski (16, 54) indicated that this was a flame spreading problem.

c. Associated Diagnostic Equipment

Most of the flame photographs were taken with a 4" x 5" Graflex Speed Graphic camera equipped with a Polaroid 4" x 5" Land Film Holder #500. The film used was Polaroid Positive/Negative Type 55 P/N which has an ASA rating of 50.

35 mm color slides of the flames were obtained using a Beseler Topcon Super D reflex camera. Extension tubes were used with this camera when closeups were required. The

film used was Kodak High Speed Ektachrome which has an ASA rating of 160.

The spectrograph used in these experiments was a Bausch and Lomb 1.5 meter stigmatic grating spectrograph, Model No. 11. First and second orders are superimposed. Filters were used to remove the second order when this was thought to be necessary. The dispersion in first order is $15 \text{ \AA}^\circ/\text{mm}$ over the wavelength range from 3700 \AA° to 7400 \AA° . The grating is blazed at 4900 \AA° . The film used in most of the experiments was Kodak #2475 Recording Film.

Densitometer traces were obtained on a Leeds and Northrup microdensitometer of the Knorr-Albers type.

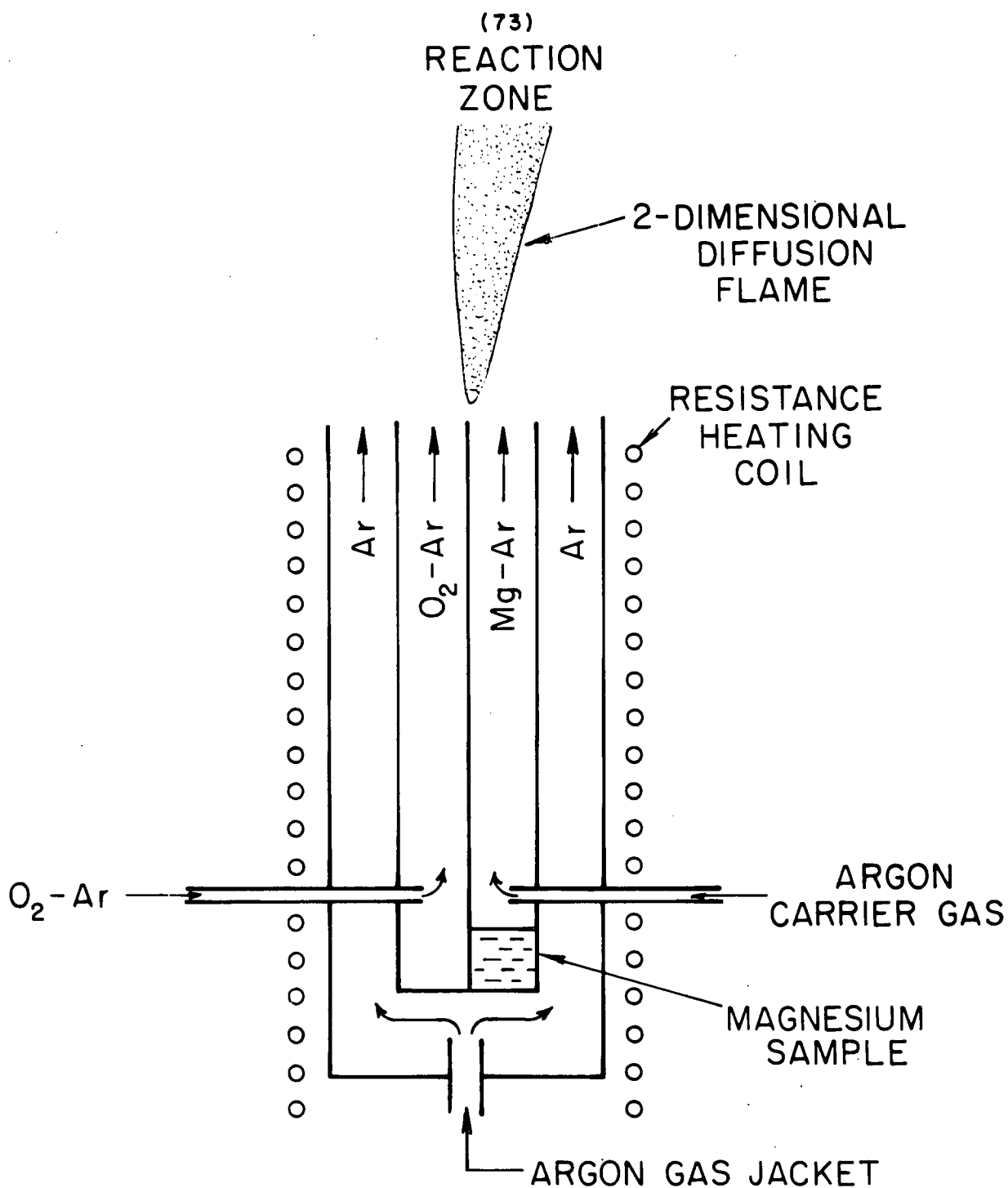
3. Two-Dimensional Diffusion Flame Burner

a. Apparatus Description

The two-dimensional diffusion flame burner to be described in this section was originally designed by Wolfhard and Parker (6, 53) for the spectroscopic examination of $\text{H}_2\text{-O}_2$, $\text{NH}_3\text{-O}_2$ and hydrocarbon -O_2 flames at atmospheric pressure. This burner design has been adapted for metal combustion studies at reduced pressures in the present investigation.

The burner is shown schematically in Figure 22. A photograph of the burner assembly is given in Figure 23.

Essentially the burner consists of two flat ducts which share one long side in common. The fuel flows in one of these ducts and the oxidizer in the other. The velocities of the two flows are matched so that at the exit of the ducts,



SCHEMATIC OF END VIEW OF 2-DIMENSIONAL DIFFUSION FLAME BURNER

(74)

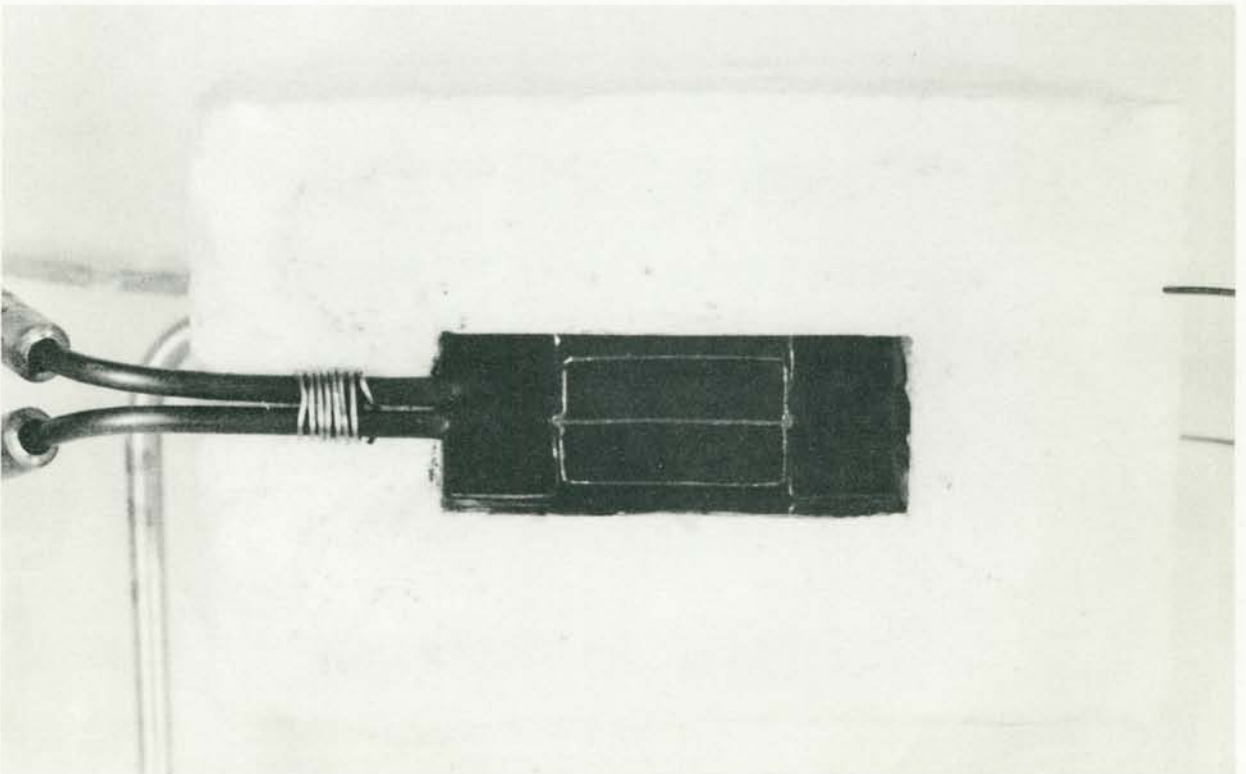
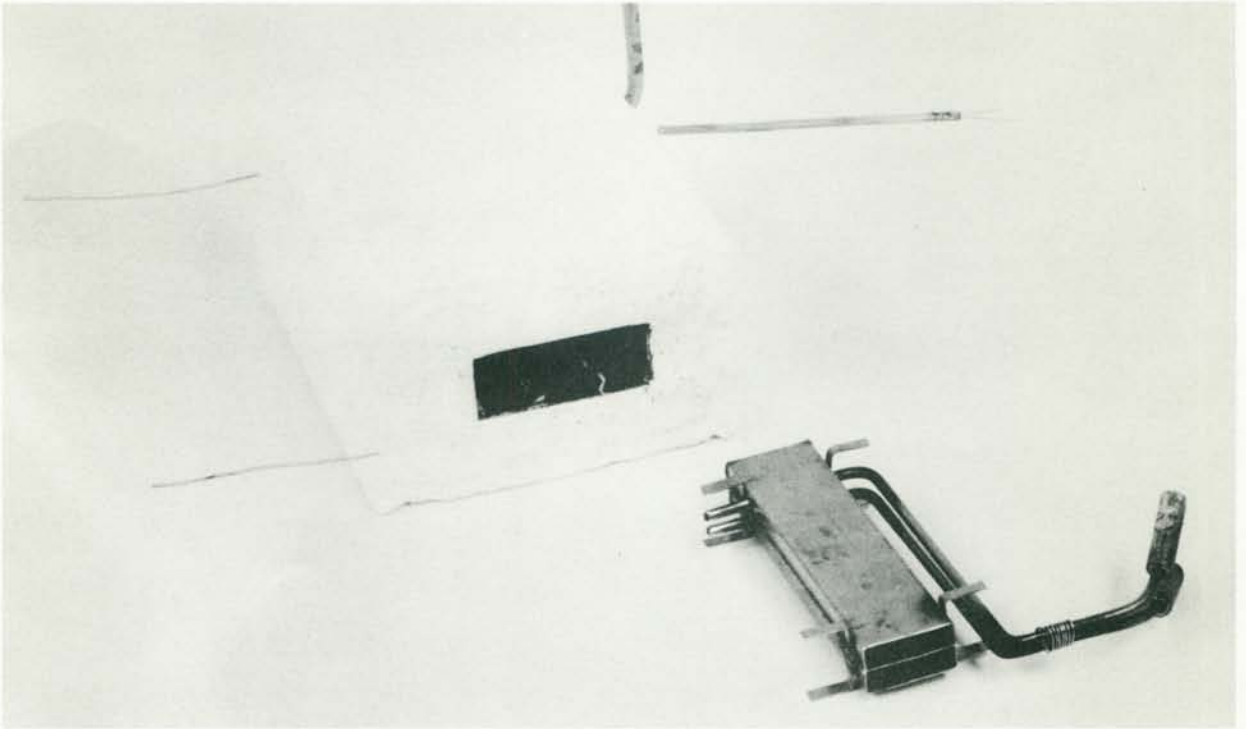


FIGURE 23

mixing occurs by diffusion. Flow rates are small so that the flow remains laminar.

In order to stabilize the flame and also to prevent entrainment of the atmosphere surrounding the flame into the flame gases, an inert gas jacket surrounds the duct assembly.

To adapt this burner for metal combustion studies, it was necessary to provide a means of heating the furnace to temperatures in excess of 1000°C in order to vaporize the metal sample and to maintain it in the vapor state as it flows along the duct.

The heating was accomplished by winding a resistance heating element around the inert gas jacket. The inner duct assembly receives its heat by conduction and by radiation from the walls of the inert gas jacket. The wire for the resistance heating element was Kanthal Grade A-1 obtained from the Kanthal Corporation. This resistance wire has a maximum temperature limit at 1375°C .

The duct dimensions were as follows: width 6 mm., depth 21 mm., height 88 mm.

The inert gas jacket was 18 mm. in width, 46 mm. in depth and 118 mm. in height.

The gas supply tubes for the carrier gas and the oxidizer mixture were 2.8 mm in diameter with 0.52 mm wall thickness.

All metal parts of the burner were constructed from 304 stainless steel.

The temperature of the burner was measured with a Pt. - Pt. 13% Rh thermocouple which was located at the base of the fuel duct in order to closely approximate the temperature of the metal sample itself rather than the furnace wall temperature.

The entire burner assembly was mounted in a combustion chamber as shown in Figure 24, to permit operation at reduced pressures.

The gas flows to the chamber were measured with Brooks Sho-Rate flow meters. Needle valves were used to control the flows.

The pressure in the chamber was maintained constant during an experiment by means of a Cartesian manostat, which had been modified slightly to increase its flow capacity.

A schematic of the apparatus is provided in Figure 25.

Figure 26 is an overall view of the apparatus showing the console, the combustion chamber, the optical components and the spectrograph.

The optical components of the system can be seen more clearly in Figure 24. The first component is an image-rotating device constructed using three first-surface mirrors (55). This is followed by a quartz lens, a filter to separate 1st and 2nd orders, a shutter and the spectrograph. Also visible on the front of the spectrograph is a bulk film holder which was designed and built for this spectro-

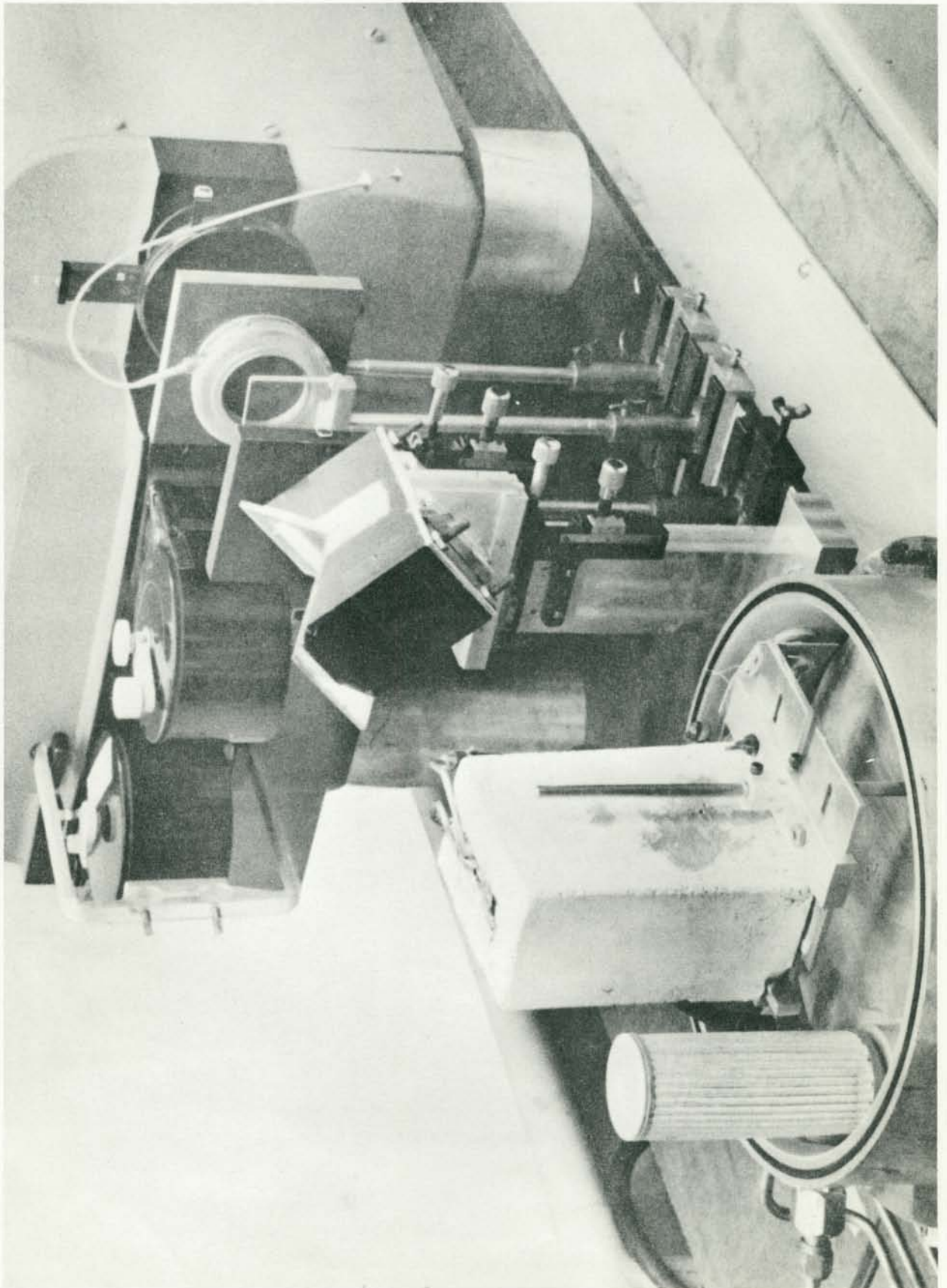
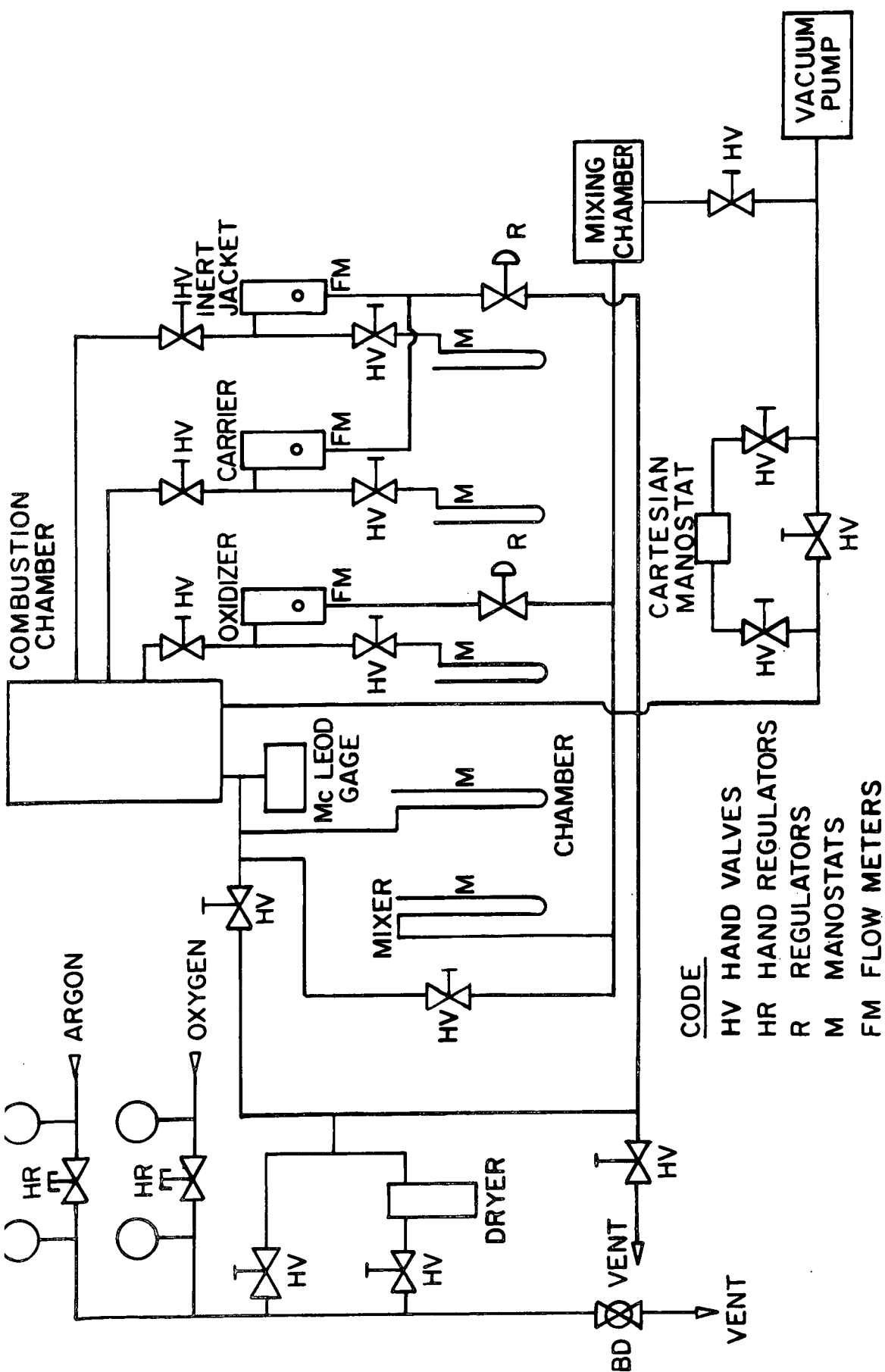


FIGURE 24



LOW PRESS. TWO DIMENSIONAL DIFFUSION FLAME BURNER
FLOW SCHEMATIC

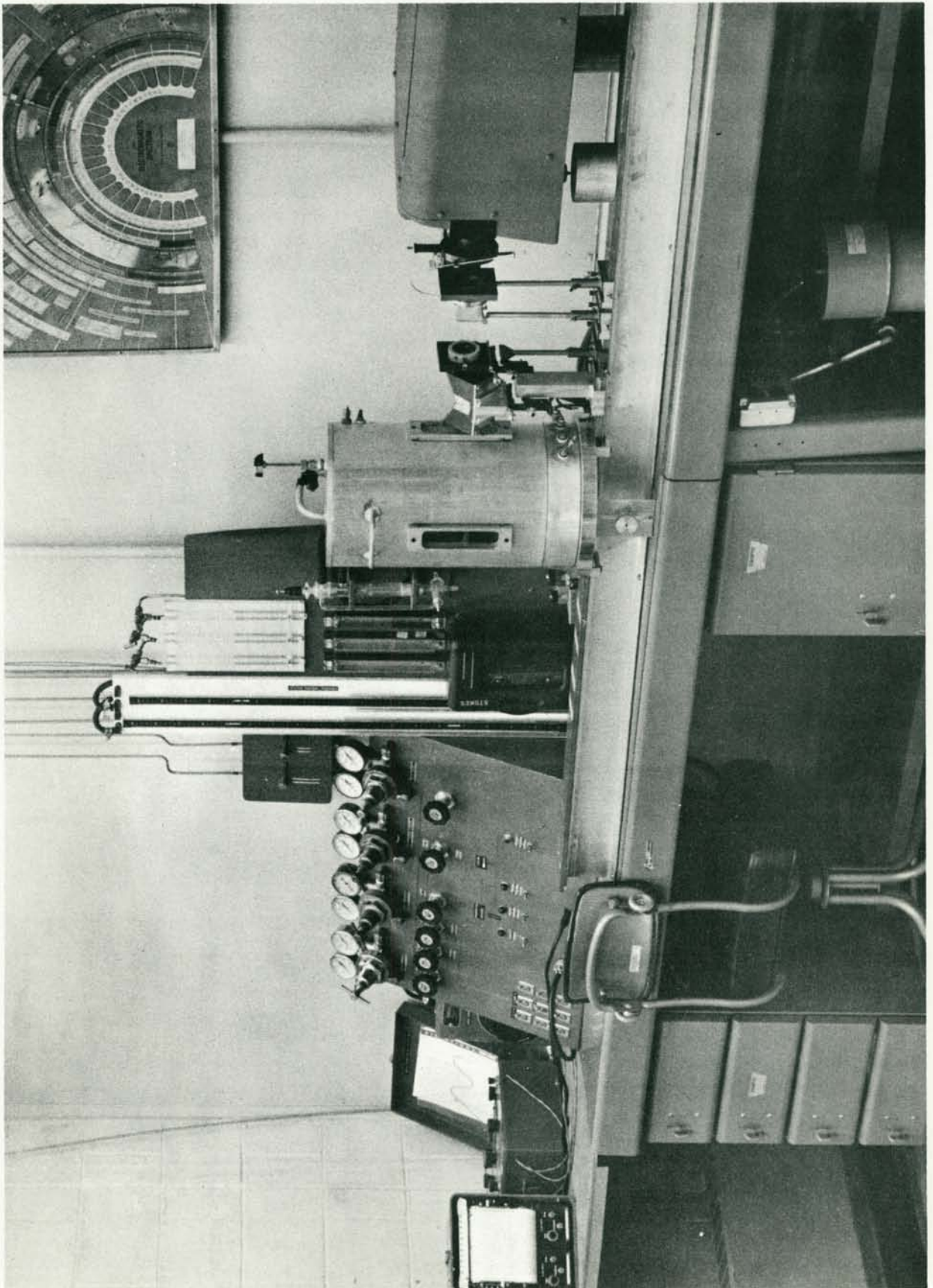


FIGURE 26

graph. This bulk film loader hold up to 100 feet of film and permitted several spectra to be obtained during a single burner experiment.

b. Associated Diagnostic Equipment

The cameras, films, spectrograph, etc., were the same as reported earlier for the wire-burning experiments.

c. Procedure

The metal sample was placed in the remote control metal loader which consisted of a small container with a hinged bottom which could be opened by lowering the container toward the burner assembly, thus pivoting the hinged bottom.

The chamber was then closed and evacuated. It was filled with Argon and re-evacuated several times. It was then filled with Argon to the desired pressure level for the experiment. The Cartesian manostat was then set for this pressure.

The power to the resistance heating element was turned on and the burner was heated up to the desired temperature for the experiment. This heating period was typically 20 minutes.

The gas flows were then set at their pre-determined levels using the flow meters.

When the chamber temperature, the gas flows and the chamber pressure were all steady, the metal sample was added to the burner using the remote control metal loader.

The flame, which appeared at the exit of the burner ducts almost immediately, was quite steady and could be maintained for several minutes.

Spectra, photographs and visual observations were obtained during the duration of the steady flame.

CHAPTER V - EXPERIMENTAL OBSERVATIONS FOR THE COMBUSTION OF MAGNESIUM, CALCIUM AND STRONTIUM

This chapter is a description of the observations of the combustion of magnesium, calcium and strontium in two different experiments. The first part of the chapter is concerned with the studies in which metal wires¹ were mounted between electrodes and heated to the point of ignition by passing electrical current through the sample. The second part of the chapter is an account of the experiments performed in the two-dimensional diffusion flame burner described in Chapter IV.

1. Wire Experiments

Magnesium, calcium and strontium were all studied in the wire burning apparatus described in the previous chapter although they were not all studied to the same extent. Calcium was studied more extensively than strontium. The results for strontium confirmed that its combustion behavior was similar to that of calcium and thus fewer experiments were performed with strontium. Magnesium was studied extensively by Brzustowski (16, 54). Some of the experiments performed by Brzustowski were repeated. In other cases Brzustowski's data were re-examined in the light of recent spectroscopic data, results, etc. In general the lack of symmetry in the magnesium wire experiments suggested that information could be obtained more readily from the symmetrical calcium and strontium flames.

¹Wires, ribbons or strands. See Chapter IV for details.

a. Calcium Wire Experiments

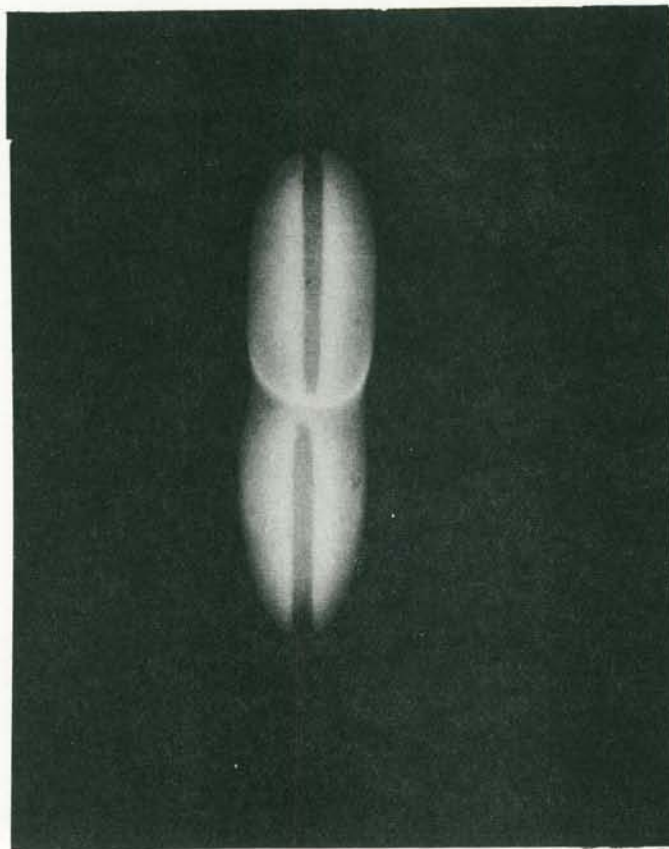
(i) Visual and Photographic Observations

Almost all of the experiments were performed at total pressures of 50 torr in an atmosphere of 20% oxygen and 80% argon. Experiments indicated that the flame observed under these conditions was representative of the main combustion features observed at other pressures over the range from 5 or 10 torr to 500 torr, the main difference is the physical dimensions of the flame.

A typical flame photograph for a calcium wire burning in an atmosphere of 20% oxygen and 80% argon at a total pressure of 50 torr is reproduced in Figure 27. The important observation in this photograph is the existence of a two zone structure; namely, an inner zone of predominantly orange radiation lying close to the wire and extending to about half the radius of the luminous envelope which surrounds the wire, and an outer zone which appears white in color and contains radiating condensed oxide particles in a molten and/or solid state.

These observations of an inner zone of radiation close to the wire were not in accord with the previous interpretation of metal flame structure based on photographic observations and a collapsed flame zone model (15).

In order to define and interpret the nature of this inner orange zone of radiation the following experiments were performed.



CALCIUM WIRE BURNING IN 20% O₂,
80% Ar AT 50 mm Hg TOTAL PRESSURE.

(ii) Photographs Through Narrow Band Interference Filters at Selected Wavelengths

Photographs of the calcium flame, burning under the same conditions as described above for Figure 27, were taken through narrow band interference filters having a half-width of 100 \AA with wavelengths centered in the following three selected regions:

- (1) 6250 \AA - the radiation passed by the filter included bands attributed to calcium oxide and continuum radiation from the condensed oxide particles. The lines of calcium which lie in the orange region of the spectrum do not fall within the wavelength region passed by the filter.
- (2) 4990 \AA - the radiation passed by the filter is due to the continuum radiation from the condensed oxide particles. This spectral region contains neither lines of calcium nor bands of calcium oxide.
- (3) 4200 \AA - Since it was not possible to select one of the orange lines of Ca without also including radiation from the bands attributed to calcium oxide, a decision was made to select a spectral region which included the strong resonance line of calcium at 4226.73 \AA . The radiation passed by the filter thus includes this Ca radiation plus the continuum radiation of the condensed oxide particles.

The photographs taken through these interference filters at 6250 \AA , 4990 \AA and 4200 \AA are reproduced in Figures 28, 29 and 30 respectively. It is to be noted that Figure 28, which includes radiation attributed to bands of calcium oxide, is the only photograph exhibiting the two zone structure which was observed in Figure 27, a non-filtered photograph. These experiments indicated that calcium oxide existed and radiated in the inner orange zone of the flame, an unexpected result on the basis of previous flame structure models.

It appeared illogical that calcium oxide vapor should be radiating strongly in a location near the wire surface and that calcium vapor evaporating from the wire should not show the same dependence (as indicated by a comparison of Figure 28 and 30). A possible explanation was that with a filter half width of 100 \AA° , the amount of continuum radiation due to the condensed oxide particles overshadowed the amount of radiation contributed by the Ca resonance line. As a result this experiment was repeated with a filter having a half width of only 12 \AA° . This filter reduces by a factor of eight the amount of continuum radiation due to condensed oxide particles, and retains the same contribution from the Ca resonance line. The photograph taken through this interference filter centered at 4231 \AA° is reproduced in Figure 31. The two zone flame structure is again apparent indicating that calcium vapor as well as calcium oxide vapor is radiating strongly in the inner zone close to the wire surface.

(iii) Space-Resolved Spectroscopic Observations

To determine the relative locations in the flame of the various radiating species, space-resolved spectra were obtained for the flames of calcium wires burning in an atmosphere of 20% oxygen and 80% argon at a total pressure of 50 torr. A schematic representation of the relative position of the spectrograph slit with respect to the cylindrically symmetric calcium wire flame is presented in Figure 32. Enlarged portions of the spectrum are also reproduced in this figure.

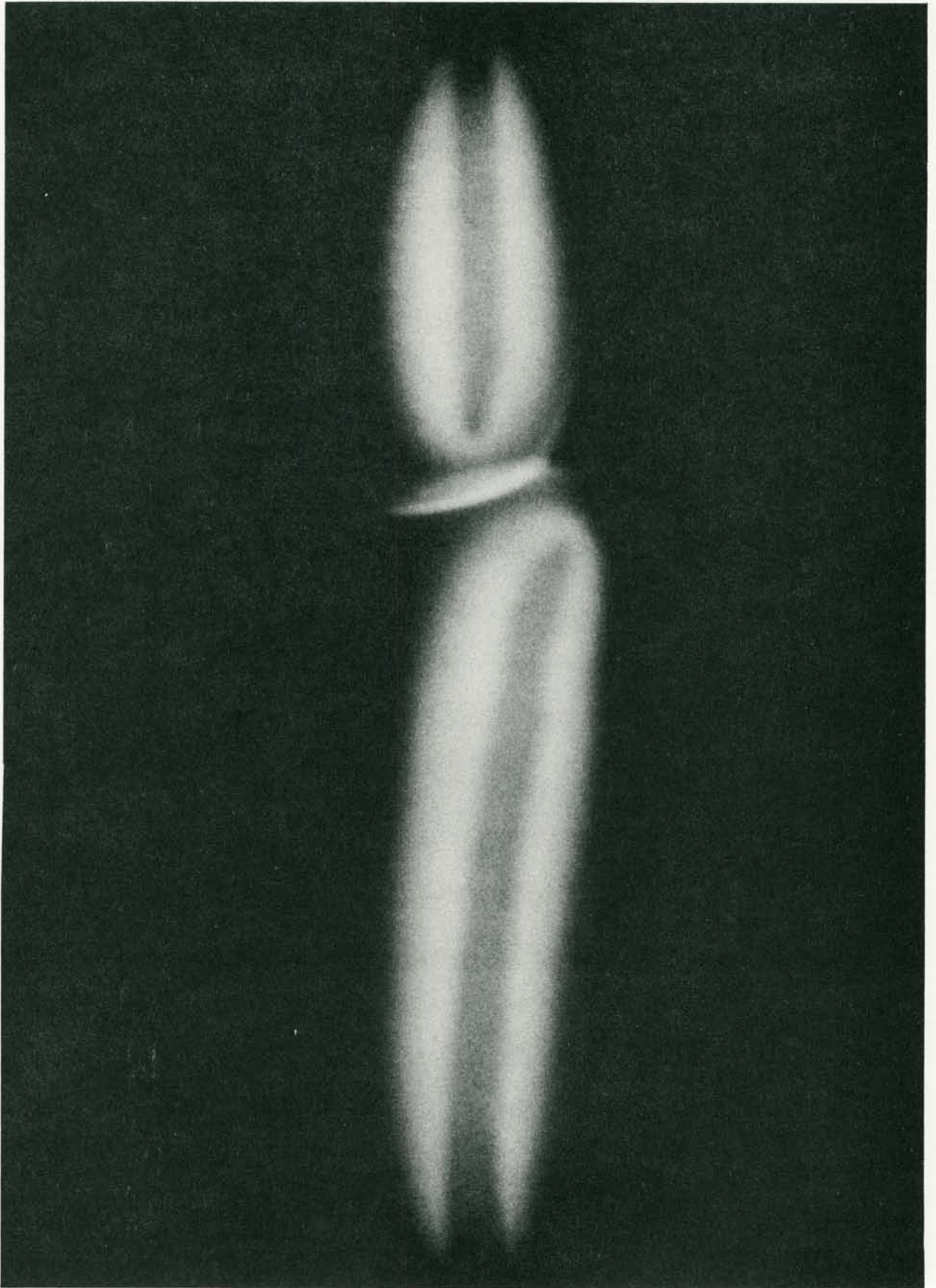


FIGURE 28

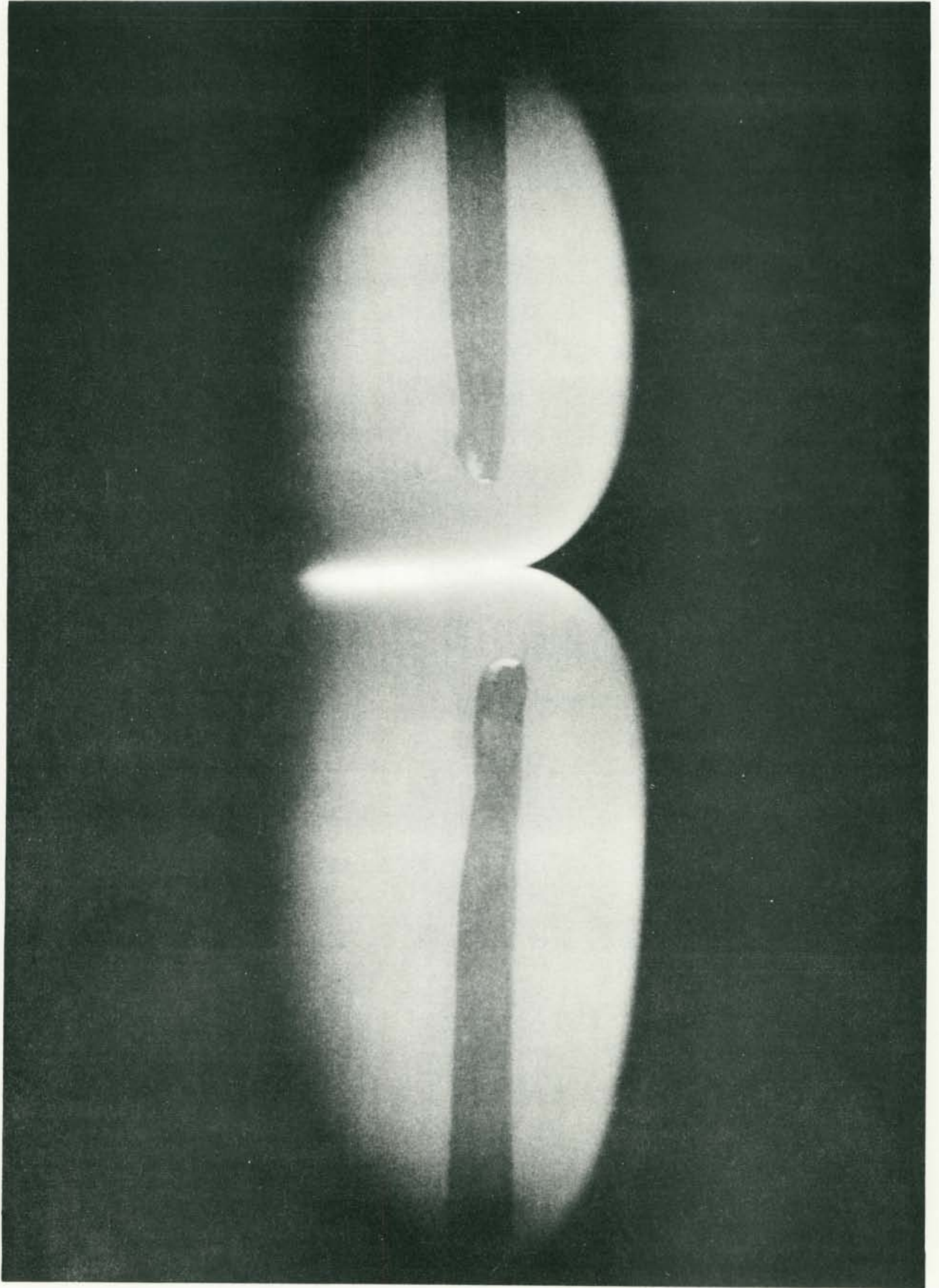


FIGURE 29

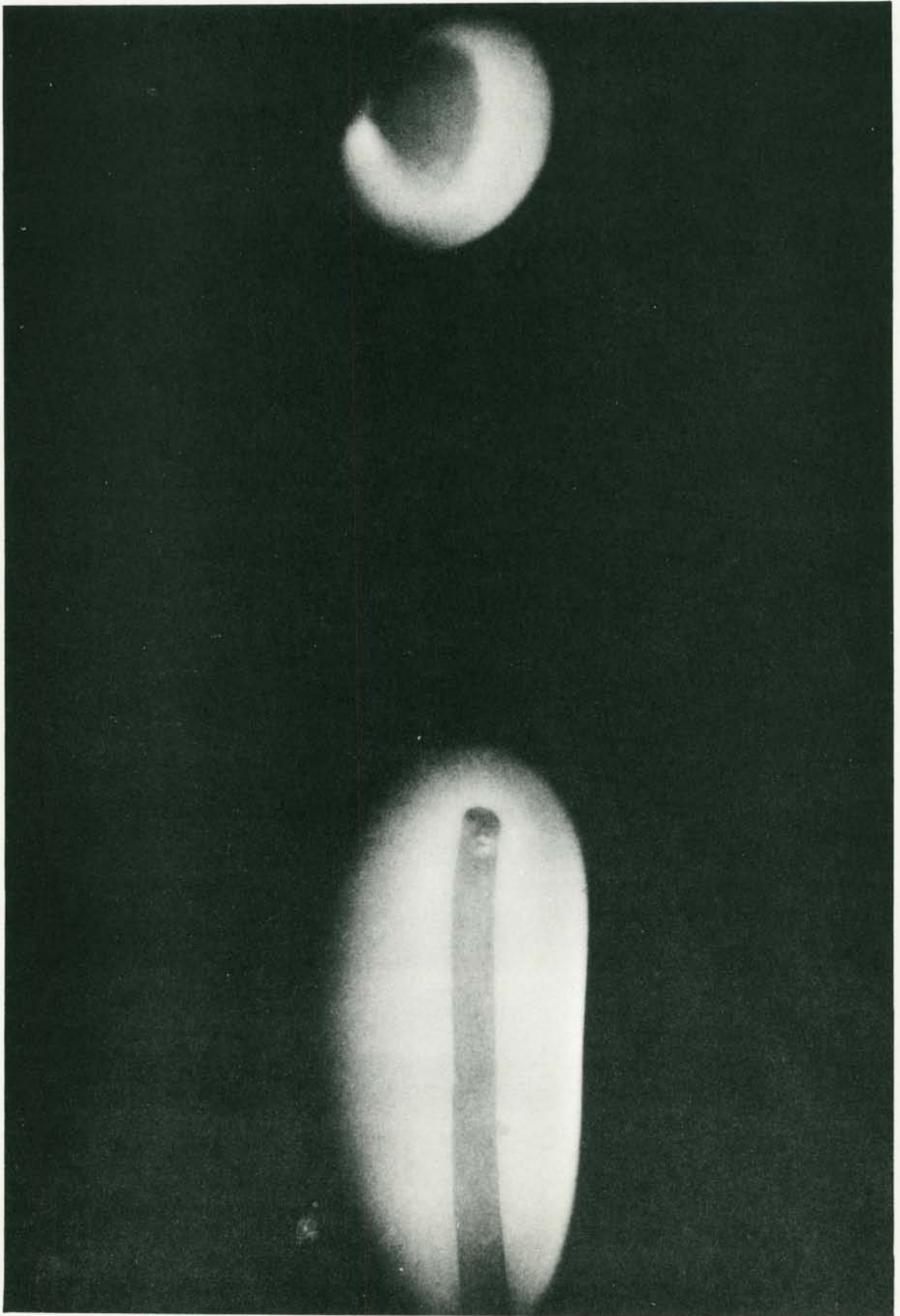


FIGURE 30

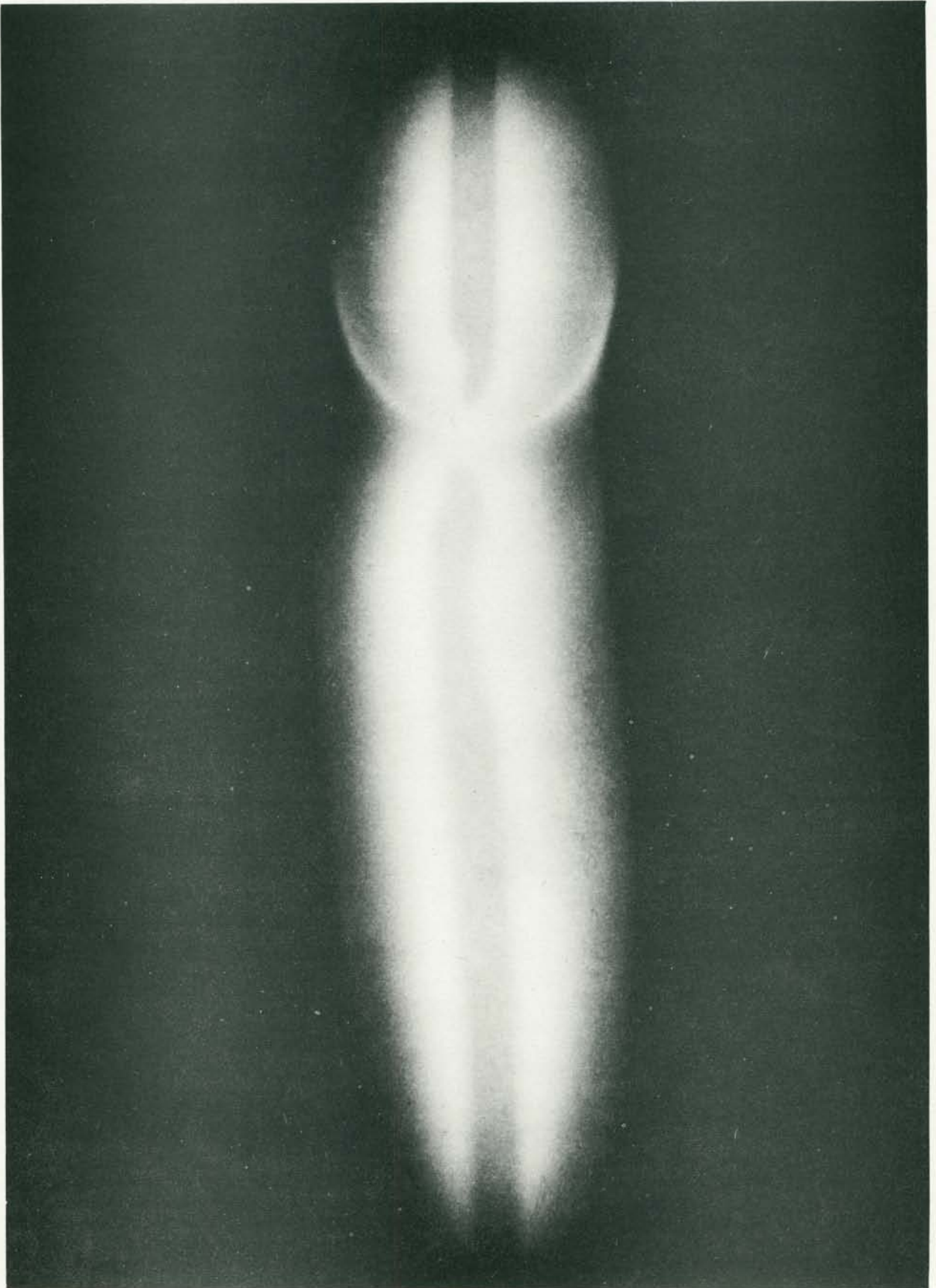


FIGURE 31

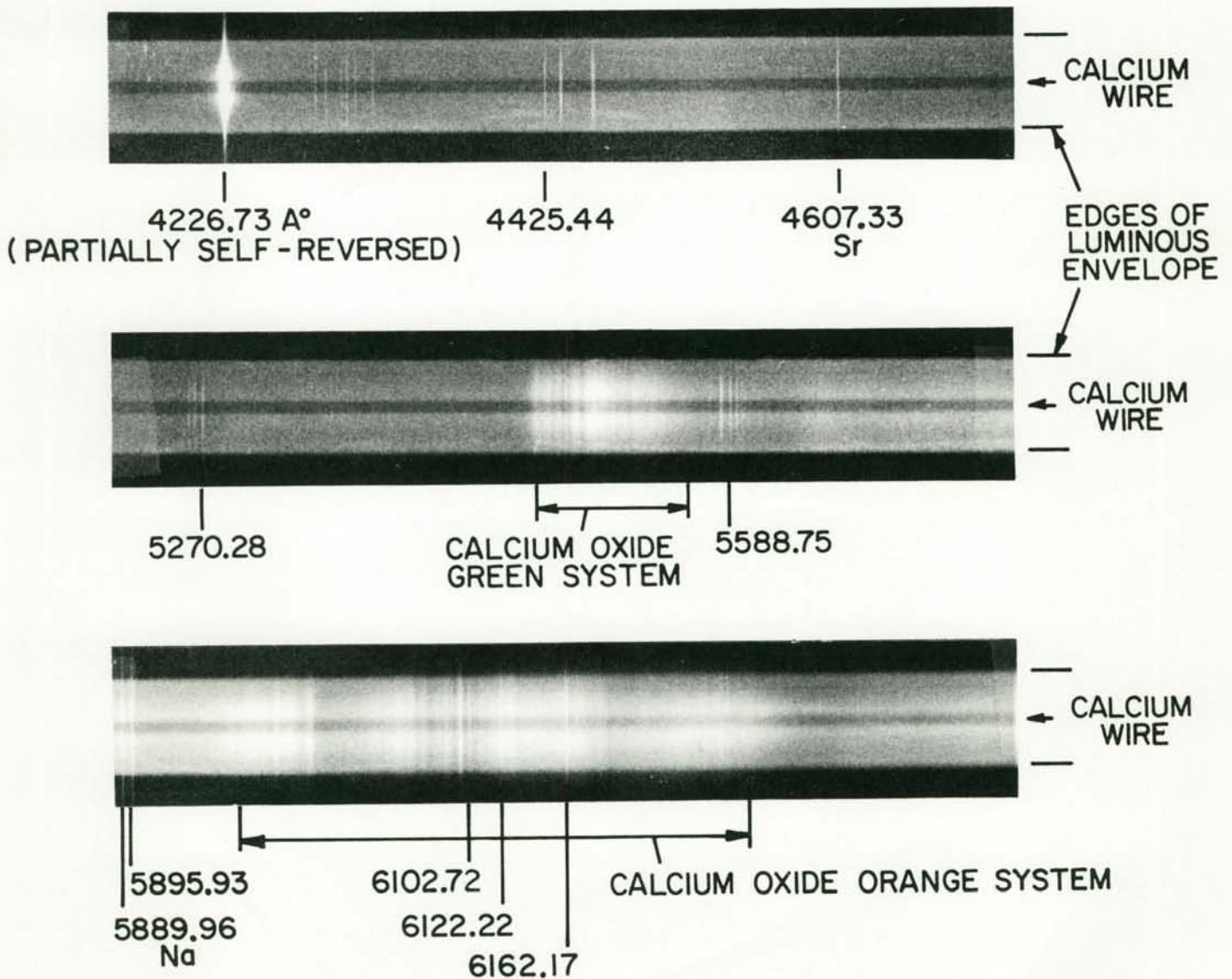
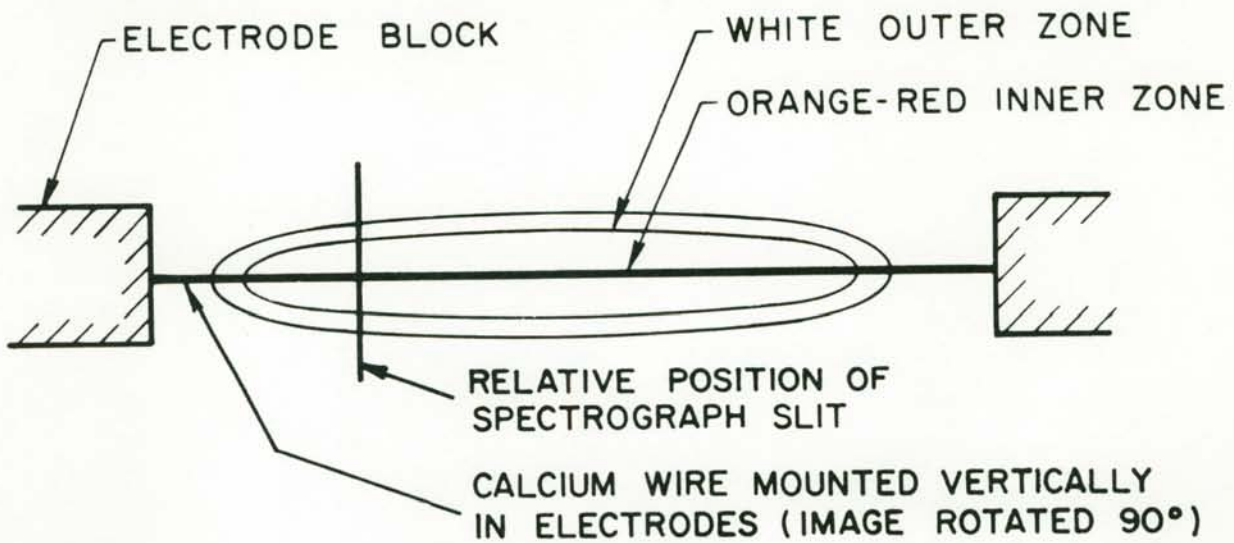
The streak running horizontally through the spectrum indicates the position of the wire. Note that the upper and lower edges of the continuum radiation in the spectrum are due to the edges of the luminous envelope of the flame and are not a result of the height of the spectrograph slit. As indicated in the schematic, the ends of the slit extend beyond the luminous envelope of the flame on both sides.

Figure 33 is a reproduction of a densitometer trace of a typical calcium flame spectrum.

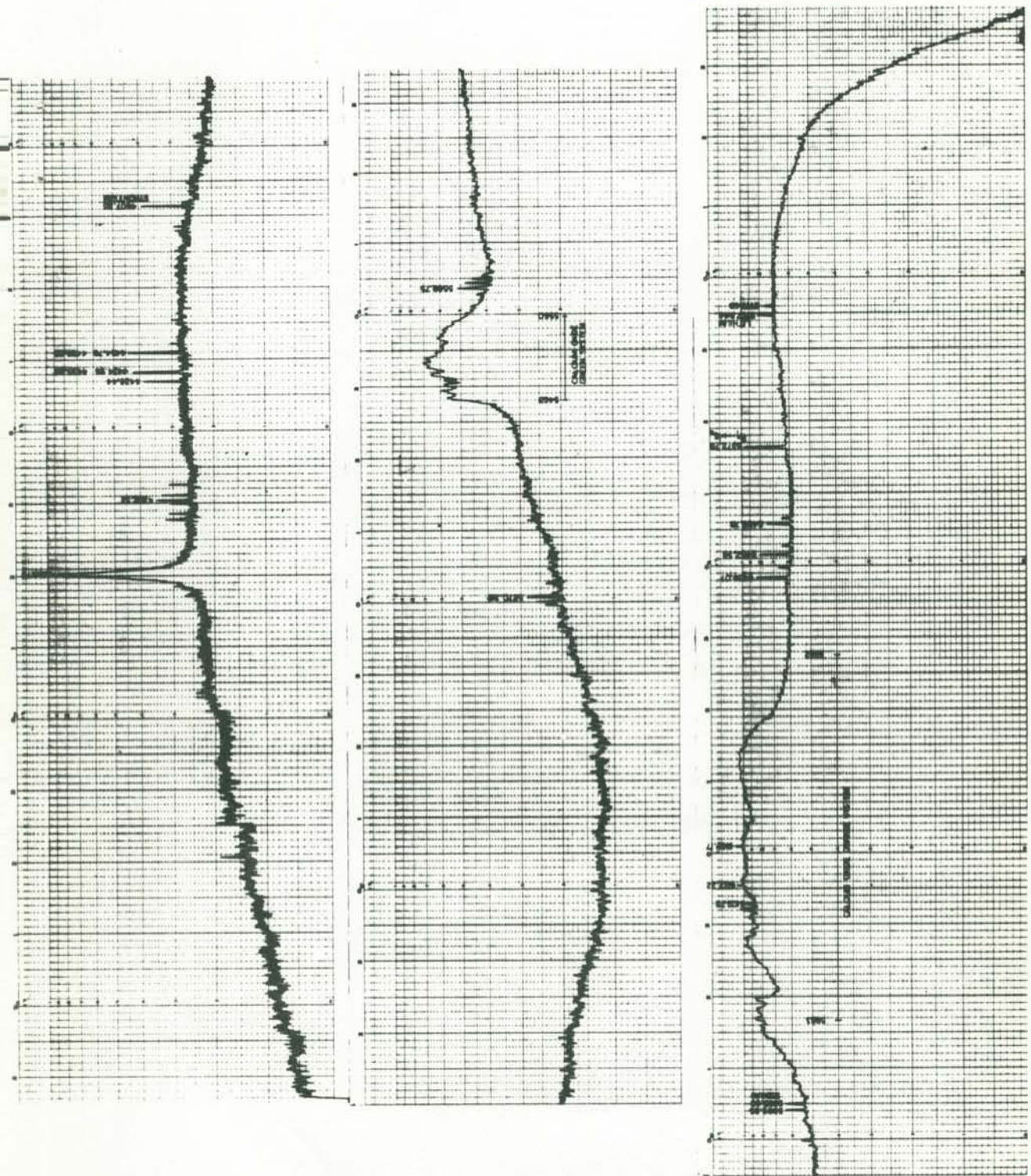
The identification of the atomic lines present in the spectra was straight forward and the numerous lines which were identified are listed in Table 9.

The spectral features attributed to molecular species were not as simple to identify. All of the known systems of CaO corresponding to transitions between singlet states of the diatomic oxide were not observed. The CaO band systems listed by Pearse and Gaydon (29) as "Meggers' Infra-Red Bands" and the "Extreme Red System" would both fall outside the spectral region of the particular spectrograph used in these investigations. However, the "Blue System" and the "Ultra-Violet System" are within the spectral range observed in these studies, but both systems were missing in the spectra.

The bands that are observed in the spectra lie in the green and orange regions and are diffuse in appearance. Bands in the green and orange regions have been ascribed both to CaOH and an oxide of calcium, not necessarily CaO, but possibly a polyatomic or polymeric specie.



SPACE-RESOLVED FLAME SPECTRUM OF CALCIUM
AT 50mm Hg, 20% O₂, 80% Ar



PRINCIPAL FEATURES OF THE Ca - O₂ FLAME SPECTRUM
(WIRE EXPERIMENTS)

(94)
TABLE 9

SPECTRAL LINES OBSERVED IN THE CALCIUM FLAMES (WIRE EXPERIMENTS)

<u>λ [Å]</u>	<u>SPECIE</u>	<u>ENERGY LEVELS [K]</u>	<u>COMMENTS</u>
3933.67	CaII	0-25414	very weak
3968.47	CaII	0-25192	very weak
4226.73	CaI	0-23652	self-reversed
4283.01	CaI	15210-38552	
4289.36	CaI	15158-38465	
4298.99	CaI	15210-38465	
4302.53	CaI	15316-38552	
4307.74	CaI	15210-38418	
4318.65	CaI	15316-38465	
4425.44	CaI	15158-37748	
4434.96	CaI	15210-37752	
4435.69	CaI	15210-37748	
4454.78	CaI	15316-37757	
4455.89	CaI	15316-37752	
4581.40	CaI	20349-42171	very weak
4585.87	CaI	20371-42171	very weak
4607.33	Sr	0-21698	impurity
4878.13	CaI	21850-42344	very weak
5261.70	CaI	20335-39355	
5262.25	CaI	20335-39333	
5264.24	CaI	20349-39340	
5265.56	CaI	20349-39335	
5270.28	CaI	20371-39340	
5349.47	CaI	21850-40538	very weak
5581.97	CaI	20349-38259	
5588.75	CaI	20371-38259	
5594.45	CaI	20349-38219	
5598.47	CaI	20335-38192	weak
5857.46	CaI	23652-40720	
5889.96	Na	0-16973	impurity
5895.93	Na	0-16956	impurity
6102.72	CaI	15158-31540	
6122.22	CaI	15210-31540	
6162.17	CaI	15316-31540	
6439.07	CaI	20371-35897	
6449.81	CaI	20335-35835	
6462.56	CaI	20349-35819	
6471.66	CaI	20371-35819	
6493.78	CaI	20335-35730	
6499.65	CaI	20349-35730	
6572.78	CaI	0-15210	$\left. \begin{array}{l} {}^3P_1 \rightarrow {}^1S_0 \\ \text{inter-system line} \\ \text{impurity} \end{array} \right\}$
6707.84	Li	0-14904	
6717.68	CaI	21850-36732	

Although some of the green bands of CaOH and calcium oxide overlap one another in the region from 5530 to 5570 \AA , the bands observed in the region from 5473 to 5530 \AA do belong to the system assigned to calcium oxide. In addition a plate comparison with the spectrum of calcium oxide reproduced in Ref. (29), appeared to confirm the identification of these bands as the green system of calcium oxide.

The orange-red bands of CaOH and the orange system of calcium oxide also fall in overlapping regions of the spectrum. The bands observed in the flame spectrum were identified as those of calcium oxide on the basis of the plate comparison mentioned above, and the fact that some structure is observed in the spectra whereas the orange-red bands of CaOH are described as being "very diffuse".

Although the presence of bands of CaOH cannot be ruled out entirely on the basis of the above assignments, it seemed logical that in an experiment in which relatively dry gases were used, the most intense spectral features observed would correspond to the oxide rather than the hydroxide band systems.

Since in the burner experiments to be described later in this chapter it appeared that hydroxide bands might be appearing in the burner flame spectra, some experiments were performed in the wire-burning apparatus in which water vapor was introduced into the chamber gases. These results are also reported later in this chapter.

The space-resolved spectra reinforce the observations from the interference filter-selected wavelength experiments. The Ca resonance line at $4226.73 \text{ \AA}^{\circ}$ as well as numerous other Ca lines and the band systems in the green and orange wavelength regions attributed to calcium oxide, appear to have their peak intensity a short distance from the wire surface but well within the luminous envelope of the flame.

The Ca resonance line at $4226.73 \text{ \AA}^{\circ}$ is observed to be self-reversed over the central portion of its length. However, it is not self-reversed over the remainder of its length which corresponds to locations still within the luminous envelope but further to the edge of the flame.

b. Strontium Wire Experiments

(i) Visual and Photographic Observations

Flame photographs of strontium wires burning in an atmosphere of 20% oxygen and 80% argon at 50 torr total pressure indicate that the flame structure for strontium appears to be very similar to that for calcium. A typical flame photograph for the conditions mentioned above is reproduced in Figure 34. The two zone flame structure, which was reported in the previous section for the case of calcium, is also evident in the strontium experiments. The overall size of the luminous envelope and also the size of the inner zone of colored radiation appear to be the same for both the strontium and calcium flames.

(ii) Space-Resolved Spectroscopic Observations

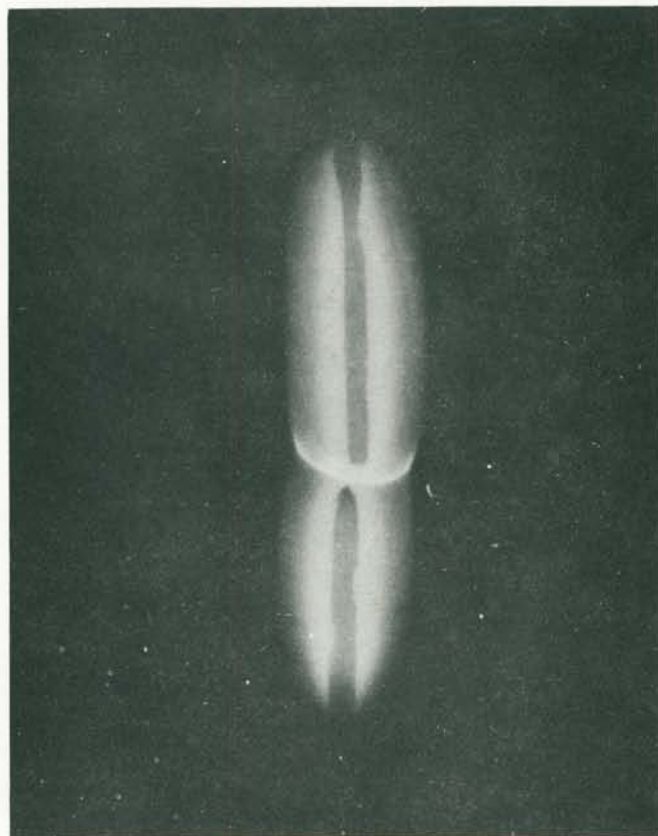
Enlarged portions of a space-resolved spectrum for a strontium wire burning under the conditions outlined above are reproduced in Figure 35. A densitometer trace of this spectrum is presented in Figure 36.

As in the case of calcium the identification of the atomic lines presented no problem, but the identification of the molecular bands observed presented somewhat more difficulty. Table 10 contains a list of the spectral lines which were identified in these spectra.

Of the three band systems assigned to transitions between singlet states of the diatomic oxide SrO , two of the systems, namely the blue and ultra-violet systems, fall within the spectral region observed in these experiments but neither system was observed in the flame spectra.

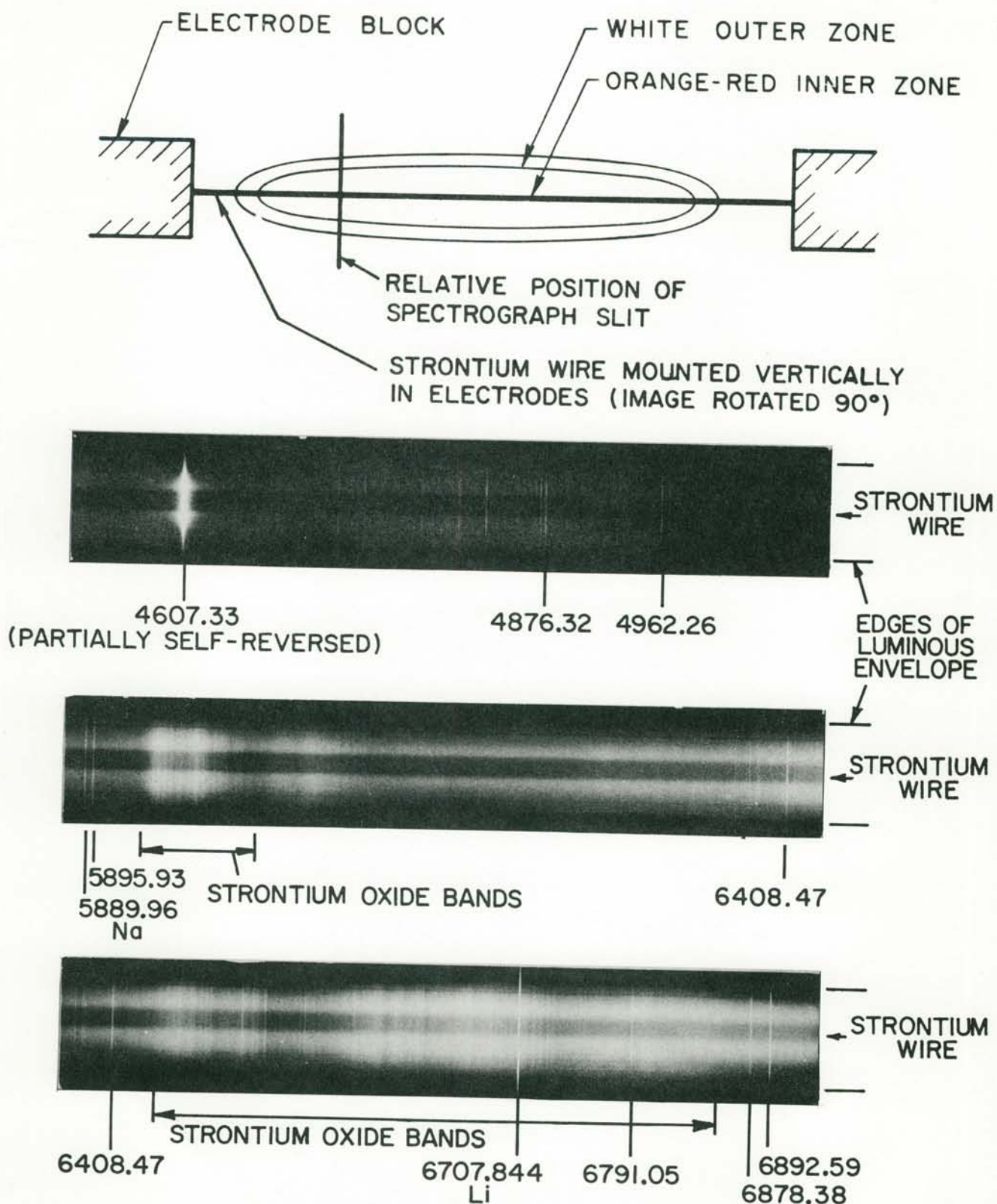
The bands which were observed in the spectra occurred in the regions where bands of SrOH and bands of a strontium oxide (possibly a polyatomic or polymeric specie) exist in overlapping regions.

The band system near the Na lines, i.e., at wavelengths of about 5950 \AA was attributed to strontium oxide since the bands of SrOH occur at slightly longer wavelengths. This assignment to the oxide rather than the hydroxide is demonstrated much more conclusively later in this chapter when the experiments to determine the effect of water vapor are reported.



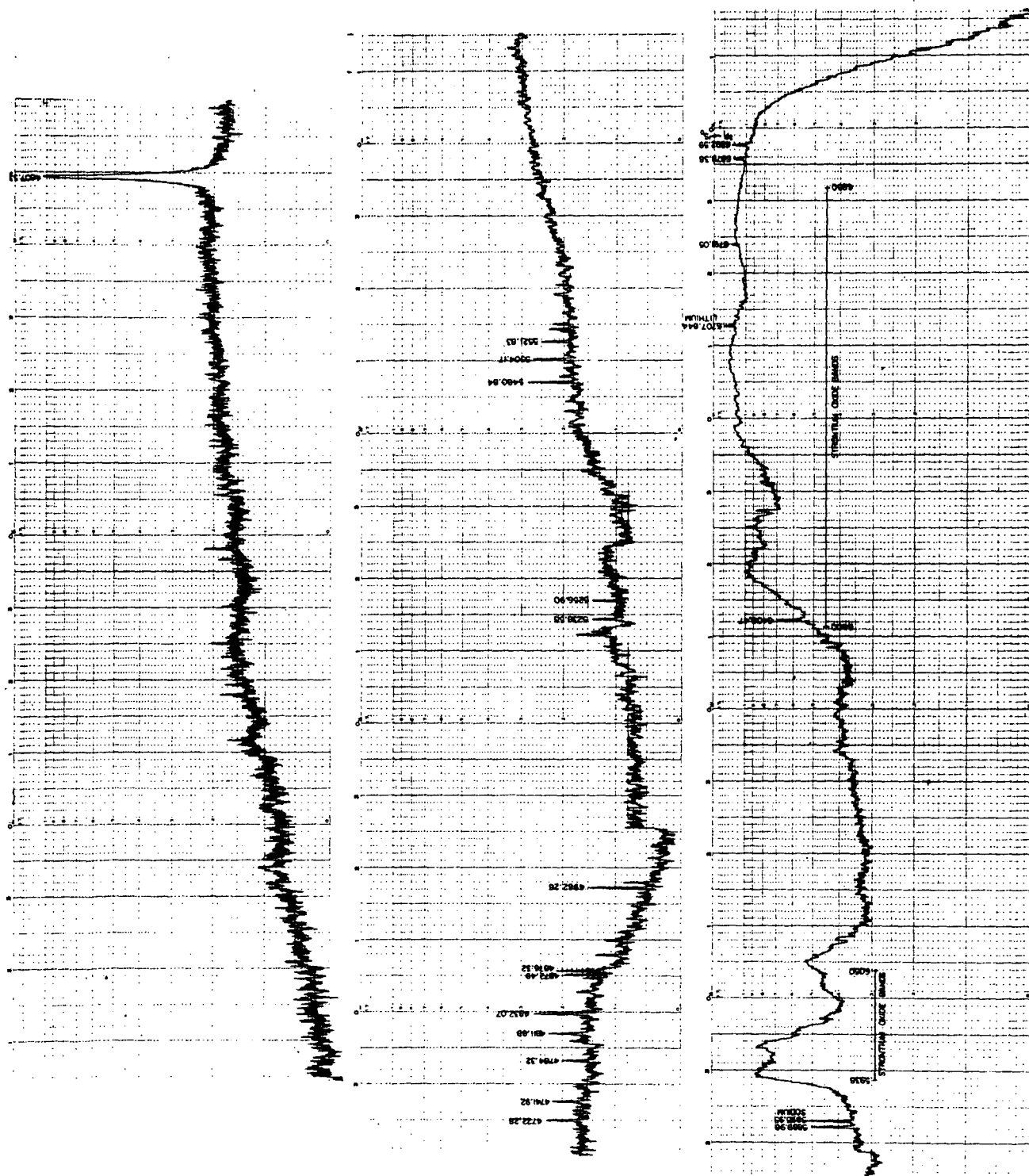
STRONTIUM WIRE BURNING IN 20% O₂,
80% Ar AT 50mm Hg TOTAL PRESSURE.

(99)



SPACE - RESOLVED FLAME SPECTRUM OF STRONTIUM
AT 50mm Hg, 20% O₂, 80% Ar

FIGURE 35



(101)
TABLE 10

SPECTRAL LINES OBSERVED IN THE STRONTIUM FLAMES (WIRE EXPERIMENTS)

<u>λ [A°]</u>	<u>SPECIE</u>	<u>ENERGY LEVELS [K]</u>	<u>COMMENTS</u>
4077.71	SrII	0-24517	very weak
4215.52	SrII	0-23715	very weak
4226.73	Ca	0-23652	impurity
4319.05	SrI		
4319.12	SrI		
4337.66	SrI		
4337.89	SrI		
4607.33	SrI	0-21698	self-reversed
4722.28	SrI	14504-35675	
4741.92	SrI	14318-35400	
4784.32	SrI	14504-35400	
4811.88	SrI	14899-35675	
4832.07	SrI	14504-35194	
4868.70	SrI	18219-38752	very weak
4872.49	SrI	14504-35022	
4876.06	SrI	14504-35007	
4876.32	SrI	14899-35400	
4891.98	SrI	18319-38755	very weak
4962.26	SrI	14899-35045	
4967.94	SrI	14899-35022	
5156.07	SrI	20150-39539	very weak
5222.20	SrI	18159-37302	" "
5225.11	SrI	18159-37292	" "
5229.27	SrI	18219-37336	" "
5238.55	SrI	18219-37302	" "
5256.90	SrI	18319-37336	
5450.84	SrI	18219-36560	
5480.84	SrI	18319-36560	
5486.12	SrI	18159-36382	very weak
5504.17	SrI	18219-36382	
5521.83	SrI	18159-36264	
5534.81	SrI	18319-36382	
5540.05	SrI	18219-36264	
5889.96	Na	0-16973	impurity
5895.93	Na	0-16956	impurity
6345.75	SrI	18219-33973	very weak
6363.94	SrI	18159-33868	very weak
6369.96	SrI	18159-33853	
6380.75	SrI	18159-33827	
6386.50	SrI	18319-33973	
6388.24	SrI	18219-33868	
6408.47	SrI	18319-33919	
6504.00	SrI	18219-33590	
6546.79	SrI	18319-33590	
6550.26	SrI	21698-36961	
6707.844	Li	0-14904	impurity
6791.05	SrI	14318-29039	
6878.38	SrI	14504-29039	
6892.59	SrI	0-14503	inter-system line $^3P_1 \rightarrow ^1S_0$

The lines at 6617.26 and 6643.54 A° are obscured by the band systems in this region.

The bands in the region from 6400 to 6850 \AA° were also attributed to the oxide. The description of the oxide bands as possessing "strong complex structure" (29) appeared to characterize the observed bands more suitably than the description of the overlapping SrOH bands which are termed "diffuse".

As indicated in the case of calcium, water vapor should have been present in only trace amounts since dry gases were used in the experiments. It would be surprising if the hydroxide bands could be the major emitter observed, although there is probably some small contribution from the hydroxide bands.

The similarities of the strontium spectrum of Figure 35 to the corresponding spectrum of the calcium flame should be noted. The profiles of the lines and bands show the same spatial variations, and indicate that for strontium as well as calcium the zone of radiation lying close to the wire and extending to about half the radius of the luminous envelope contains both the metal and metal oxide vapors at their peak intensity.

Note again that the resonance line at 4607.33 \AA° for strontium is self-reversed over the inner portion of its length, but that it is not self-reversed over the remainder of its length corresponding to the outer zone of the flame. These observations are the same as were reported for the corresponding line in the case of calcium.

c. Magnesium Wire Experiments

(i) Visual and Photographic Observations

The flames of magnesium ribbons burning in an atmosphere of 20% oxygen and 80% argon at a total pressure of 50 torr were observed to be highly asymmetric, in contrast to the flames of calcium and strontium which possessed cylindrical symmetry to a fair degree. A typical flame photograph of magnesium for the conditions mentioned above is reproduced in Figure 37.

It was felt that the lack of symmetry in the case of magnesium could be due to the fact that the metal sample was in ribbon form rather than the wire or strand shape used for calcium and strontium. Some attempts were made to burn wires or strands of magnesium, but it did not produce the desired effect on the symmetry of the flame.

Another more likely cause of the asymmetry is the surface oxide coating present on the magnesium samples. If this coating ruptures it produces a local "jet" of magnesium vapor. The interaction of these vapor streams may be the distorting effect on the flame symmetry.

It is possible that the lack of symmetry is one of the few differences when comparing the flames of Mg, Ca and Sr. The spectroscopic features reported for Mg flames by Brzustowski (16, 54) are certainly consistent with the observations reported for Ca and Sr in the previous two sections of this report. The two-dimensional diffusion flame burner experiments to be described later also suggest

that Mg, Ca and Sr have common combustion behavior.

(ii) Spectroscopic Observations

The spectroscopic features reported by Brzustowski (16, 54) for magnesium ribbon flames can be compared to the results reported earlier for Ca and Sr.

The resonance line of Mg at $2852.13 \text{ \AA}^{\circ}$ is observed to be self-reversed. However, since these spectra were not space-resolved it is not possible to determine whether the line would exhibit the same type of spatial variation as was observed in the symmetrical Ca and Sr flames.

Brzustowski observed two band systems, the green band system of MgO, corresponding to the transition $B'\Sigma \rightarrow X'\Sigma$, and a complex group of bands in the UV which were un-analyzed but which were attributed to an oxide of magnesium, possibly a polyatomic or polymeric specie. Brzustowski labeled these bands in the UV as $(\text{MgO})_n$ with the limitations of this notation understood to mean either MgO or a polymeric specie.

Since the time of Brzustowski's experiments, two new band systems of MgO have been reported in the literature (27, 32, 34, 35) for this UV region for magnesium oxide. Since it had been expected that the complexity of the bands observed by Brzustowski was possibly caused by a polymeric specie rather than an overlapping of several band systems of MgO, Brzustowski's spectroscopic data were re-examined on the basis of this new information reported in the literature.

This re-examination showed that both of the newly



MAGNESIUM WIRE BURNING IN 20% O₂ ,
80% Ar AT 50 mm Hg TOTAL PRESSURE.

FIGURE 37

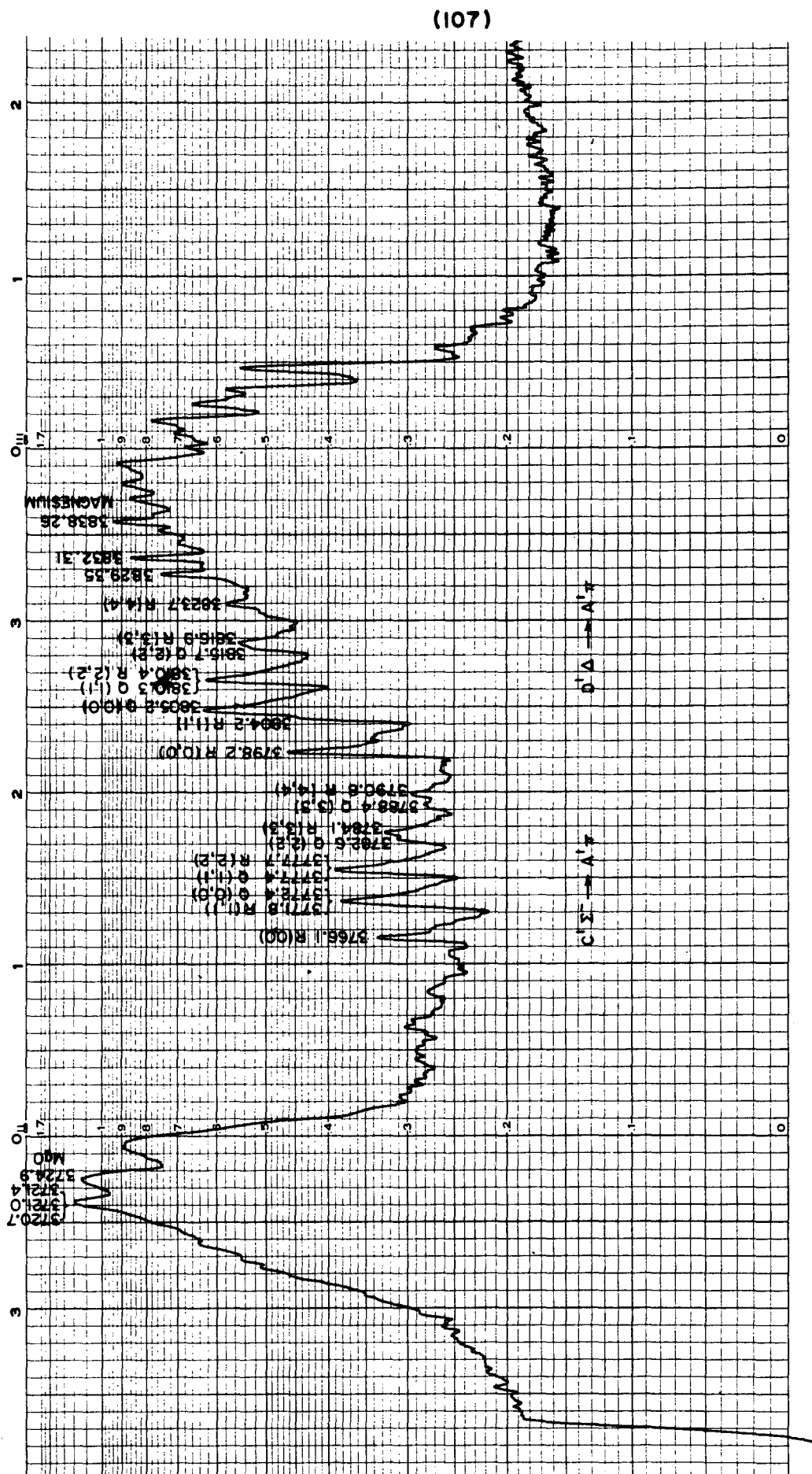
analyzed band systems, the $C'\Sigma^- \rightarrow A'\pi$ and $D'\Delta \rightarrow A'\pi$, were observed in the magnesium flame spectra. Other features observed in the UV region are still unassigned, and it is important to note that the three strong features which Brzustowski identified and labeled at 3721.4, 3725.7 and 3731.8 \AA are still not analyzed and are subject to some question regarding the emitter. A densitometer trace of this spectral region for a magnesium ribbon burning in an atmosphere of 30% O_2 and 70% Ar at a total pressure of 100 torr is reproduced in Figure 38.

The main features of the spectra observed by Brzustowski are tabulated in Table 11 for comparison with the results reported earlier for Ca and Sr.

d. Wire Experiments - Effects of Water Vapor

In the burner experiments which will be described later in this chapter, in particular in the strontium experiments, it appeared that small amounts of water vapor in the system resulted in the observance of hydroxide bands in the spectra. To confirm these observations, it was decided that some of the wire-burning experiments should be repeated to determine whether the addition of water vapor to the chamber gases would also lead to an enhancement of the hydroxide bands at the expense of the oxide bands.

The spectra in "dry" and "moist" gases for the flames of magnesium, calcium and strontium are shown in Figures 39, 40 and 41 respectively. These spectra were taken with a McPherson Model 216.5 half-meter spectrograph using



UV BAND SYSTEMS OF THE $\text{Mg} - \text{O}_2$ FLAME SPECTRUM
(WIRE EXPERIMENT)

TABLE 11SPECTRAL FEATURES OBSERVED IN THE MAGNESIUM FLAMES (WIRE EXPERIMENTS)Ref. Brzustowski (16, 54)

λ [A°]	SPECIE	ENERGY LEVELS [K]	COMMENTS
2852.13	MgI	0-35051	self-reversed
3091.08	"	21850-54192	weak
3092.99	"	21870-54192	"
3096.90	"	21911-54192	"
3329.93	"	21850-51872	"
3332.15	"	21870-51872	"
3336.68	"	21911-51872	"
3829.35	"	21850-47957	
3832.31	"	21870-47957	
3838.26	"	21911-47957	
4030.75	Mn	0-24802	impurity
4033.07	Mn	0-24788	"
4034.49	Mn	0-24779	"
4571.15	MgI	0-21870	inter-system line $^3P_1 \rightarrow ^1S_0$
5167.34	MgI	21850-41197	
5172.70	"	21870-41197	
5183.62	"	21911-41197	
5889.96	Na	0-16973	impurity
5895.93	Na	0-16956	"

In addition to the above atomic species, the MgO green band system $B'\Sigma \rightarrow X'\Sigma$ 5007.3 A° and complex bands in the UV were observed. The $C'\Sigma^- \rightarrow A'\Pi$ and $D'\Delta \rightarrow A'\Pi$ UV systems which have recently been analyzed were identified among the complex bands in the UV. Other UV bands are still unanalyzed.

Polaroid Film Type 57 with an ASA rating of 3000. The region of the spectrum observed was centered about 4000 A°, 6000A° and 6300 A° for the flames of Mg, Ca and Sr respectively. These wavelength regions permitted the observation of the following regions: the UV region for magnesium in which the bands of MgOH and the $C \rightarrow A$ and $D \rightarrow A$ systems of MgO overlap; the green and orange regions for calcium in which the bands of CaOH and two systems attributed to an oxide of calcium overlap; the region from 5950 A° to 6100 A° where bands of SrOH and an oxide of strontium overlap.

A comparison of the spectra in Figures 39, 40 and 41 does confirm the identification of the band systems in both the wire experiments reported earlier in this chapter and the burner experiments reported below. In the wire experiments the predominant emitter is the oxide, whereas in the burner experiments the presence of the hydroxide bands, in the region where oxide and hydroxide bands overlap, is confirmed.

2. Two-Dimensional Diffusion Flame Burner Experiments

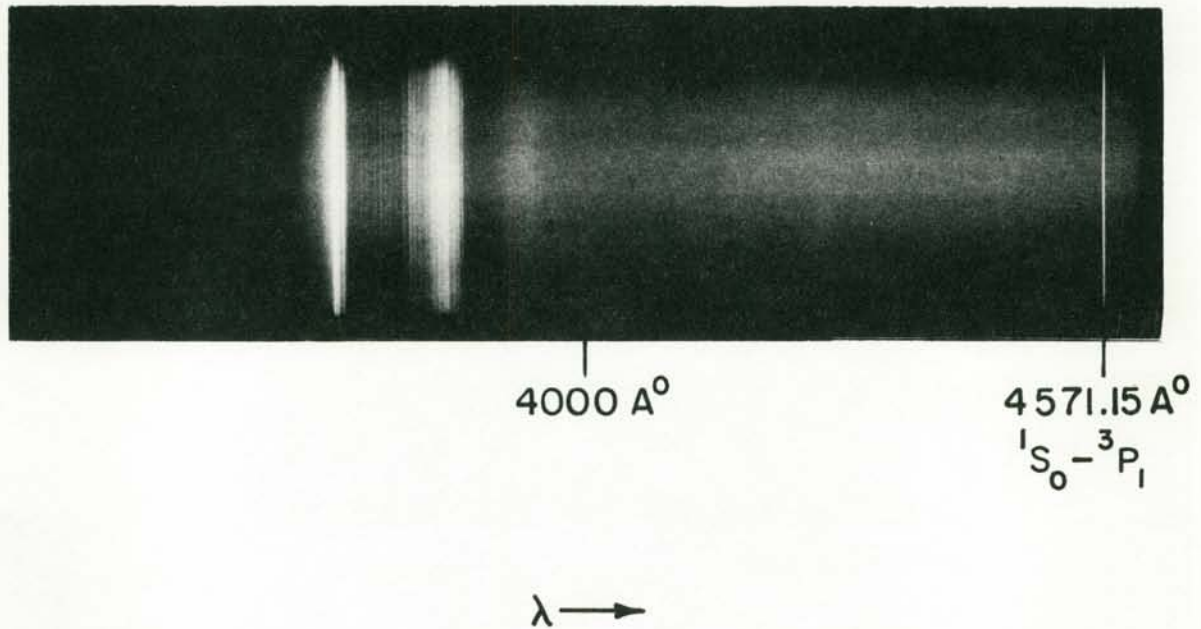
The experiments in the two-dimensional diffusion flame burner were conducted at pressures of 100 or 200 torr because of limitations of the apparatus at both higher and lower pressures. The oxidizer mixture was 10% Oxygen and 90% Argon in all but a few of the experiments. The carrier gas for the metal vapor was argon. The combustion chamber was filled with argon prior to the experiment.

a. Magnesium Burner Experiments

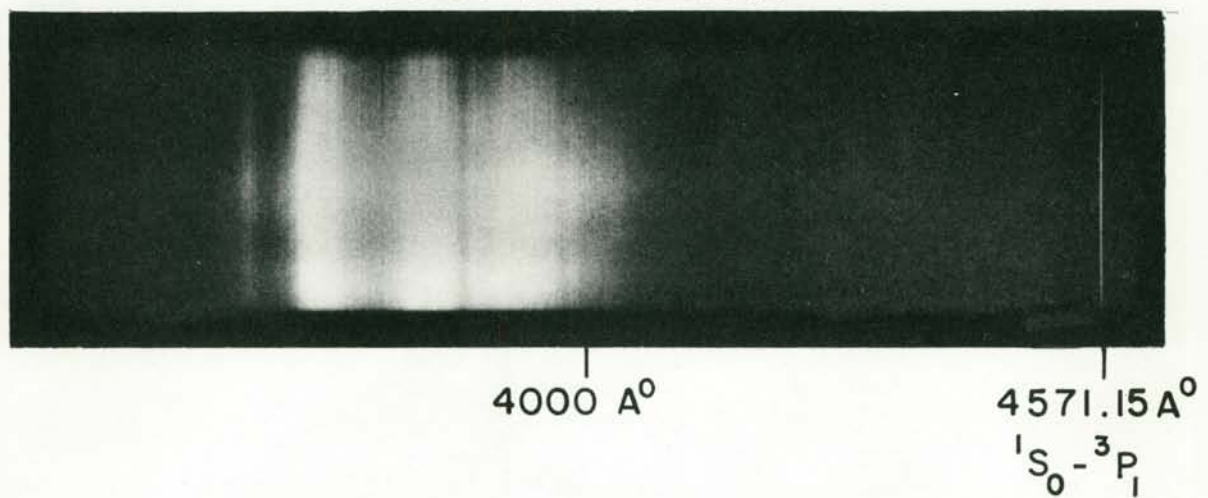
Because of its higher vapor pressure, magnesium was the metal used in the initial experiments in the two-dimensional diffusion flame burner. More experiments have been performed for magnesium than for either of the other two metals, calcium and strontium, but the experimental observations suggest common features in their combustion behavior for all three of these metals. The magnesium results will be presented in somewhat more detail than those for calcium and strontium

(110)

DRY ATMOSPHERE



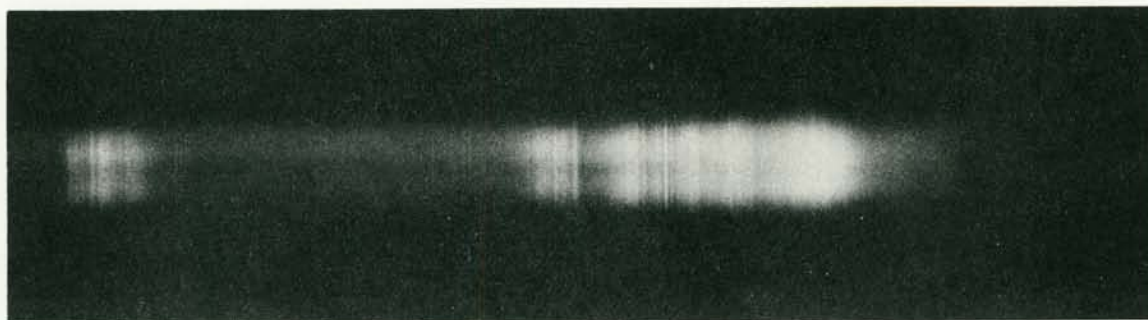
MOIST ATMOSPHERE



EFFECT OF WATER VAPOR
MAGNESIUM WIRE EXPERIMENT

(III)

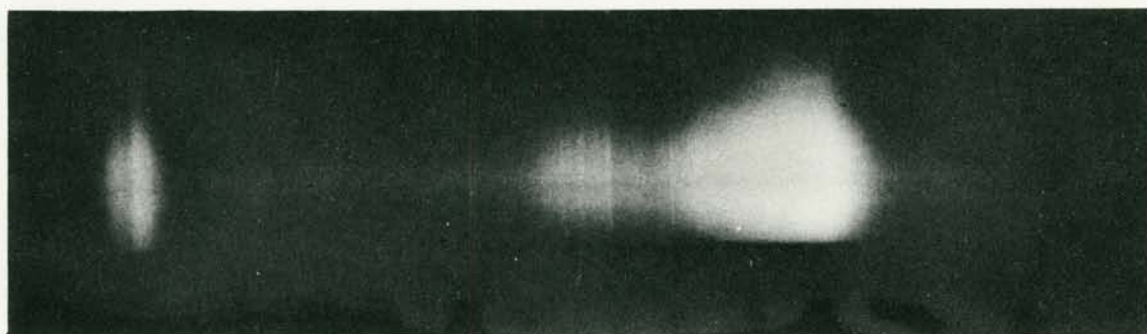
DRY ATMOSPHERE



|
6000 A°

$\lambda \rightarrow$

MOIST ATMOSPHERE



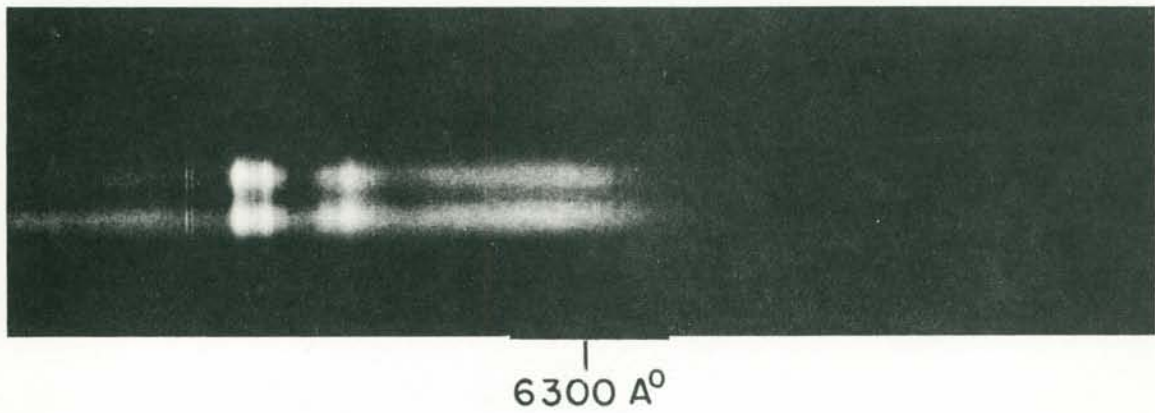
|
6000 A°

EFFECT OF WATER VAPOR
CALCIUM WIRE EXPERIMENT

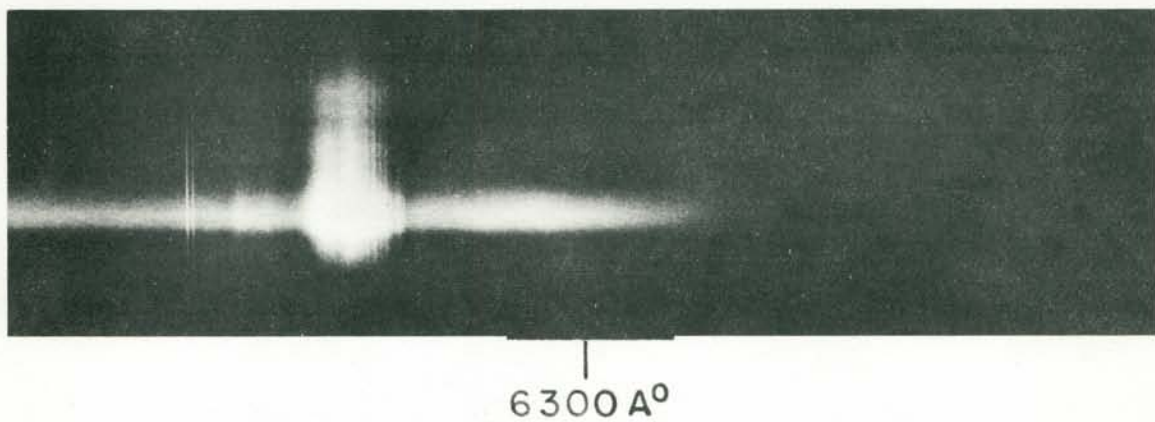
FIGURE 40

(112)

DRY ATMOSPHERE



MOIST ATMOSPHERE



EFFECT OF WATER VAPOR
STRONTIUM WIRE EXPERIMENT

FIGURE 41

but it should be noted that they are probably typical observations for the alkaline-earth metals.

(i) Visual Observations

When the metal sample was placed in the pre-heated burner assembly in which all the gas flows were already established, a flame appeared almost immediately at the exit of the fuel and oxidizer ducts. The flame appeared to extend to the duct exit, i.e., no dark space was observed between the end of the ducts and the start of the luminosity.

The flame was wedge-shaped with the thickness of the wedge increasing gradually as one moved from the duct exit to positions further from the burner. The central region of the wedge when viewed end-on appeared to have the highest luminosity but the variation in intensity across the flame was gradual.

The flames observed were quite steady and could be maintained for a period of several minutes.

One of the problems encountered initially was the buildup of a deposit on the lip of the metal divider between the two ducts. For the conditions under which these experiments were eventually performed, i.e., furnace temperature, flow rates, oxidizer mixtures, etc., it was observed that although a deposit still formed, it did not appear to distort the flame geometry or influence the gross features of the flame as the deposit grew in size.

The overall duration of the experiment was a com-

promise to allow a reasonable amount of time for spectroscopic observations before the buildup of the deposit at the burner exit affected the flame significantly and before the amount of oxide generated in the chamber coated the chamber windows appreciably.

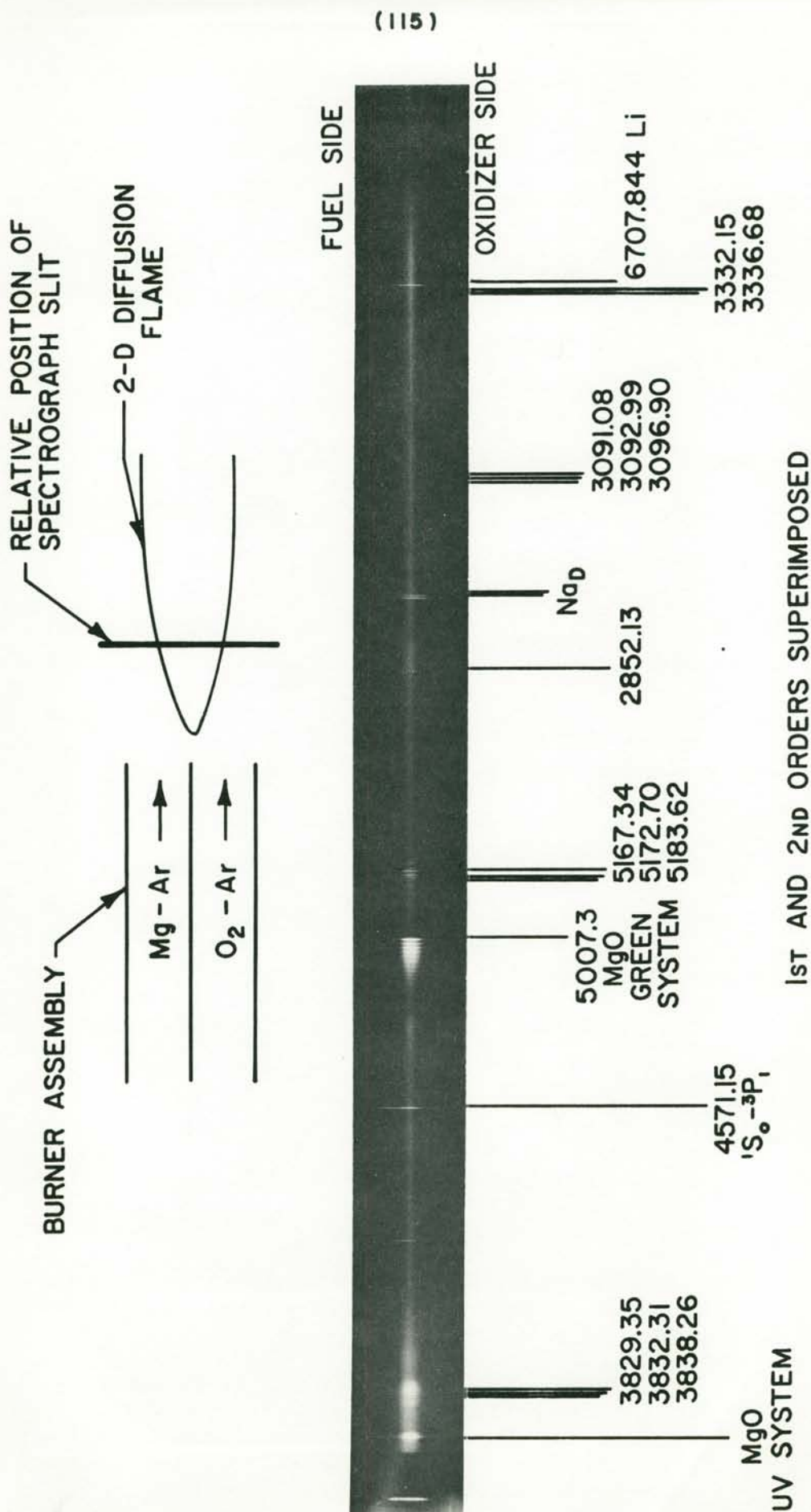
(ii) Space-Resolved Spectroscopic Observations

To determine the relative locations in the flame of the various radiating species, space-resolved spectra of the two-dimensional diffusion flames were obtained as indicated in the schematic in Figure 42. The portion of the flame viewed by the spectograph was a region approximately 12 mm above the burner top. This distance corresponds to about half of the overall flame length.

A typical space-resolved spectrum of a magnesium flame for these experiments is reproduced in Figure 42. The details of the spatial variation of the lines and bands observed can be seen more clearly in the enlarged photographs of certain regions of this spectrum which are presented in Figures 43 and 44.

The species observed in these spectra were the same for the magnesium burner experiments as they were for the magnesium wire experiments with the following exceptions:

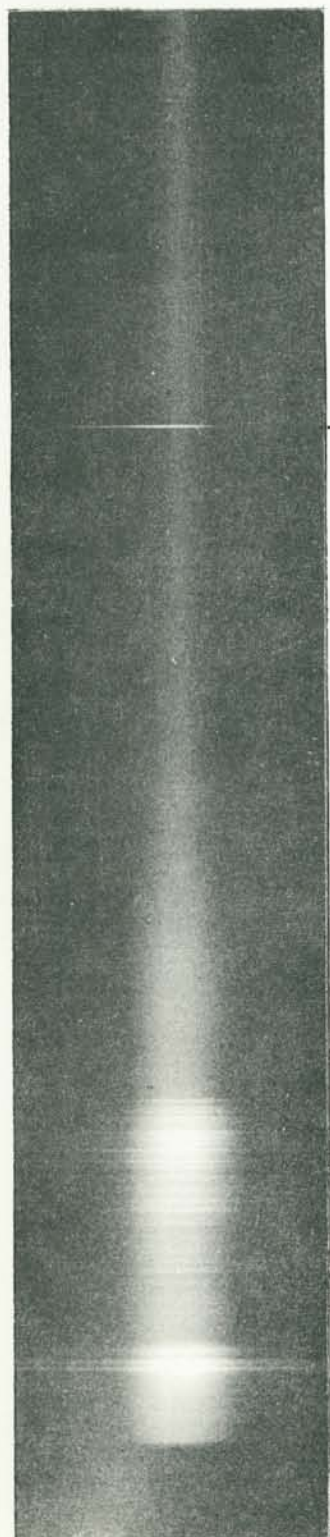
- (1) The MgO "red system" which was not observed in the wire experiments was observed weakly in these burner experiments.
- (2) Different impurity lines were observed. The manganese lines observed in the Mg wire experiments were not seen in the burner experiments. The resonance lines of both Ca and Li were observed in the Mg burner spectra.



SPECTRUM OF MAGNESIUM 2-D DIFFUSION FLAME
TOTAL PRESSURE 200mm Hg OXIDIZER MIXTURE 10%O₂-90%Ar

FIGURE 42

OXIDIZER
SIDE
FUEL
SIDE



3829.35
3832.31
3838.26

MgO
UV SYSTEMS

4226.73Ca

(116)

OXIDIZER
SIDE
FUEL
SIDE



4571.15
 $1S_0 - 3P_1$

MgO 5007.3

5167.34
5172.70
5183.62

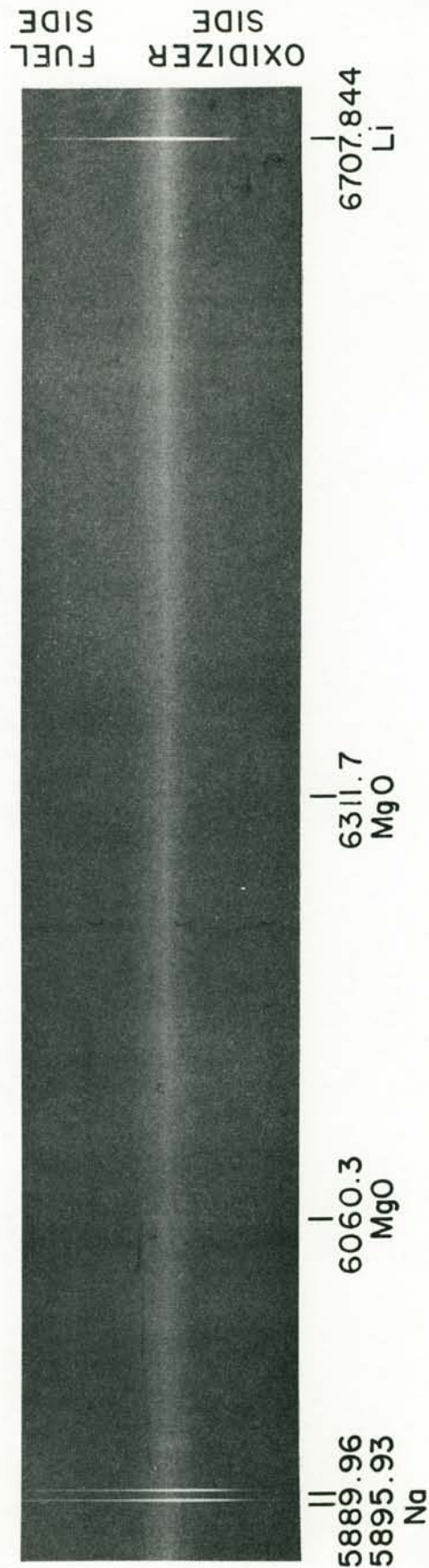
SPECTRUM OF MAGNESIUM 2-D DIFFUSION FLAME

TOTAL PRESSURE 200mm Hg OXIDIZER MIXTURE 10%O₂ - 90% Ar

FIGURE 43



(117)



SPECTRUM OF MAGNESIUM 2-D DIFFUSION FLAME

TOTAL PRESSURE 200 mm Hg OXIDIZER MIXTURE 10% O₂ - 90% Ar

FIGURE 44

Since the magnesium in the wire experiments and the burner experiments came from different sources it is not surprising that the observed impurity lines do not correspond in the two experiments. It should be noted however that the Li line at 6707.844 \AA was observed in the burner spectra of Mg, Ca and Sr and it is likely that this impurity arises from some part of the burner assembly rather than the metal sample itself.

3. The amounts of water vapor present as impurity in the chamber gases appeared to be more of a problem in the burner experiments than in the previously reported wire experiments. Thus, the complex bands in the UV probably contain a greater contribution from MgOH than was observed in the wire experiments although all of the strong features including the $C \rightarrow A$ and $D \rightarrow A$ transitions for MgO were observed in the magnesium burner spectra.

The important features of these burner spectra are the intensity variations of the various lines and bands with respect to their location in the flame. A convenient reference line is the narrow streak of continuum present in the middle of the spectrum which is most likely due to emission by the hot condensed oxide particles. In the following paragraphs reference will be made to the fuel side and the oxidizer side of the flame relative to this region of continuum radiation. The fuel and oxidizer sides of the flame are indicated in Figures 42, 43 and 44.

The continuum radiation was always relatively weak in intensity in comparison with the line and band emission observed. In addition, as indicated above, it is confined to a rather narrow region of the flame.

Lines of Mg as well as several impurities are observed to extend to both the oxidizer and fuel sides of

this continuum streak. In most cases, the peak intensity of these lines was near or coincided with the location of the continuum radiation, although some radiation was observed at locations reasonably distant from this continuum streak.

The resonance line of Mg at 2852.13 \AA is observed in second order. It is quite weak in intensity and is observed to be self-reversed. It is also wedge-shaped in appearance, being much broader on the fuel side of the continuum streak and narrowing in breadth as one moves toward the oxidizer side.

The red, green and two UV band systems of MgO are all observed in these spectra. The peak intensity of these band systems appears to coincide with the location of continuum radiation in the flame, but the bands are observed in emission on both the fuel and oxidizer sides of this continuum streak.

Bands in the UV which are not a part of the C-A and D-A transitions of MgO but are believed to be MgO bands are also observed. Three of these features extend rather far from the region of continuum radiation although their intensity is greatly reduced in these regions.

b. Calcium Burner Experiments

(i) Visual Observations

As in the case of magnesium, steady flames were observed at the exit of the ducts for the case of calcium. The flame appeared slightly smaller in overall dimensions

with a somewhat thinner wedge shape as well. The flame appeared to extend to the burner lip with no evidence of a dark zone between the burner itself and the onset of radiation.

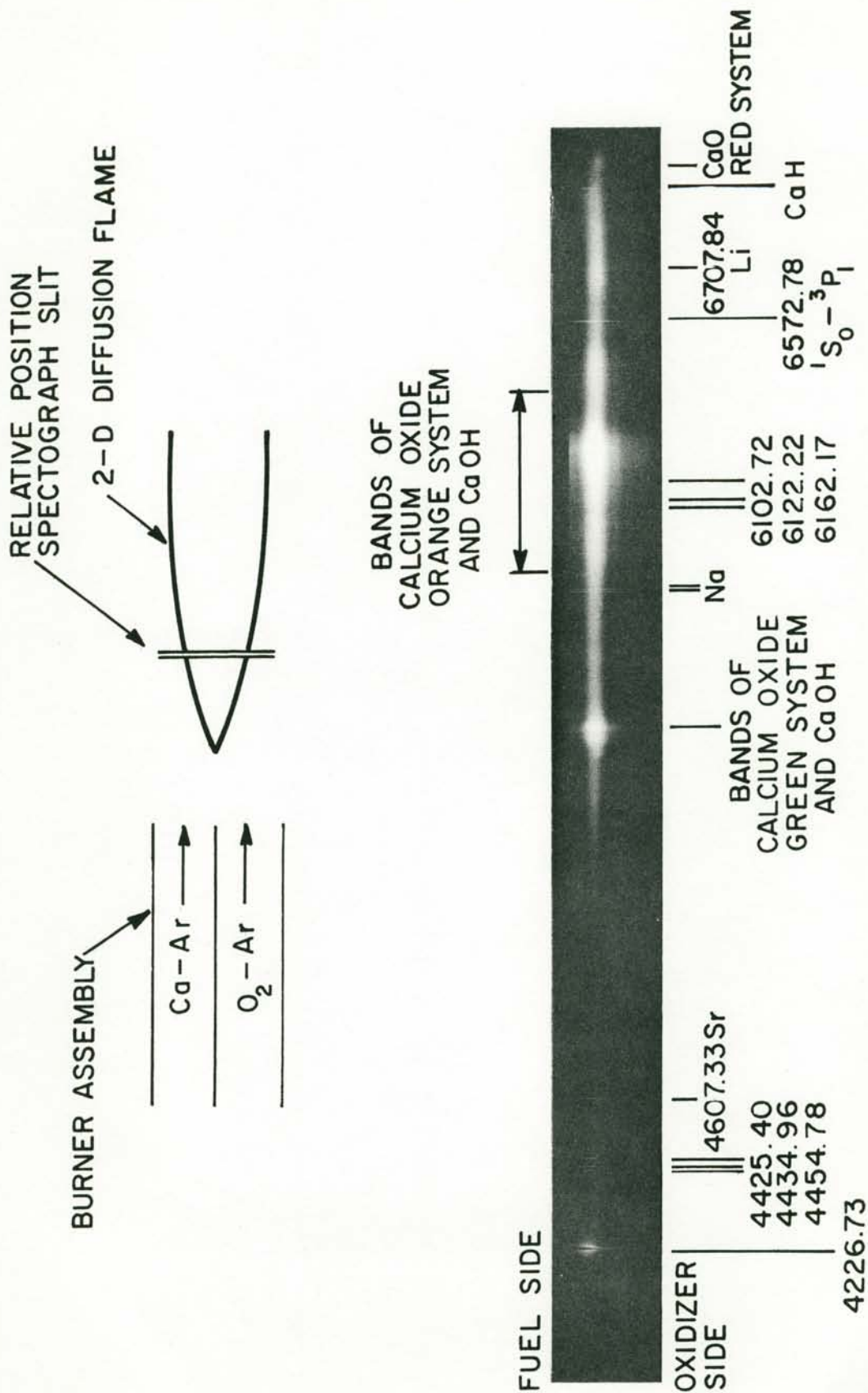
The problems with the growth of the deposit on the metal separation between the ducts were much reduced. The deposit remained much smaller than in the case of magnesium and did not appear to distort the flame.

(ii) Space-Resolved Spectroscopic Observations

A typical space-resolved spectrum for a two-dimensional calcium diffusion flame is reproduced in Figure 45. Enlargements of particular regions of this spectrum illustrating the spatial variation of the intensity of the lines and bands are provided in Figures 46 and 47.

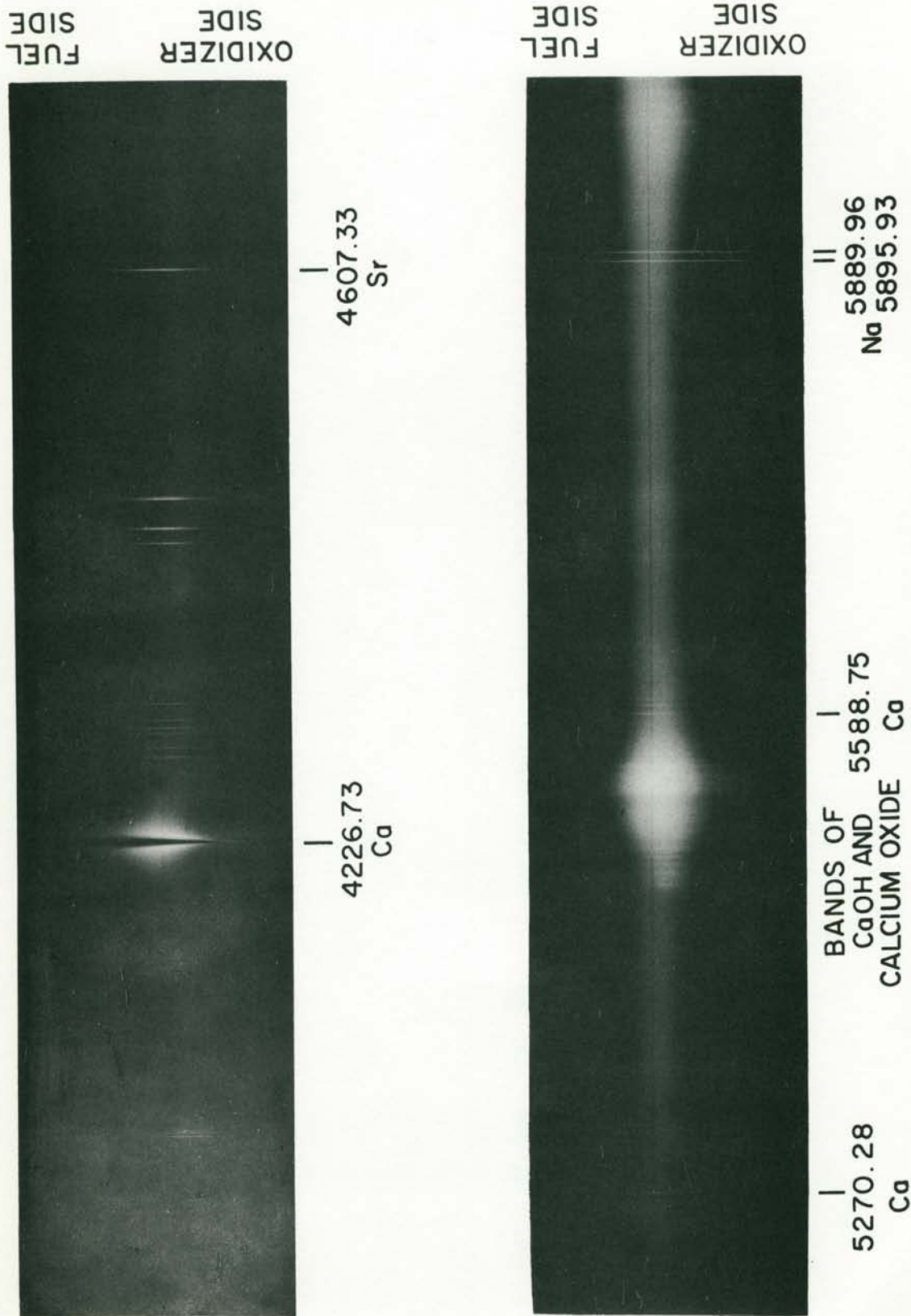
The species identified in these spectra are the same as those identified for the calcium flames in the wire experiments with the following exceptions:

- (1) The green bands due to the hydroxide CaOH are observed in addition to the bands of the green system of calcium oxide. In the orange region it is more difficult to determine which emitter predominates. This can be substantiated by the spectra taken in "dry" and "moist" atmospheres reported earlier in this chapter.
- (2) Bands of CaH were observed in the region near 6920 \AA .
- (3) The weak bands observed at slightly longer wavelengths than the CaH bands, appear to be the first few bands of the CaO "extreme red system" the great majority of which falls outside the range of the spectrograph used in these investigations.



SPECTRUM OF CALCIUM 2-D DIFFUSION FLAME

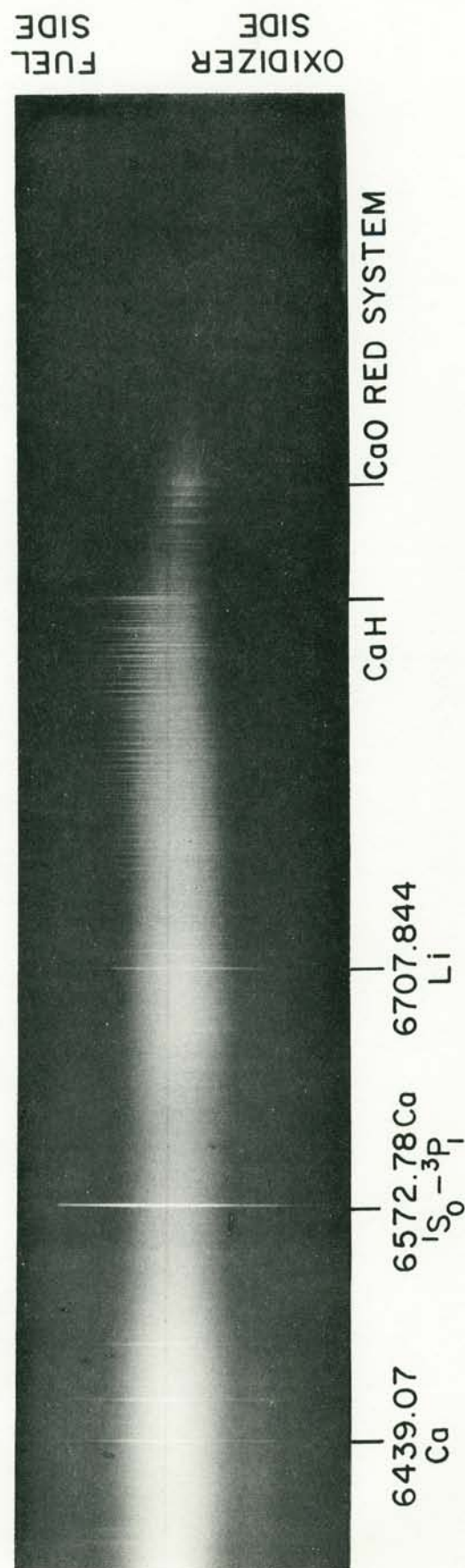
TOTAL PRESSURE 200 mm Hg OXIDIZER MIXTURE 10% O_2 -90% Ar



SPECTRUM OF CALCIUM 2-D DIFFUSION FLAME
 TOTAL PRESSURE 200mm Hg OXIDIZER MIXTURE 10% O₂ - 90% Ar



(123)



SPECTRUM OF CALCIUM 2-D DIFFUSION FLAME
TOTAL PRESSURE 200 mm Hg OXIDIZER MIXTURE 10%O₂-90%Ar

The variation in intensity as a function of location in the flame indicates that the magnesium and calcium flames are quite similar. The continuum radiation is weak in intensity relative to the lines and bands observed. As in the case of magnesium, this continuum radiation is confined to a rather narrow region of the flame. Bands of the oxide and hydroxide as well as numerous lines of the metal and several lines due to impurities extend beyond the region of continuum radiation on both the fuel and oxidizer sides of the flame.

The resonance line of Ca at 4226.73 \AA is self-reversed. It is wedge-shaped as was the corresponding line for Mg, with the broad edge of the wedge on the fuel side, and the tapering of the line width occurring as one moves towards the oxidizer side of the flame.

c. Strontium Burner Experiments

(i) Visual Observations

The visual observations for the strontium two-dimensional diffusion flame are in almost all respects the same as those for the calcium flame. The growth of the deposit at the lip of the burner was also less troublesome than in the case of magnesium.

The flames observed were quite steady and no trouble was experienced in obtaining sufficient exposure times for spectroscopic observations.

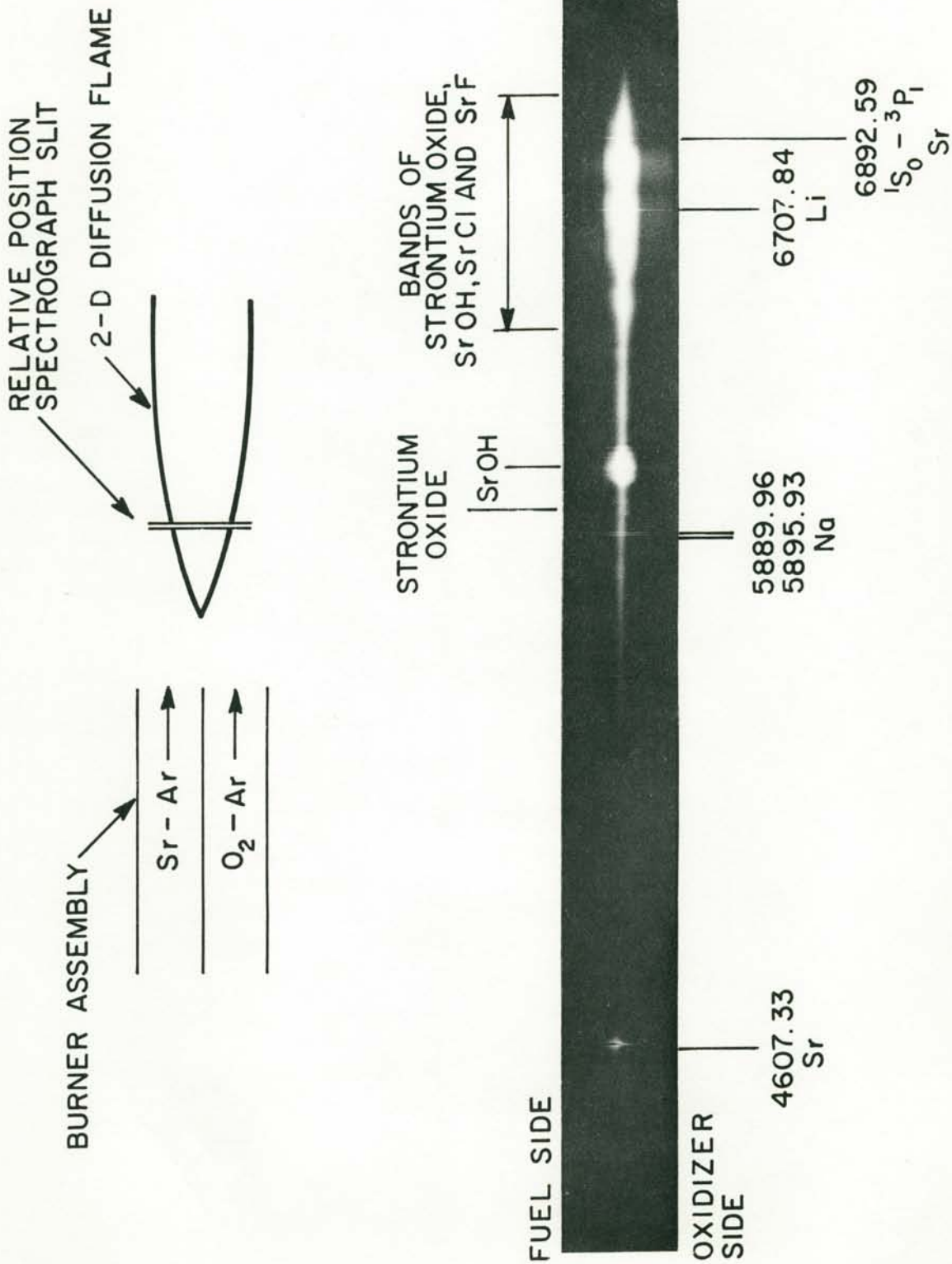
(ii) Space-Resolved Spectroscopic Observations

A typical spectrum of a strontium flame for these burner experiments is reproduced in Figure 48. Enlargements of particular regions of this spectrum are presented in Figures 49 and 50 to illustrate more clearly the spatial variation of the spectral features observed.

The spectral features observed in these burner spectra were the same as those identified in the strontium wire experiments with the following exceptions:

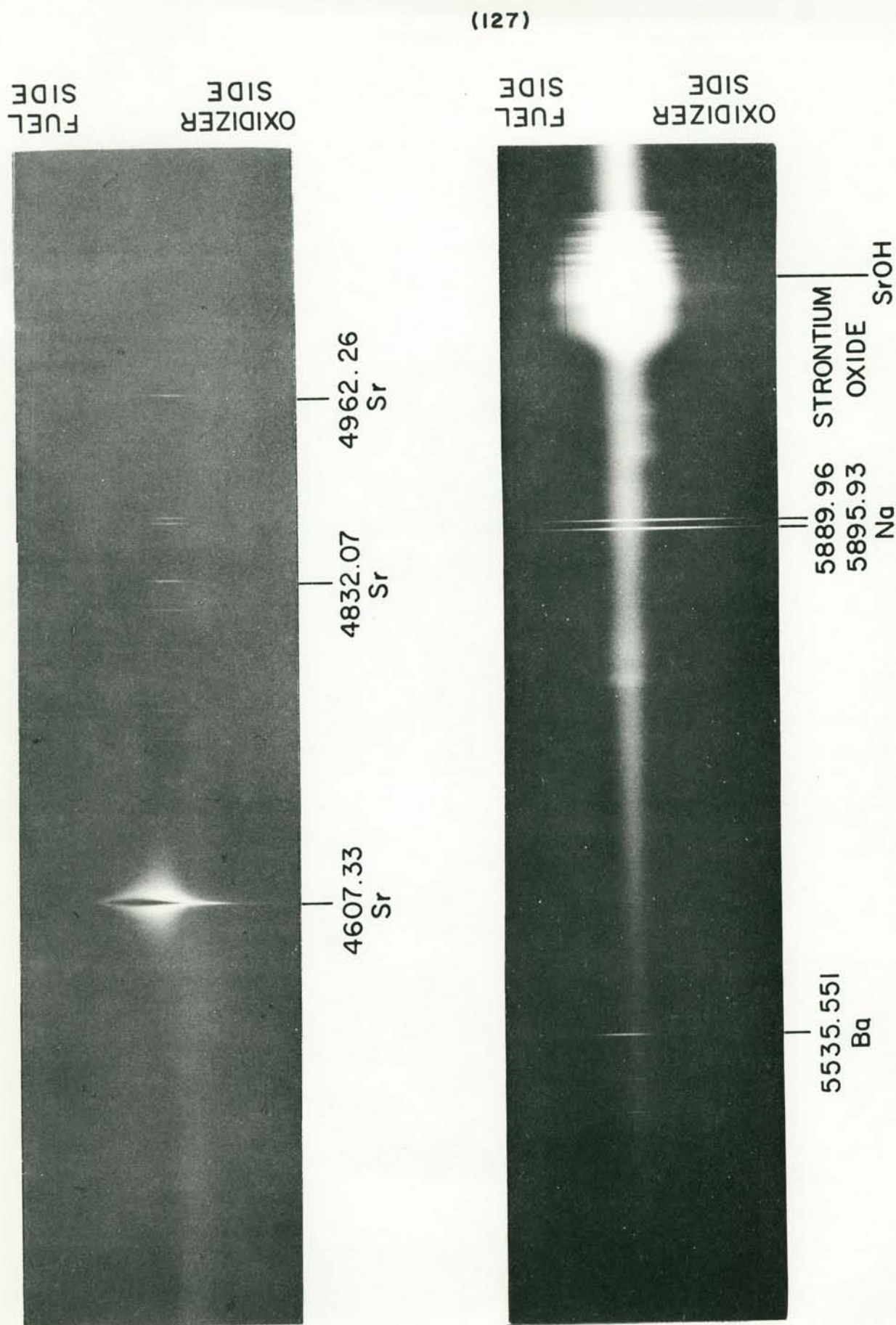
- (1) The bands due to SrOH in the region near 6050 \AA appeared much more strongly than the oxide bands which partially overlap the hydroxide bands. This observation was confirmed by the wire experiments in "dry" and "moist" atmospheres reported earlier in this chapter. Plate comparison of the spectra in Figure 41 illustrates that the addition of water vapor results in an enhancement of the same bands that were observed in the strontium burner spectra and attributed to SrOH .
- (2) A tentative identification was made for bands of SrCl at 6744.7 and 6613.7 \AA respectively and bands of SrF were identified at 6632.7 and 6512.0 \AA respectively. These bands are clearly marked and are violet degraded. This description fits both the strontium chloride and strontium fluoride systems. It does not fit the descriptions of either the SrO or SrOH systems which lie in overlapping regions of the spectrum.

The intensity variation, as a function of position in the flame, for the lines and bands of the metal and metal oxide vapor as well as the lines due to several impurities show a similarity to the corresponding observations in the magnesium and calcium flames.



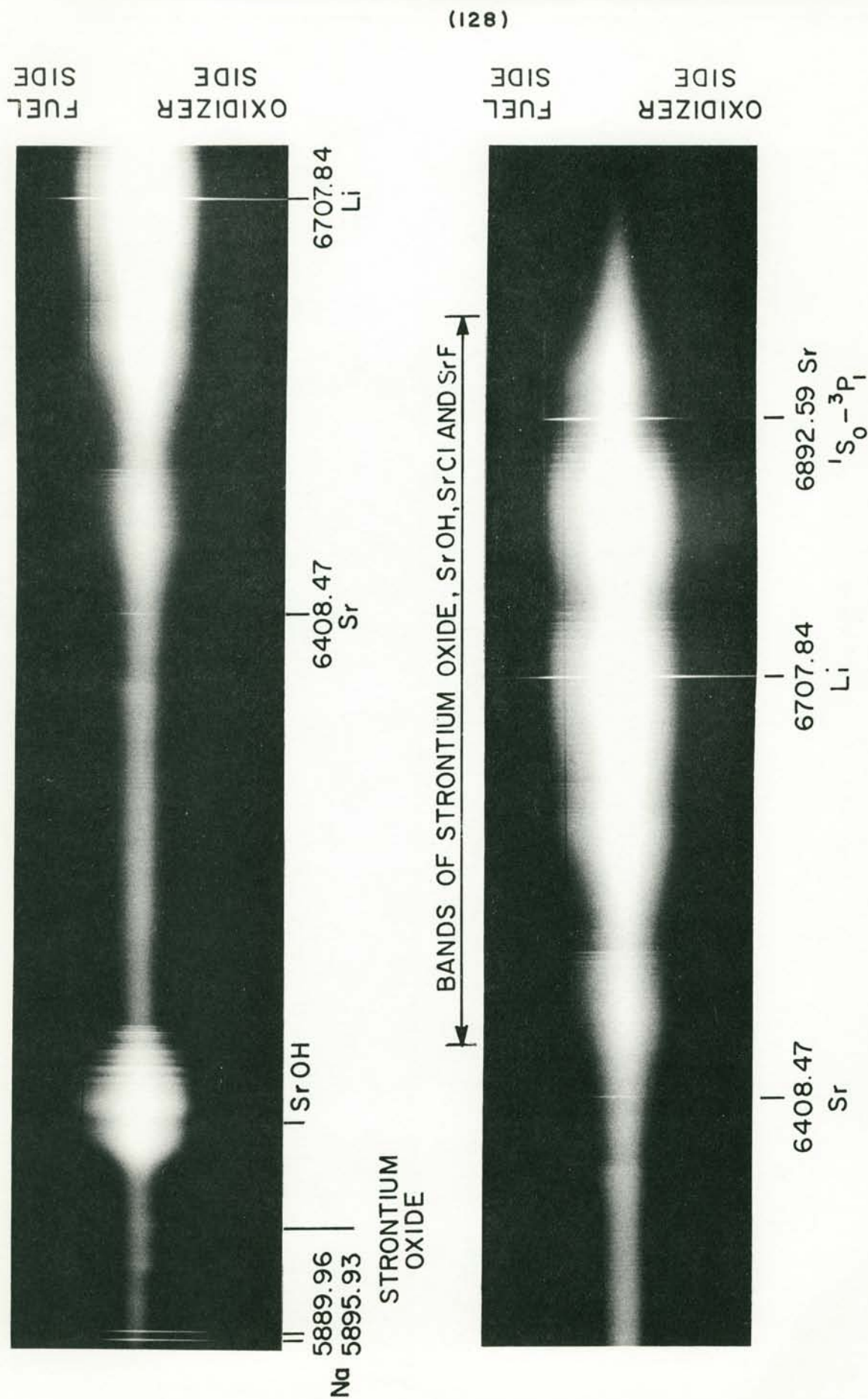
SPECTRUM OF STRONTIUM 2-D DIFFUSION FLAME

TOTAL PRESSURE 200mm Hg OXIDIZER MIXTURE 10% O_2 - 90% Ar



SPECTRUM OF STRONTIUM 2-D DIFFUSION FLAME

TOTAL PRESSURE 200 mm Hg OXIDIZER MIXTURE 10% O₂ - 90% Ar



SPECTRUM OF STRONTIUM 2-D DIFFUSION FLAME

TOTAL PRESSURE 200 mm Hg OXIDIZER MIXTURE 10% O_2 - 90% Ar

The continuum radiation is observed to be rather weak in intensity relative to the line and band radiation. In addition, it is confined to a rather narrow region of the flame.

Most of the lines and bands have their peak intensity located near or coincident with the location of the flame emitting the continuum radiation, although the radiation from these vapor species does extend to locations on both the fuel and oxidizer sides of this continuum streak.

The resonance line of Sr at 4607.33 \AA shows the same self-reversed and wedge-shaped profile that was observed for the corresponding lines of Mg and Ca.

CHAPTER VI - DISCUSSION AND INTERPRETATION OF EXPERIMENTAL OBSERVATIONS

In this chapter an attempt is made to interpret the observations reported in the previous chapter on the basis of the flame model of Brzustowski and Glassman (15). Discrepancies between these observations and the Brzustowski-Glassman model are noted. A new model for the flame structure which accounts for the observations of the present investigation and for the results of other investigators will be outlined in Chapter VII.

1. Comments on the Spectroscopic Observations

Although specific comments will be made in sections 2 and 4 of this chapter for the spectroscopic observations of each of the metals calcium, strontium and magnesium for both the wire and burner experiments, it is appropriate to make some general comments first.

In Chapter III it was pointed out that much confusion still exists regarding the band systems attributed to the oxides of the alkaline-earth metals. In most cases there has been an observation of a complex series of bands that have not been analyzed, and although they are assigned to an oxide, it is not certain that the emitter is not polymeric or polyatomic. In any case, it is generally suggested that the complexity of these bands rules out the likelihood that they are due to transitions between singlet states, and that triplet states are one possibility; the other possibility is a polymeric or polyatomic emitter.

The above postulates regarding the emitter of these bands are particularly interesting in view of the spectroscopic observations in the wire experiments for the flames of calcium, strontium and magnesium. For both calcium and strontium, none of the analyzed band systems assigned to transitions between singlet states of the simple oxides, CaO and SrO , are observed. Instead the two band systems which are observed for each of these flames are the complex systems that are still unanalyzed. In the case of magnesium, spectroscopic observations showed that one of the analyzed band systems, the green bands for the $B'\Sigma \rightarrow X'\Sigma$ transition in MgO , is observed, but in addition a complex system of bands in the UV is present.

One might postulate that a possible explanation for the spectroscopic observations noted above is that conditions in the flame are favorable to the production of polymeric and/or polyatomic oxides of the alkaline-earth metals, or at least that triplet states of the simple oxide are favored in comparison to the singlet states. Such information is very important to the determination of flame structure since it might be an indication of the individual kinetic steps involved in the overall reaction.

However, when one also considers the spectroscopic observations for the burner experiments in addition to some new spectroscopic information in the literature, it appears less likely that the conditions in the flame favor polymeric or polyatomic emitters or triplet states instead of singlet states of the diatomic oxide.

In the case of magnesium the experiments of Brewer and Trajmar (27), Brewer, Trajmar and Berg (32), Trajmar and Ewing (34, 35) and Green (36) have shown that many of the complex bands in the UV that had been unanalyzed and thought to be due to a polymeric or polyatomic oxide, or transitions between triplet states of MgO are in fact none of these. Two new band systems corresponding to the transitions $C'\Sigma \rightarrow A'\pi$ and $D'\Delta \rightarrow A'\pi$ between two new singlet states ($C'\Sigma^-$ and $D'\Delta$) and a previously known singlet state ($A'\pi$) of MgO have been found among the complex UV bands. Although a few features existing in the UV spectra of magnesium flames are still not contained in the newly identified band systems mentioned above, it is not likely that they are due to an oxide other than MgO, i.e., they are probably neither polymeric or polyatomic (27). Since most of the bands observed in the UV region in the spectra of magnesium flames thus correspond to transitions between singlet states of MgO, the suggestion that these flames may be a source favorable to the production of triplet states and polyatomic or polymeric oxides must be looked at somewhat doubtfully.

In the case of calcium and strontium it is a possibility that the complexity of the unanalyzed bands attributed to their oxides could also be due to an overlapping of band systems corresponding to transitions between singlet states as was found for magnesium. The recent work of Hauge (37) in which an oxygen isotope substitution experiment was performed to identify the emitter of the green and orange band systems

attributed to calcium oxide, has not resolved this problem and the identity of the emitters is still in doubt.

The results of the burner experiments for calcium showed that one of the analyzed band systems of the diatomic oxide CaO , the "extreme red system", did appear weakly in the spectra. Most of the "extreme red system" falls outside the range of the spectrograph used in the present investigation, but a few weak bands lie within the region of the spectrum observed. The corresponding system for Sr falls outside the spectral region observed. The absence of the analyzed band systems in the spectra in the wire experiments is most likely due to a lack of intensity (i.e., these systems would be observed if exposure times were not limited by the duration of the flame).

2. Wire Burning Experiments

a. Calcium

The appearance of an inner zone of orange radiation extending from a point near the wire surface to a position at about half the radius of the luminous envelope, can not be explained on the basis of the Brzustowski-Glassman flame model. In the Brzustowski-Glassman model the reaction zone is assumed to be a collapsed front at the outer edge of the luminous envelope. The only specie assumed to be present between this collapsed reaction zone and the wire surface is metal vapor. If the inner zone of the flame is hot enough to cause the metal vapor to radiate, then the radiation should not fall off at half radius, since in the Brzustowski-Glassman model the maxi-

mum temperature is thought to occur at the collapsed flame front at the outer edge of the luminous envelope.

The photographs of the calcium flame at selected wavelength regions of the spectrum using narrow pass interference filters, demonstrate that the inner zone of radiation is indeed more than just metal vapor as the Brzustowski-Glassman model indicates. CaO vapor is present in this inner region of the flame, and the radiation appears to extend to locations quite near the wire surface. Even if one were to relax one of the assumptions of the Brzustowski-Glassman model, which is that all combustion products formed in the flame front diffuse outwards and back-diffusion of products can be neglected, it is still not possible to explain why the radiation of the CaO vapor is concentrated in the inner half of the luminous envelope. As pointed out in Appendix A, the amount of CaO vapor in the evaporation products is a small fraction of the total species evaporated so that the maximum concentration of CaO vapor would be expected at the location where the largest amount of evaporation occurred, namely the high temperature collapsed reaction zone in the case of the Brzustowski-Glassman model. It is not likely that the temperature variation over a distance of about half the flame radius could so drastically alter the amount of oxide vapor dissociated as to cause the absence of CaO radiation from the region where one expected both the highest concentration and the highest temperature and instead account for the concentration of CaO vapor radiation

in the inner half of the luminous envelope. If the CaO vapor in the inner half of the luminous envelope is not the result of back-diffusion of evaporated products, it must be the result of reaction occurring in the inner zone.

The space-resolved spectra of the calcium flame reinforce the observations of the selected wavelength experiments mentioned above. Reference to Figure 32 shows that both band systems attributed to the oxide show an intensity variation which peaks in the inner radiation zone between the wire and about half the radius of the luminous envelope. The spectral lines due to calcium vapor show the same type of intensity variation as a function of distance from the wire. Most of these lines do not extend beyond the edges of the luminous envelope, although the calcium resonance line at $4226.73 \text{ \AA}^{\circ}$ is observed to do so. It is believed that the effect is real and not due to film halation or light reflections within the spectrograph during exposure.

The shape and intensity variation of this calcium resonance line does indicate the possible variation of the flame temperature as a function of the radius. This line is extremely broad in the inner radiation zone close to the wire, where the concentration of Ca vapor is highest. The line is also self-reversed in this region. As one moves further from the wire, the line width tapers off rapidly, the self reversal disappears and the line appears in emission in the outer regions of the luminous envelope. If this line corresponds to equilibrium

excitation of the calcium vapor for the flame temperature, it indicates that the inner radiation zone of the flame is indeed the region of highest temperature since the colder calcium vapor from the outer zone of the flame absorbs the radiation from the hotter calcium vapor in the inner zone causing the resonance line to be self-reversed over a portion of its length. It is important to note that the resonance line does appear in emission while still within the limits of the luminous envelope, an indication that it is not cold Ca vapor in the combustion chamber which causes the self-reversal, but rather that the regions of hot Ca vapor and cold Ca vapor are both within the flame itself.

However, if the excitation of the Ca vapor does not correspond to equilibrium at the flame temperature, one can only say that the electronic temperature of the Ca vapor is highest in the inner zone and that chemiluminescence may be responsible for the Ca vapor radiation.

b. Strontium

All of the comments in the preceding section for calcium can be extended to the case of strontium. The visual and photographic observations indicate a bright zone of orange-red radiation well inside the luminous envelope. As in the case of calcium, the space-resolved spectra for strontium flames indicate that the spectral band systems attributed to strontium oxide and the spectral lines due to the strontium vapor have a spatial intensity variation which confirms the fact that both metal and metal oxide vapor radiate strongly

in the inner region of the flame.

The resonance line for strontium at 4607.33 \AA has the same characteristic appearance as the equivalent line for calcium, i.e., it is self-reversed over the middle portion of its length, but is in emission in regions still within the luminous envelope. Thus the comments expressed above about the temperature variation as a function of radius are also appropriate for the case of strontium.

c. Magnesium

Since the magnesium flame lacks the symmetry of the calcium and strontium flames, very little can be said about the flame structure based on visual and photographic observations. The flame has a characteristic blue-green color, but this colored radiation does not appear to be confined to the inner regions of the luminous envelope as for calcium and strontium. The edges of the luminous envelope are also not clearly defined.

The resonance line for magnesium is observed to be self-reversed. However, since space-resolved spectra were not obtained for magnesium flames due to the lack of symmetry, it is not certain where the location of the cold magnesium vapor is, i.e., whether it is still within the luminous envelope or whether it is outside the flame itself.

3. Effect of Water Vapor

Figures 39, 40, and 41 of Chapter V which provide a comparison of the flame spectra of Mg, Ca and Sr respective-

ly in both "dry" and "moist" atmospheres illustrate that the predominant emitters in the case of the wire experiments are the systems attributed to the respective oxides, rather than the hydroxides. However, in view of the difficulties involved in completely removing all traces of water vapor, it is likely that there will always be some small contribution from the hydroxide. Also, as was pointed out in Chapter III, Schofield (24) indicates that the dihydroxide has been shown to be more important than the diatomic oxide in flames containing hydrogen, except perhaps in flames of very high temperature with very low water content. Considering the high temperatures expected in metal flames and the attempts made in these investigations to keep the amount of water vapor at a low level, it is felt that the role played by the hydroxide and/or dihydroxide may be unimportant.

In the burner experiments to be reported in the following sections of this chapter, it became obvious from the spectra that the contribution from the hydroxide bands was greater than it was in the wire experiments. Since the gases used were from the same source in both cases, and the metal samples came from a common source, it appeared that the water vapor problems in the burner experiments were connected in some way with the apparatus itself, perhaps the refractory casting surrounding the burner assembly. Thus far no attempts have been made to eliminate this difficulty since other investigators (36) have stated that despite a concerted effort

it was not possible to eliminate entirely the spectral evidence indicating the presence of water vapor. If the water vapor cannot be removed entirely, it would seem to be more fruitful to attempt to determine its possible role in the combustion behavior of these metals. The lack of thermochemical data for the hydroxide and dihydroxide makes it almost impossible to assess the importance of small amounts of water vapor in these flames.

4. Two-Dimensional Diffusion Flame Burner Experiments

The general observation that magnesium, calcium and strontium burner flames possess many common features in their spectra, e.g. resonance line shape, narrow continuum streak, similar spatial intensity variation of lines and bands, etc., suggests that a common flame structure model may be applicable to all of these metals.

All of the spectral features observed in the wire experiments are also observed in the burner experiments. The presence of hydroxide bands in the burner spectra of Ca and Sr particularly, appears to reduce the intensity of the bands attributed to the oxide which occur in overlapping regions of the spectrum. However, the same band systems attributed to the oxide are seen in both the wire and 2-D burner experiments, with the exception that the longer available exposure times in the burner experiments also permit the observation of the MgO "red system" and the CaO "extreme red" system, one of the known systems of CaO. This is an important observation

since it indicates that the absence of the known systems of CaO in the spectra of the wire experiments is most likely just due to a lack of intensity.

The consumption of the metal vapor as it diffuses toward the oxidizer side of the flame can be followed by observing the variation of the profile of the resonance line as a function of the distance from the fuel side of the flame in the direction of the region of continuum radiation. There are competing effects on the line intensity. The temperature is increasing and the concentration of metal vapor is decreasing because of the diffusive gradient and because of reaction of the metal vapor. It can be seen from the burner spectra, particularly for the resonance lines of calcium and strontium, that the emission profile broadens considerably at first showing the effect of higher temperature which appears to overcome the counter-acting decrease in metal vapor concentration. Still further across the flame the rapid decrease in metal vapor concentration is shown by significant reduction of the line breadth over a very small distance in the flame.

CHAPTER VII - DISCUSSION OF A NEW FLAME STRUCTURE MODEL

This chapter is a description of a new model for the flame structure of vapor phase metal diffusion flames, in particular the flames of the alkaline-earth metals Mg, Ca and Sr. The initial sections of the chapter discuss the experimental observations which indicate that a reaction region is located in the inner zone of the flame, close to the metal surface. Arguments based on observations from this investigation and from the work of other investigators suggest that a thermal excitation mechanism is the main source of the observed radiation for the metal and metal oxide vapor. Based on a thermal excitation mechanism for the resonance line and the observation regarding the self-reversal of this line over a portion of its length, it is possible to determine the relative temperatures for the two different zones observed in the flame, namely that the inner zone is the high temperature region of the flame.

Since the heat of condensation of the oxide accounts for a major heat release in the flame, it is possible to infer the location in which condensation occurs from a knowledge of the temperature variation in the flame. The predicted location of the condensation region based on the above argument is consistent with what would be expected on the basis of homogeneous gas phase reactions in the inner zone forming a supersaturated oxide vapor thus leading to rapid nucleation of the oxide.

The nature of the condensed oxide particles and of their movements within the flame are then discussed.

The presence of the condensed oxide particles in the reaction zone raises the possibility of heterogeneous reaction on the surface of the condensed oxide competing with homogeneous reaction. Although the relative roles played by these two reaction mechanisms are not completely resolved, the determination of other flame characteristics as mentioned above allows one to predict the regions of the flame in which heterogeneous reaction may predominate.

A comparison is made of the possible kinetic steps leading to the formation of oxide vapor by homogeneous reaction.

Thus, the proposed flame structure model contributes information on the following items: the location of the reaction zone, the nature of the radiation from this zone, the relative temperatures of the two zones observed in the flame, the region in which condensation is likely to occur, the size and movement of the condensed oxide species in the flame, the regions of the flame in which heterogeneous reaction might be expected to be important, and the possible kinetic steps producing oxide vapor by homogeneous reaction.

1. Zone of Reaction

It was pointed out in Chapter II that one of the most commonly accepted flame models is that of Brzustowski and Glassman characterized by a collapsed reaction zone.

In the Brzustowski-Glassman model the reaction zone is thought to be located near the edge of the luminous envelope of the flame. The peak flame temperature, which is expected to be near the boiling point of the oxide, is thought to coincide with the narrow reaction zone.

The present investigation demonstrates that reaction takes place in the inner regions of the luminous envelope, namely the zone of colored radiation located near the metal surface. This conclusion is based on both the photographic observations in which narrow band pass interference filters were used to isolated selected wavelength regions of the spectrum and the space-resolved spectroscopic observations. These experiments demonstrate conclusively the presence of oxide vapor in this inner flame zone. The argument presented in Chapter VI showed that it is unlikely that back-diffusion of evaporated (and largely dissociated) oxide products is responsible for the oxide concentration in the inner zone. The alternative explanation is that reaction is responsible for the generation of oxide vapor in this zone of colored radiation.

2. Thermal or Chemiluminescent Excitation

If metal oxide vapor is formed by reaction in the inner zone it is important to ascertain whether nucleation and condensation also occur in this region. A knowledge of the temperature variation in the flame could be an indication of condensation since the high temperature region would be

expected to coincide with the large release of heat accompanying condensation. For example, in the case of magnesium oxide the standard heat of formation of the oxide vapor is + 1.00 kilocalories per mole, whereas the condensation of the oxide vapor releases about 113 kilocalories per mole (7).

In order to determine whether the inner zone of the flame is indeed a high temperature zone, one is interested in knowing whether the observed radiation is due to a thermal or a chemiluminescent excitation mechanism.

Because the inner zone is a region of reaction, there is almost certainly some deviation from equilibrium conditions, and it is expected that some of the radiation would be attributable to chemiluminescent excitation. The goal here is not to identify the source of the chemiluminescence but rather to answer the simpler question of whether the inner zone of the flame is at a higher temperature than the outer zone. This knowledge of the temperature profile would thus serve as an indication of whether condensation and heat release are occurring in the inner zone of the flame.

Consider the spatial variation of the radiation from the metal vapor as indicated in the spectra of Figure 32 and 35. Although a portion of this radiation may be attributed to possible chemiluminescent excitation, there must be a contribution from thermal excitation of the metal vapor. It is expected that the flame temperature will be near the boiling point of the oxide. For the oxides of interest in this in-

vestigation, at pressures of about 50 torr, the temperatures may exceed 3000°K . If temperatures of this magnitude are reached in the outer regions of the flame as the Brzustowski-Glassman model indicates, the contribution from thermal excitation of the metal vapor should be clearly evident. However, the space-resolved spectroscopic observations indicate that only a few of the calcium lines are observed to extend to the regions of the flame corresponding to the outer zone. Based on the gradual reduction in intensity of these calcium lines as a function of the distance from the inner zone it seems unlikely that two distinct processes account for the radiation from the inner and outer zones of the flame. If strong chemiluminescence accounts for essentially all of the radiation in the inner "lower temperature" zone, and thermal excitation accounts for radiation from the outer "higher temperature" zone (with a temperature peak near the outer edge of the luminous envelope), one would expect an intensity variation with distance which would have two maxima, one in each zone. The gradual decay in intensity with distance which is observed suggests instead that a single process dominates the excitation.

The results of the 2-D burner experiments appear to support the possibility that much of the radiation observed can be explained on the basis of thermal excitation. In the spectra of these experiments, the peak intensity of the lines and bands appears to coincide with the region of the flame

emitting the continuum radiation due to the condensed oxide particles. Also the spatial intensity variation of the oxide band systems shows a rather symmetrical pattern about this continuum region. These observations would be consistent with a thermal excitation mechanism in which the peak temperature region might be expected to coincide with the region of continuum radiation from the condensed oxide particles.

In the following section, arguments will be presented which favor thermal excitation as the main source of the observed emissions.

b. Supporting Evidence for Thermal Excitation - Temperature Measurements in Metal Flames

Wolfhard and Parker (10) measured the flame temperature of a magnesium - air flame by means of an absolute intensity measurement. Their results indicated a significant variation of the emissivity with wavelength, the emissivity growing larger as the UV region was approached. On the assumption that the emissivity approached a value of unity at wavelengths in the region 2400 to 2800 Å⁰, their measured flame temperature was approximately 3100°K. This value is in reasonably good agreement with the boiling point of magnesium oxide. The measured color temperature was in excess of 3900°K, a number which they indicated was an unrealistic value for the flame. Wolfhard and Parker indicated that because of the effects of the small oxide particles on the flame emissivity, color temperatures were of no significance. With flames of greater optical depth, Wolfhard and Parker expected that emissivity in the visible region of the spectrum would

be higher than indicated by their results.

This last statement may be the explanation of the results of Scartazzini (11) who measured the flame temperature of a magnesium-oxygen flame. His results indicated flame emissivities of nearly unity in the visible regions of the spectrum. Measured temperatures reached a maximum of about 2900°K which compares reasonably with 3100°K measured by Wolfhard and Parker. Color temperatures were found to be about 4000°K , a value also in good agreement with the color temperature measured by Wolfhard and Parker, but considered to be too high a temperature for the flame.

Nazimova and Sokolov investigated the possibility of chemiluminescence in a magnesium-oxygen flame. They measured a temperature for the magnesium oxide vapor by using intensity ratios of pairs of band heads of the MgO green system which corresponds to the transition from the $B'\Sigma$ state to the $X'\Sigma$ state. Their observations indicated that the radiation from the oxide vapor corresponded to an equilibrium situation with a temperature of 3000°K . This value compares favorably with the temperatures of 2900°K and 3100°K measured by Wolfhard and Parker (10), and Scartazzini (11) respectively. In addition, Nazimova and Sokolov determined a temperature for the magnesium vapor using ratios of line intensities. The average temperature for these measurements is about 3100°K although there is a greater spread in the individual values than for the corre-

sponding measurements for the MgO vapor.

On the basis of the equilibrium nature of the radiation, and on the agreement between the temperature determined for both the oxide vapor and the metal vapor, Nazimova and Sokolov conclude that the excitation of the MgO and Mg corresponds to thermal excitation, not chemiluminescence.

The good agreement of the temperatures determined by Wolfhard and Parker (10) and Scartazzini (11) which were not based on the Mg or MgO vapor radiation but included the radiation from the condensed oxide particles) with the temperatures for Mg and MgO determined by Nazimova and Sokolov is additional support for a thermal excitation mechanism.

Although all of the above investigations are for magnesium flames, there does appear to be some support for a thermal excitation mechanism for both calcium and strontium flames as well. Parkinson and Nicholls (57, 58) studied the radiation emitted from alkaline-earth oxide samples in a shock tube¹. The species observed to radiate in these shock

¹Parkinson and Nicholls indicate that atomic vapors are probably evaporated from the oxide samples. These atomic vapors which are heated thermally in the hot gases behind the shock wave react to give the resulting spectra. It is important to note that it is a reacting system leading to the radiation, as opposed to thermal excitation of oxide vapor evaporated from the sample. The vaporization studies reported in Appendix A confirm the fact that atomic species, rather than molecular species are expected to be the major evaporation products. Thus, the results of these shock-tube studies are applicable to the present investigation of metal flames.

tube studies are the same species identified in the flame spectra in the present investigation. For magnesium oxide the green system $B'\Sigma \rightarrow X''\Sigma$ and the complex bands in the UV around 3800\AA^0 were observed. For calcium oxide, the green and orange bond systems attributed to an oxide (possibly polymeric or polyatomic) were observed. For strontium oxide, two similar unanalyzed systems that are attributed to an oxide which may also be polyatomic or polymeric were observed. Since these unanalyzed systems are so complex, the type of investigation performed by Nazimova and Sokolov for the bands of MgO cannot be performed for the bands due to the oxides of calcium and strontium. In these shock tube studies the temperature was varied by varying the shock strength. Changes in the spectra were then noted as a function of the shock Mach number. Nicholls, Parkinson and Reeves (59) stated that "in general, the strongest features which might be expected from a thermal excitation standpoint appear. . . . The change from molecular to atomic spectra with increasing temperature . . . suggests a general thermal excitation mechanism. This is consistent with the intensity distribution of each spectrum."

It thus appears that in reacting systems of alkaline-earth metals and oxygen a thermal excitation mechanism is responsible for the major emissions.

3. Relative Temperatures in the Two Flame Zones

It was pointed out in Chapter VI that the resonance line of Ca and Sr in the space-resolved spectra of the wire

experiments is self-reversed over a portion of its length. Since the radiation appears to be due largely to a thermal excitation mechanism, the self reversal thus indicates that the inner zone of the flame is hotter than the outer region. In order for the flame to have its highest temperature region located in the inner zone of the flame, one would expect that condensation is also occurring throughout the zone of colored radiation. The following section presents additional arguments indicating that the inner zone is the location of the condensation.

4. Location of Condensed Oxide Particles in the Flame

As was indicated earlier in this chapter, the spectroscopic observations confirmed the presence of oxide vapor in the inner zone of the flame. Having demonstrated that the oxide vapor is most likely generated by reaction in this zone of the flame, a logical argument can be made for the existence of condensed oxide particles in this zone.

Courtney (60) defines the various stages of condensation as nucleation, growth and agglomeration. He indicates that the process of nucleation is generally the slow step in condensation, and thus this aspect deserves closer attention. The rate of nucleation increases rapidly with the degree of supersaturation. In a reacting metal-oxygen system the degree of supersaturation can become very large. Courtney cites as an example the adiabatic reaction of a stoichiometric mixture of Mg vapor and oxygen at a temper-

ature of 600°C and a total pressure of 1 torr. Calculations indicate that the supersaturation of the uncondensed vapor is a number of the order of 10^{20} , an extremely large value in comparison with corresponding values for other systems such as water vapor condensation which have been studied more extensively. Typically, a supersaturation of 6 for a water vapor experiment at -10°C indicates condensation in about 50 msec (61). The extremely high value for the calculated supersaturation in the above example for Mg-O_2 reaction is taken as an indication that nucleation should be a very rapid process. Markstein (21) also comments that the reaction to form oxide vapor would probably generate a large supersaturation and nucleation would occur rapidly. For the flame conditions of the present investigation similar calculations indicate a supersaturation value expressed in powers of ten. These arguments lead to the conclusion that the generation of oxide vapor by reaction in the inner zone of the flame will also lead to nucleation and condensation of oxide particles in this zone. The large heat release accompanying condensation can indeed make the inner zone of the flame a high temperature region. The interpretation of the flame radiation on the basis of thermal excitation thus appears to be a consistent explanation of the flame structure.

The work discussed in this section indicates that particles do condense in the inner zone of the flame. In order to discuss particle movement in the flame, it is of

interest to know the size of particles likely to be encountered in metal flames. The next section describes the particle sizes and section 6 discusses particle movement in the flame.

5. Oxide Particle Sizes

The sizes of oxide particles which form in metal-oxygen flames have been reported by several investigators. There appears to be general agreement that the particle diameters are submicron in size.

A very rough estimate is available from the work of Wolfhard and Parker (10). They state that the bluish color of the smoke from a magnesium-air flame can be taken as an indication that the particle size is less than the wavelength of light. Thus, for a magnesium flame at atmospheric pressure an approximate limit for the oxide particle diameter is 5000 \AA .

Markstein (21, 62) reports particle diameters of 50 or 100 \AA for MgO particles generated in his dilute diffusion flame experiments at pressures in the range 2 to 20 torr. These values are based on electron microscope and x-ray diffraction measurements.

Courtney (63) also studied the reaction of Mg vapor and O_2 at low pressures of about 1 torr. Electron microscope measurements indicated a particle size of 100 \AA .

Gouldin (64, 65) has determined an upper limit for the particle sizes for MgO , CaO and SrO particles formed in metal flames at low pressures identical to those reported in

the wire-burning studies in this investigation. The electron micrographs for these particles indicate sizes of about 400 \AA for CaO and SrO, and somewhat larger particles 500 \AA to 1000 \AA for MgO. In Gouldin's experiments the particles were sampled from the atmosphere outside the flame itself. It was thought that the particles in this region would have experienced their full growth history and as such would be representative of the larger particles formed in the flame.

6. Particle Movement in the Flame

An important consideration of the flame model of Brzustowski and Glassman (15) is based on the indication that condensed oxide particles are probably formed in the flame zone itself. The conditions under which these particles are likely to be transported out of the flame zone are also outlined. In the Brzustowski-Glassman model (15), the film BC is a zone in which the inward diffusion of oxidizer is opposed by the outward flow of gaseous combustion products. It is stated that "condensed oxide particles can be transported out of the flame zone only if there is a bulk outward gas velocity in BC". The conditions under which a bulk gas velocity outward can be expected are determined by a parameter α which is the fraction of oxide vaporized. It should be noted that α is a function of the radius since it decreases due to further condensation of the products as they move outward. Thus, even though the particles can be swept

from the flame zone, it is likely that a region will occur where the particles pile up.

Simply stated, the criterion for outward bulk velocity is that "more than one mole of gaseous products is formed in the flame for every mole of oxidizer consumed".

Brzustowski's experimental results correlate well with the considerations expressed above regarding the movement of condensed oxide particles. In the combustion map for magnesium burning over a wide pressure range (50 torr to 30 atm) and oxidizer mole fraction ($X_{O_2} = 0.1$ to 1.0), regions are observed in which the condensed products collect in a heavy deposit in the flame zone itself. In fact, in some instances the deposit actually extinguishes the flame. These observations are taken as an indication that there is no bulk outward gas velocity in the film BC.

In other regions of the combustion map, Brzustowski observes that the heavy deposits of oxide do not form in the flame. The absence of heavy deposits is taken as an indication that the particles are being carried out of the flame zone by an outward bulk gas velocity.

The conditions under which Brzustowski observes no heavy deposits in the flame, are comparable to the conditions under which the present investigation was performed, namely low oxidizer mole fractions and low pressures. Thus, it is not at all surprising that heavy deposits are not observed to form in the flames of Ca and Sr as well. The absence of

deposits is likely an indication that an outward bulk gas velocity exists to carry the oxide particles from the inner zone of colored radiation, to the outer zone of the flame.

In addition to the outward bulk gas velocity produced by the gaseous oxide products, there is also the possibility that metal vapor passes unreacted through the inner zone of predominantly homogeneous reaction. The outward bulk velocity due to this metal vapor is also expected to decrease with increasing radius due to depletion by heterogeneous reaction on the oxide smoke particles, if this reaction mechanism is significant in the outer zone of the flame.

Still another effect which would move the oxide particles from the hot reaction zone toward the cooler outer zone of the flame is the mechanism of thermophoresis which is also called the thermomechanical effect or the radiometer effect. It is "a force which particles experience in a temperature gradient; it results from the unbalance in molecular collisions on the hot and cold side of a particle". (66).

The possible role of thermophoresis was brought to the attention of the author some time ago in discussions held in this laboratory. Recently, there has been reported some experimental evidence in the case of aluminum combustion (67) which indicates that thermophoresis may be an important mechanism for the movement of small oxide particles. A quenched sample of a burning aluminum particle with its wake

of oxide smoke was observed to have a dark zone (no particles) separating a large oxide particle from the fine smoke present in the wake.

In the flames of Ca and Sr in the present investigation, it is expected that the effect would be largest in the inner reaction zone of the flame since the velocity due to thermophoresis is directly proportional to the temperature gradient. The size of the particles also determines the magnitude of the effect. Thermophoresis forces are largest for particles which are small compared to the mean free path. In the present study an entire range of particle sizes are expected ranging from nuclei consisting of perhaps several atoms up to particle diameters of typically 100 \AA^0 , a number still small compared to the mean free path. Thus in the inner zone of the flame where the particles originate, their very small size would make them subject to significant forces due to the thermophoresis effect.

The presence of condensed oxide deposits throughout the flame raises the possibility of heterogeneous reaction on these particles competing with homogeneous reaction. The following section discusses the evidence regarding heterogeneous reaction.

7. Homogeneous versus Heterogeneous Reaction

The question regarding the relative roles of heterogeneous and homogeneous reaction is still subject to

a great deal of uncertainty and speculation. In the present investigation it is shown that the inner zone of the flame is a reaction zone in which radiation from the metal vapor and metal oxide vapor is observed. The oxide vapor is probably the result of homogeneous reaction since very little oxide vapor is expected in the evaporation products of the oxides. However, it is also pointed out in an earlier section of this chapter, that nucleation is expected to occur rapidly in these flames, and thus condensed oxide particles are expected to exist in the inner zone of the flame. The presence of the particles in this zone raises the old question about the relative importance of the homogeneous and heterogeneous reaction paths. In this regard the recent results of Markstein (23) are highly significant. He studied the growth of MgO deposits on a heated nichrome surface, to determine the effect of temperature on the collision efficiency β , the fraction of collisions of Mg atoms with the surface that result in MgO formation. Over the temperature range from 410 to 840°K the collision efficiency dropped from a value of nearly unity, to a value of 0.02. Although Markstein indicates that the temperature dependence demonstrated for only a limited temperature range should not be taken as "unqualified evidence" that heterogeneous reaction will be unimportant at high temperatures, it is an indication that previous anomalies in the spectral

observations of various investigators studying Mg-O_2 systems may be resolved by this latest evidence on the possible temperature dependence of the heterogeneous reaction path. Markstein indicates that for the conditions present in the experiments of Courtney (63) and Brzustowski and Glassman (16, 54), the high temperature of the oxide particles may have greatly reduced the heterogeneous reaction mechanism.

Assuming that the effect of temperature on the collision efficiency β does not reverse itself at temperatures higher than 840°K , heterogeneous reaction would probably play a minor role in the reaction zone in the inner flame region. In the outer region of the flame where it appears to be cooler (on the basis of the results of this investigation) a heterogeneous mechanism may still account for some of the reaction.

In the following section of this chapter a comparison is made of the possible kinetic steps for the formation of oxide vapor.

8. Possible Reaction Steps for the Production of Oxide Vapor

Markstein (21) considers most of the possible reaction steps for the formation of MgO vapor including three body reactions, reactions involving the dimer of the alkaline-earth metal, and the possibility of the formation of the peroxide. For the conditions of his experiment, in

particular for pressures in the range from 2 to 20 torr, he excludes three body reactions. In view of the fact that Markstein has recently shown (23) a strong dependence of the collision efficiency (for surface reaction of Mg on oxide particles) on temperature it is probably worthwhile to investigate the possibility of three body reactions competing with bimolecular reactions in the formation of MgO molecules, in particular for conditions where the MgO particles might be at a high temperature and heterogeneous reaction might be suppressed.

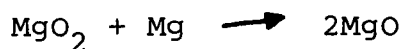
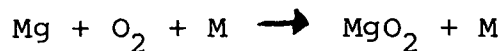
Three body reactions for which the activation energy is small may be expected in some cases to compete favorably with bimolecular reactions such as:



in which the activation energy must be at least equal to 28 kcal. This possibility, suggested by Walsh in the comments following the paper by Markstein (21), is discussed below.

(a) Reaction Steps Involving the Alkaline-Earth Peroxide

The reaction steps involving the alkaline-earth peroxide might be the following:

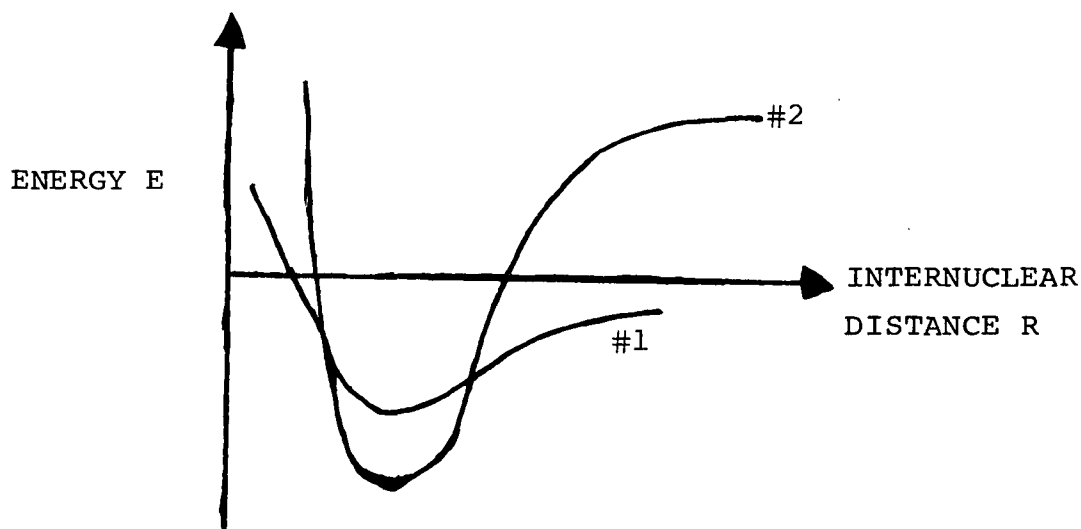


Markstein dismissed this reaction mechanism for several reasons, one of which was the fact that the alkaline-

earth peroxides have not been observed experimentally in the gas phase.

Recently, a set of reaction steps has been proposed by Gordon et al (68) which involves the peroxide, not as a stable species, but rather as a reaction intermediate. Whereas, a normal complex formed by the interaction of a metal atom and an oxygen molecule might be expected to have a lifetime of one vibrational period, typically 10^{-13} seconds, the peroxide is postulated to have a longer lifetime as a result of curve crossing, "intersystem crossing between the triplet surface and an excited triplet surface".

The postulated mechanism can be explained as follows, if one considers the situation depicted below. For the sake of simplicity the two-dimensional representation showing a curve representing the energy as a function of internuclear distance has been used, rather than the more complex three-dimensional picture of a surface representing the energy as a function of the two internuclear distances for a triatomic specie.



Consider curve #1 to represent the energy state for the complex formed from ground states of the metal atom and the oxygen molecule. Curve #2 represents a bound excited state. Suppose that a crossing from curve #1 to the excited state, curve #2, occurs once in every one thousand encounters. After the crossing has occurred, the MgO_2 would be expected to remain in the bound excited state for period of time because the probability that it will cross back to its original state again would be expected to be also about one in every one thousand encounters. Thus, the lifetime of the MgO_2 intermediate increases from one vibrational period of about 10^{-13} seconds to about one thousand vibrational periods or 10^{-10} seconds. The lifetime of the reaction intermediate is obviously determined by the assumption that one makes regarding the probability that a crossing from one triplet surface to another will occur.

The reaction steps leading to the formation of MgO by this mechanism could be significant in comparison with other possible mechanisms since all steps involve only the major species Mg and O_2 . However, there is no direct experimental evidence to indicate that this mechanism is actually taking place, and the likelihood of these reaction steps being important is subject to the hypotheses noted above regarding the proposed interaction of the energy states of the triatomic specie MgO_2 .

(b) Reaction Steps Involving the Alkaline-Earth Metal Dimer

In the flames of interest, metal vapor is continually vaporized from the metal surface and if the concentration of the dimer Mg_2 in this vapor is sufficiently high, then a bimolecular reaction involving the Mg_2 dimer and an oxygen atom may be expected to compete favorably with other three body reactions for the formation of MgO .



In order to determine whether or not the dimer could exist in sufficient quantities to be important in the formation of oxide vapor, the existing literature was analyzed. The analysis is summarized briefly below along with calculations estimating the amount of dimer.

() Evidence for the Existence of the Alkaline-Earth Metal Dimer

The spectroscopic evidence indicates the possibility of the dimer for both Mg_2 and Ca_2 . Hamada (70) lists the spectral features which he has attributed to the dimer. Other investigators (71) reported observing in absorption the same features reported by Hamada for Mg_2 . The observation of these Mg_2 bands in absorption occurred in a vaporization study of Mg_3N_2 . The above two references appear to be the only spectroscopic evidence regarding the existence of the dimer.

A recent compilation of high temperature mass-spectrometric studies (72) indicates that mass spectrometric

observations have been performed for the vapors of Be and Sr. For Be, Nikitin and Gorokhov (73) performed a mass-spectrometric analysis of the species vaporized from an effusion cell over the temperature range from 1410°K to 1620°K . They conclude that for these experimental conditions, "the only component of the vapor is atomic beryllium". Their results thus confirm the findings of Chupka et al (74) which were subject to some doubt because of the studies of Amonenko et al (75). For Sr, the investigation of Boerboom et al, (76), for the temperature range 500°C to 650°C , indicates that the vapor effusing from a Knudsen cell contained only Sr atoms. The accuracy of their detection thus placed an upper limit on the amount of dimer or other polyatomic species as 1 part in 10^6 .

Some mass-spectrometric measurements were also performed by Mellor (77) for the vaporization of Mg and Ca at relatively low temperatures, approximately 285°C for Mg, and 290°C and 350°C for Ca. The observations indicated that within the limits of detection, no dimer was present in the vapors of either Mg or Ca.

Mellor has also performed calculations to estimate the mole fraction of dimer expected when Mg and Ca vaporize at temperatures in the range appropriate to metal diffusion flames (Brzustowski and Glassman (15) indicated that the metal surface temperature is several hundred degrees lower than the metal boiling point.) The calculations for the

equilibrium amount of dimer, based on the value of the second virial coefficient, follow the method outlined by Stogryn and Hirschfelder (78, 79). Table 12 summarizes Mellor's calculations for Ca and Mg.

TABLE 12
MOLE FRACTION OF DIMER VERSUS TEMPERATURE

<u>T^{°K}</u>	<u>X_{Mg₂}</u>
707	9.5 x 10 ⁻⁸
884	5.9 x 10 ⁻⁶
1060	5.4 x 10 ⁻⁵
1238	3.5 x 10 ⁻⁴
1414	1.2 x 10 ⁻³

<u>T^{°K}</u>	<u>X_{Ca₂}</u>
864	1.5 x 10 ⁻⁷
1080	7.1 x 10 ⁻⁶
1295	8.3 x 10 ⁻⁵
1510	3.3 x 10 ⁻⁴

Boiling point of Mg @ 1 atm = 1376^{°K}

Boiling point of Mg @ 50 torr = 1100^{°K}

Boiling point of Ca @ 1 atm = 1762^{°K}

Boiling point of Ca @ 50 torr = 1400^{°K}

An inspection of the values presented in Table 12 illustrates that the bimolecular reaction



will probably not be competitive with the termolecular reaction



except at very low pressures where the ratio of two-body to three-body collisions overcomes the large concentration differences between Mg and Mg₂, typically 5 or 6 orders of magnitude. The ratio of two-body to three-body reactions is about 10³ at one atmosphere and the number scales according to the inverse of the pressure, so that for a ratio of 10⁶ we require a pressure of 10⁻³ atm, or slightly less than 1 torr.

The possible reaction steps for the formation of oxide vapor can be summarized as follows. The bimolecular step



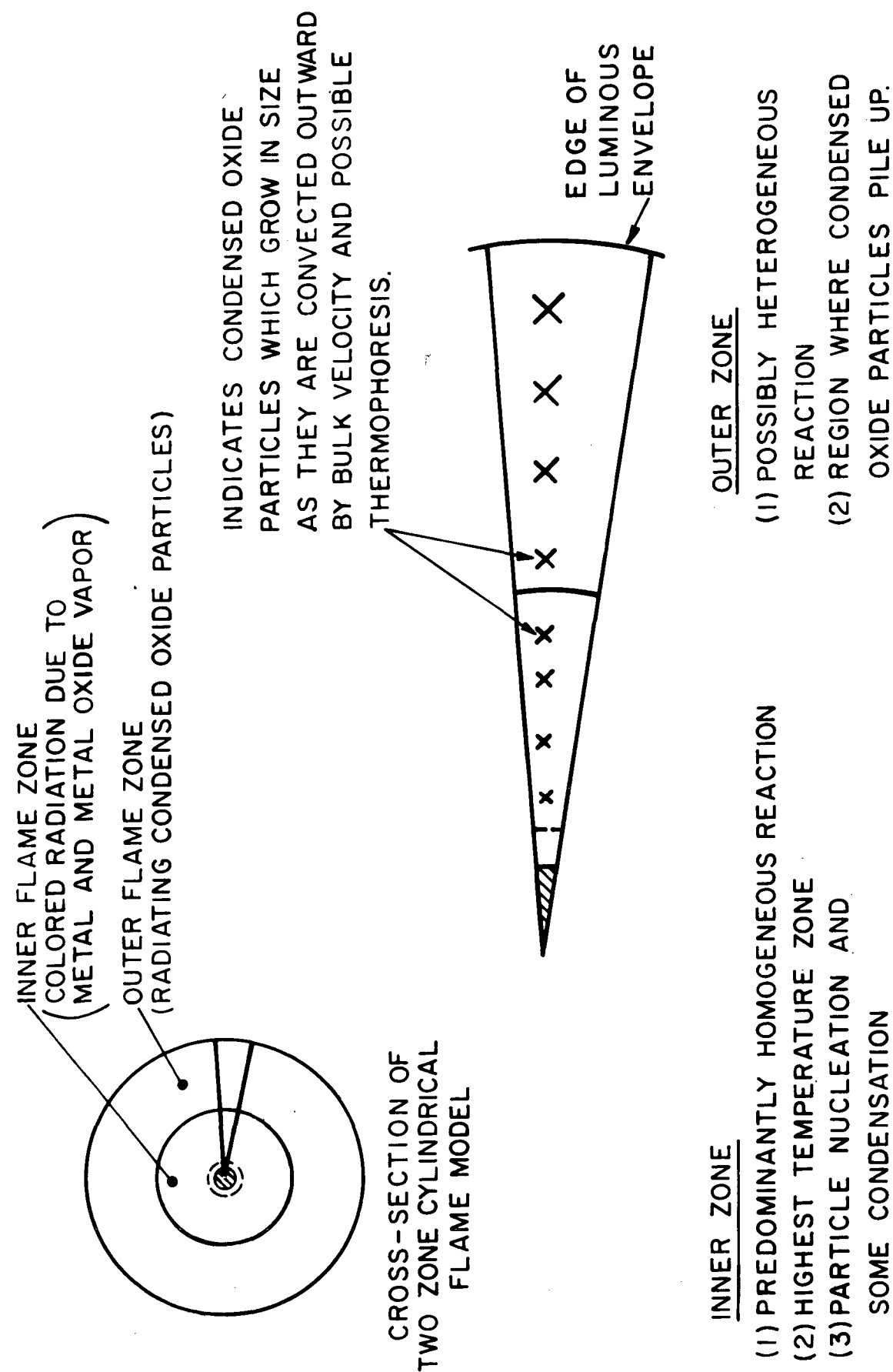
is endothermic by 28 kilocalories per mole and it is expected that three body reactions with a low activation energy can compete favorably with this step. The steps involving the peroxide MgO₂ as an intermediate are based on postulated curve crossings to increase the lifetime of the MgO₂ and there is no direct evidence to support this mechanism. The steps involving the metal dimer Mg₂ will not be competitive with the three-body reaction



except at pressures of about 1 torr.

A schematic of the flame structure proposed in this chapter is presented in Figure 51.

The next chapter summarizes the new model and compares it with the previous models which are discussed in Chapter II.



SCHEMATIC REPRESENTATION OF FLAME STRUCTURE

CHAPTER VIII - SUMMARY OF FLAME MODEL

The present investigation has shown that a reaction region exists in the inner zone of the luminous envelope surrounding the metal sample. The production of oxide vapor by homogeneous reaction causes a supersaturation of oxide vapor leading to rapid nucleation. Thus the inner reaction zone is expected to be a high temperature region of the flame due to the liberation of the heat of condensation. It was demonstrated that the major contribution to the observed radiation is due to a thermal excitation mechanism, although some contribution from chemiluminescent radiation may occur in the inner reaction zone. Based on the thermal nature of the radiation, the self-reversal over a portion of their length of the resonance lines of the metals Ca and Sr respectively, indicates that the inner zone of colored radiation in the flame is hotter than the outer zone.

If the trend shown by Markstein's results (23) illustrating the decrease of collision efficiency (for surface reaction) with increasing temperature continues at higher temperatures, it is anticipated that the inner reaction zone of the flames of Ca and Sr is thus a zone of predominantly homogeneous reaction. Heterogeneous reaction would tend to become more important at larger flame radii where it is expected that the temperature is decreasing.

The model described above is pictured schematically in Figure 51. A comparison of this figure with the figures

of Chapter II demonstrates the differences in the flame model as a result of the present investigation.

The flame zone does not appear to be a "collapsed reaction zone" as in the model of Brzustowski and Glassman. The peak flame temperature is not expected to be located at the outer edge of the luminous envelope. The reaction zone appears to extend to regions very close to the wire surface, and makes it difficult to determine the size of an inner zone such as in the Brzustowski - Glassman model, zone AB, which is assumed to contain only metal vapor and the inert diluent.

The model due to Coffin (9) assumes an extended reaction zone such as the present investigation indicates, but in Coffin's model this zone is assumed to contain no MgO vapor. It would be impossible to explain the spectroscopic observations of Brzustowski (16, 54), Courtney (63), and the present investigation, on the basis of Coffin's model. In addition, the two zones observed in the Ca and Sr flames, namely a reaction zone extending almost to the wire surface, and a second zone containing oxide particles surrounding the zone of colored radiation, are not distinguished by Coffin.

In the proposed extensions of the Brzustowski - Glassman model by Knipe (18), it is assumed that reaction probably proceeds predominantly by heterogeneous reaction in the case of aluminum combustion, and that this reaction proceeds at the cloud boundaries. The role played by heterogeneous reaction in the case of aluminum combustion could be significantly different than for the combustion of the

alkaline-earth oxides. Unlike the aluminum oxides, the alkaline-earth oxides are observed to have the same composition in the condensed and gaseous phases. However, Knipe's suggestion that reaction proceeds at the cloud boundaries is appropriate to the flames of the alkaline-earth metals as well, in view of the trend illustrated by Markstein's results showing a strong dependence of the heterogeneous reaction mechanism on temperature. It should be stressed, however, that Markstein's results are for a limited temperature range (410°K to 840°K) and that he states that the results should not be taken as "unqualified evidence" that heterogeneous reaction may be unimportant at higher temperatures.

The differences between the reaction mechanism proposed by Markstein and the findings of the present investigation have been indicated throughout the previous chapter. Unfortunately the relative roles played by homogeneous and heterogeneous reaction are still subject to question.

A key test of the main features of the model proposed as a result of the present investigation will be the results of a parallel experimental study in this laboratory by Gouldin (64, 65), in which flame temperature measurements will be performed on the flames of Ca and Sr as described in this report. The technique is basically a brightness-emissivity temperature measurement in which a correction will

be made for the scattering by the small condensed oxide particles in the flame. The measurements of extinction coefficient as a function of the radius of the flame will determine the regions of the flame in which oxide particles exist. The evaluation of the flame temperature as a function of the flame radius will confirm whether or not the inner zone of the flame is indeed hotter than the outer zone. The knowledge of the temperature gradient may then permit an estimate of the magnitude of the effect of thermophoresis on the movement of the small condensed oxide particles.

In summary, the work in the present thesis defines a flame structure model in which a predominantly homogeneous reaction zone is located well inside the luminous envelope. Heat release, which occurs throughout this reaction zone due to oxide vapor condensation, accounts for the excitation of the species observed to radiate. Oxide particles, formed throughout the reaction zone, are swept out of the inner zone of the flame by the bulk velocity of the gaseous product species and thermophoresis effects. Since both effects decrease with increasing distance from the reaction zone, there is a region in which the particles pile up to form the outer luminous edge of the flame which is characteristic of most metal flame photographs.

LIST OF REFERENCES

1. Grosse, A. V. and Conway, J. B., "Combustion of Metals in Oxygen", Ind. Eng. Chem. 50, 663-72 (1958).
2. Glassman, I., "Metal Combustion Processes", Amer. Rocket Soc. Preprint 938-59 (1959).
3. Ackermann, R. J. and Thorn, R. J., "Vaporization of Oxides", p. 39-88 in Progress in Ceramic Science, Vol. 1, ed. by Burke, J. E., Pergamon Press, New York, (1961).
4. Brzustowski, T. A. and Glassman, I., "Spectroscopic Investigation of Metal Combustion", p. 41-74 in Heterogeneous Combustion, Vol. 15, Wolfhard, H. G., Glassman, I., and Green, L. Jr., Editors, Academic Press, New York, (1964).
5. Mellor, A. M., "Heterogeneous Ignition of Metals: Model and Experiment", Princeton University, Dept. of Aerospace and Mechanical Sciences, Report No. 816 (1967).
6. Wolfhard, H. G. and Parker, W. G., "A New Technique for the Spectroscopic Examination of Flames at Normal Pressures", Proc. Phy. Soc. A62, 722-30 (1949).
7. Janaf Thermochemical Tables, The Dow Chemical Co., Midland, Mich., March 31, 1965.
8. Hodgman, C. D., Editor, Handbook of Chemistry and Physics, 46th Edition, Chemical Rubber Publishing Co., Cleveland, 1964.
9. Coffin, K. P., "Some Physical Aspects of the Combustion of Magnesium Ribbons", Fifth Symposium (International) on Combustion, Reinhold, New York, (1955) p. 267-76.
10. Wolfhard, H. G. and Parker, W. G., "Temperature Measurements of Flames Containing Incandescent Particles", Proc. Phy. Soc. (London) 62B, 523-9 (1949).
11. Scartazzini, H., "Combustion du magnesium en poudre dans l'oxygene", Compt. Rend. 230, 97-8 (1950).
12. Brewer, L., "The Thermodynamic Properties of the Oxides and Their Vaporization Processes", Chem. Rev. 52, 1-75 (1953).

13. Fassell, W. M., Papp, C. A., Hildenbrand, D. L. and Sernka, R. P., "The Experimental Nature of the Combustion of Metallic Powders" in Solid Propellant Rocket Research, ed. by M. Summerfield, Progress in Astronautics and Rocketry, Vol. 1, Academic Press, 1960, p. 259-69.
14. Bartlett, R. W., Ong, J. N., Fassell, W. M. and Papp, C. A., "Estimating Aluminum Particle Combustion Kinetics", Combustion and Flame, 7, 227-34 (1963).
15. Brzustowski, T. A. and Glassman, I., "Vapor-Phase Diffusion Flames in the Combustion of Magnesium and Aluminum: I. Analytical Developments", p. 75-115 Heterogeneous Combustion, Wolfhard, H. G., Glassman, I., and Green, L. Jr., Editors Academic Press, New York (1964).
16. Brzustowski, T. A., Vapor-Phase Diffusion Flames in the Combustion of Magnesium and Aluminum, Ph.D. Thesis, Princeton University, Dept. of Aero. Eng., 1962.
17. Christensen, H. C., Knipe, R. H. and Gordon, A. S., "Survey of Aluminum Particle Combustion" Pyrodynamics 3, 91-119 (1965).
18. The Metal Combustion Study Group "Aluminum Particle Combustion Progress Report, 1 April 1964-30 June 1965" Technical Progress Report 415, NOTS TP 3916 U. S. Naval Ordnance Test Station (1966).
19. Markstein, G. H., "Heterogeneous Reaction Processes in Metal Combustion 11th Symposium (International) on Combustion, The Combustion Institute, Pittsburgh, Penn. (1967).
20. Macek, A., "Fundamentals of Combustion of Single Aluminum and Beryllium Particles", 11th Symposium (International) on Combustion, The Combustion Inst., Pittsburgh, Penn. (1967).
21. Markstein, G. H., "Magnesium-Oxygen Dilute Diffusion Flame", 9th Symposium (International) on Combustion, Academic Press, New York, (1963).
22. Markstein, G. H., "Rate of Growth of Magnesium Oxide Deposits Formed by Surface Reaction of Magnesium Vapor and Oxygen", Presented at the Spring Meeting of the Western States Section of the Combustion Institute, Denver, Colorado, 25-26 April 1966.

23. Markstein, G. H., "Study of the Reaction of Magnesium Vapor and Oxygen at the Surface of MgO Deposits by Atomic-Absorption Spectrophotometry" presented at the 12th International Symposium on Combustion, Poitiers, France, July 1968.
24. Schofield, K., "The Bond Dissociation Energies of Group IIA Diatomic Oxides", Chemical Reviews 67, 707-15 (1967).
25. Gaydon, A. G., "Green and Orange Band Spectra of CaOH, CaOD and Calcium Oxide", Proc. Roy. Soc. 231, 437-45 (1955).
26. Kaufman, M., Wharton, L. and Klemperer, W., "Electronic Structure of SrO" J. Chem. Phys. 43, 943-52 (1965).
27. Brewer, L. and Trajmar, S., "Ultraviolet Bands of Magnesium Hydroxide and Oxide", J. Chem. Phys. 36, 1585-87 (1962).
28. Richards, W. G., Vergaegen, G. and Moser, C. M., "Low-Lying Energy Levels of Magnesium Oxide", J. Chem. Phys. 45, 3226-30 (1966).
29. Pearse, R. W. B. and Gaydon, A. G., The Identification of Molecular Spectra, Third Edition, John Wiley and Sons, Inc., New York (1963).
30. Pearse, R. W. B. and Gaydon, A. G., Supplement to the Third Edition of the Identification of Molecular Spectra, Chapman and Hall Ltd., (1966).
31. Herzberg, G., Molecular Spectra and Molecular Structure I Spectra of Diatomic Molecules, D. Van Nostrand Company, Inc., Princeton, New Jersey, (1950).
32. Brewer, L., Trajmar, S. and Berg, R. A., "Analysis of the Ultraviolet System of Magnesium Oxide" Astrophysical Journal 135, 955-62 (1962).
33. Pesic, D. S., "Isotope Effect in Band Spectra of Magnesium Oxide", Proc. Phy. Soc. (London) A76, 844-8 (1960).
34. Trajmar, S. and Ewing, G. E., "Identification of a New Band System of MgO in the Near Ultraviolet", J. Chem. Phys. 40, 1170-1170 (1964).
35. Trajmar, S. and Ewing, G. E., "The Near-Ultraviolet Bands of MgO: Analysis of the $D'\Delta \rightarrow A'\pi$ and $C'\Sigma \rightarrow A'\pi$ Systems", Astrophysical Journal 142, 77-83 (1965).

36. Green, D. W., "Arc Spectrum of Magnesium Oxide", University of California, Berkeley, UCRL-17878 Rev. (1968).
37. Hauge, R. H., "Spectra of CaO", Ph.D. Thesis, University of California, Berkeley, Univ. Microfilms, Ann Arbor, Michigan (1966).
38. Wharton, L., Kaufman, M. and Klemperer, W., "Electric Resonance Spectrum and Dipole Moment of BaO", J. Chem. Phys. 37, 621-6 (1962).
39. Wharton, L. and Klemperer, W., "Microwave Spectrum of BaO", J. Chem. Phys. 38, 2705-8 (1963).
40. Verhaegen, G. and Richards, W. G., "Valence Levels of Beryllium Oxide" J. Chem. Phys. 45, 1828-33 (1966).
41. Brewer, T., "Principles of High Temperature Chemistry" in Proceedings of the Robert A. Welch Foundation Conference on Chemical Research p. 47-92 Robert A. Welch Foundation, Houston, Texas 1962.
42. Drowart, J., Exsteen, G., and Verhaegen, G. "Mass Spectrometric Determination of the Dissociation Energy of the Molecules MgO, CaO, SrO and Sr₂O", Trans. Faraday Soc. 60, 1920-33 (1964).
43. Brewer, L. and Porter, R. F. "A Thermodynamic and Spectroscopic Study of Gaseous Magnesium Oxide" J. Chem. Phys. 22, 1867-77 (1954).
44. Bulewicz, E. M. and Sugden, T. M. "Determination of the Dissociation Constants and Heats of Formation of Molecules by Flame Photometry Part 5 - The Stabilities of MgO and MgOH" Trans. Faraday Soc. 55, 720-729 (1959).
45. Thrush, B. A., "The Ground State of Beryllium Oxide" Proc. Chem. Soc. 339-340 (1960) CA 55:11070g.
46. Alexander, C., Ogden, J. S. and Levy, A., "Transpiration Study of Magnesium Oxide", J. Chem. Phys. 39, 3057-3060 (1963).
47. Huldt, L. and Lagerqvist, A., "The Height of the Excited Electron States of Calcium, Strontium and Barium Oxides", Arkiv Fysik 8, 427-432 (1954) CA 49:7380e.
48. Sugden, T. M. and Schofield, K., "Heats of Dissociation of Gaseous Alkali Earth Dihydroxides" Trans. Faraday Soc. 62, 566-575 (1966)

49. Hollander, Tj., Kalff, P. J. and Alkemade, C. Th. J. "Dissociation Energies and Excitation Levels of Alkaline-Earth Oxides" J. Quant. Spectrosc. Radiat. Transfer 4, 577-579 (1964)
50. Kalff, P. J., Hollander, Tj., and Alkemade, C. Th. J. "Flame-Photometric Determination of the Dissociation Energies of the Alkaline-Earth Oxides" J. Chem. Phys. 43, 2299-2307 (1965).
51. Hofman, F. W., and Kohn, H. "Optical Cross Section of Resonance Lines Emitted by Flames Under Conditions of Partial Thermal Ionization", J. Opt. Soc. Am. 51, 512-521 (1961) CA 55, 19484e
52. Newbury, R., "Vapor Species of the Barium-Oxygen-Hydrogen System", U. S. Atomic Energy Commission Report UCRL-12225-T, Office of Technical Services, Washington, D.C. 1964 69 pages.
53. Wolfhard, H. G. and Parker, W. G., "A Spectroscopic Investigation into the Structure of Diffusion Flames", Proc. Phy. Soc. A65, 2-19 (1952).
54. Brzustowski, T. A. and Glassman, I., "Vapor-Phase Diffusion Flames in the Combustion of Magnesium and Aluminum II Experimental Observations", p. 117-158 Heterogeneous Combustion, Wolfhard, H. G., Glassman, I. and Green, L., Jr., Editors, Academic Press, New York (1964).
- a
55. Cremers, C. J. and Winter, E. R. F., "Image - Rotating Device for a Spectrograph Illumination System", Applied Spectroscopy 20, 421-423 (1966).
56. Nazimova, N. A. and Sokolov, V. A., "A Study of the Electronic-Vibrational Structure of the Spectrum of Magnesium Oxidation", Izv. Vysshikh Uchebn. Zavedenii, Fiz. p. 143-148 (1961).
57. Parkinson, W. H. and Nicholls, R. W., "Shock Excitation of Powdered Solids" Scientific Report No. 1 Contract AF 19(604)-4560 (1959) U.S. Dept. Com., Office Tech. Serv. PB Rept. 144,005 - 92 pages.
58. Nicholls, R. W. and Parkinson, W. H., "Shock Excitation of Atomic and Molecular Spectra" J. Chem. Phys. 26, 423-424 (1957).
59. Nicholls, R. W., Parkinson, W. H., and Reeves, E. M., "The Spectroscopy of Shock-Excited Powdered Solids" Applied Optics 2, 919-930 (1963).

60. Courtney, W. G., "Recent Advances in Condensation and Evaporation", ARS Journal 31, 751-756 (1961).
61. Courtney, W. G., and Budnik, C., "Colloid Propulsion Using Chemically-Formed Particles", AIAA paper 66-254, March 7-9, 1966 (27 pages).
62. Markstein, G. H., "Analysis of a Dilute Diffusion Flame Maintained by Heterogeneous Reaction", p. 177-202 Heterogeneous Combustion, Wolfhard, H. G., Glassman, I., and Green, L., Jr., Editors Academic Press, New York (1964).
63. Courtney, W. G., "Homogeneous Nucleation from Simple and Complex Systems", p. 677-699 Heterogeneous Combustion, Wolfhard, H. G., Glassman, I., and Green, L., Jr., Editors Academic Press, New York (1964).
64. Sullivan, H. F., Gouldin, F. C., and Glassman, I., "Metal Flame Structure Studies Employing Optical Techniques" presented at the Western States Section of the Combustion Institute October 1967, Preprint WSS/CI 67-40.
65. Gouldin, F. C., Personal communication, October 1968.
66. Fristrom, R. M., and Westenberg, A. A., "Flame Structure", McGraw-Hill, Inc., New York 1965.
67. Prentice, J. L., Editor, "Metal Particle Combustion Progress Report - 1 July 1965 - 1 May 1967", Naval Weapons Center NWC TP4435, China Lake, California 1968.
68. Gordon, A. S., Drew, C. M., Prentice, J. L., and Knipe, R. H., "Techniques for the Study of the Combustion of Metals", AIAA Journal 6, 577-583 (1968).
69. Gordon, A. S., Personal communication, November 1967.
70. Hamada, H., "On the Molecular Spectra of Mercury, Zinc, Cadmium, Magnesium and Thallium", Phil. Mag. 12, 50-67 (1931).
71. Soulen, J. R., Sthapitanonda, P., and Margrave, J. L., "Vaporization of Inorganic Substances: B_2O_3 , TeO_2 and Mg_3N_2 " J. Phys. Chem. 59, 132-136 (1955).
72. Grimley, R. T. in Characterization of High Temperature Vapors edited by Margrave, J. L., John Wiley and Sons, Inc., New York 1967.

73. Nikitin, O. T., and Gorokhov, L. N., "The Composition of Beryllium Vapour" Russian Journal of Inorganic Chemistry, 6, 111 (1961) CA 57:16105e
74. Chupka, W. A., Berkowitz, J., Giese, C. F., and Inghram, M. G., J. Phys. Chem. 62, 611 (1958)
75. Amonenko, V. M., Ryabchikov, L. N., Tikhinskii, G. F., and Finkel, V. A., Dokl. Akad. Nauk. SSSR, 128, 977 (1959)
76. Boerboom, A. J. H., Reyn, H. W., and Kistemaker, J., "Heat of Sublimation and Vapour Pressure of Strontium", Physica 30, 254-257 (1964)
77. Mellor, A. M., Personal Communication, Feb., April and August 1968.
78. Stogryn, D. E., and Hirschfelder, J. O., "Contribution of Bound, Metastable and Free Molecules to the Second Virial Coefficient and Some Properties of Double Molecules", J. Chem. Phys. 31, 1531-1545 (1959)
79. Stogryn, D. E., and Hirschfelder, J. O., "Errata" J. Chem. Phys. 33, 942-943 (1960)
80. Toropov, N. A., and Barzakovskii, V. P., "Evaporation of Oxides of Alkaline Earth Elements and Energy Characteristics of Gaseous RO Molecules" in High-Temperature Chemistry of Silicates and Other Oxide Systems translated by Turton, C. N., and Turton, T. I. Consultants Bureau, New York 1966
81. Kubaschewski, O., and Hopkins, B. E., "Oxidation of Metals and Alloys" Second Edition, Butterworths, London 1962
82. Chupka, W. A., Berkowitz, J. and Giese, C. F. "Vaporization of Beryllium Oxide and Its Reaction With Tungsten" J. Chem. Phys. 30, 827-834 (1959)
83. Theard, L. P., and Hildenbrand, D. L., "Heat of Formation of $\text{Be}_2\text{O}(\text{g})$ by Mass Spectrometry" J. Chem. Phys. 41, 3416-3420 (1964)
84. Porter, R. F., Chupka, W. A., and Inghram, M. G., "On the Dissociation Energies of SrO and MgO Molecules" J. Chem. Phys. 23, 1347-48 (1955)
85. Plumlee, R. H., and Smith, L. P., "Mass Spectrometric Study of Solids I. Preliminary Study of Sublimation Characteristics of Oxide Cathode Materials", J. Appl. Phys. 21, 811-819 (1950)

86. Aldrich, L. T., "The Evaporation Products of Barium Oxide from Various Base Metals and of Strontium Oxide from Platinum" J. Appl. Phys. 22, 1168-1174 (1951)
87. Pelchowitch, I., "Evaporation Products of Alkaline-Earth Oxides", Phillips Research Reports 9, 44-79 (1956)
88. Bickel, P. W., and Holroyd, L. V., "Mass Spectrometric Study of the Evaporation Products of Strontium Oxide on Platinum" J. Chem. Phys. 22, 1793-1795 (1954)
89. Inghram, M. G., Chupka, W. A., and Porter, R. F., "Mass Spectrometric Study of Barium Oxide Vapor", J. Chem. Phys. 23, 2159-65 (1955)

APPENDIX A - VAPORIZATION OF THE ALKALINE-EARTH OXIDES

This section describes the vaporization behavior of the alkaline-earth oxides as reported in the literature. The large majority of this information is contained in a survey article by Ackermann and Thorn (3). New high-temperature mass-spectrometric data for CaO is referenced in a recent publication edited by Margrave (72). Other recent survey articles on the alkaline-earth oxides which also discuss the vaporization behavior are written by Schofield (24) and Toropov and Barzakovskii (80).

A knowledge of the vaporization species is very important for thermochemical calculations since previously reported values for the heat of sublimation, vapor pressures, etc., are in error because of the assumptions regarding the vaporization species. A great deal of the previous work was carried out in reducing rather than neutral environments because the investigators failed to assess the influence of components of their apparatus which reacted with the oxide (3).

Although dioxides or peroxides are known to exist for the alkaline-earth metals, they all decompose at reasonably low temperatures (3, 81). Upon decomposition they yield monoxides and oxygen (3).

The vaporization behavior of the monoxides or diatomic oxides does not appear to follow a predictable

pattern. MgO and CaO are the only gaseous species to have been identified for magnesium and calcium, whereas the suboxides Be_2O , Sr_2O and Ba_2O have all been observed in addition to the monoxide for beryllium, strontium and barium respectively (24). Schofield (24) also reports that polymers have been observed for barium and beryllium, $(\text{BaO})_2$ and $(\text{BeO})_n$ $n=1, \dots, 6$. The extent of dissociation upon vaporization also varies irregularly or unpredictably for these oxides. Table 13 contains a listing of the fraction of molecular species observed in the vaporization products at comparable pressures for sublimation of the monoxides "in vacuo" (3).

TABLE 13
SUBLIMATION OF THE MONOXIDES IN VACUO

<u>Specie</u>	<u>Temp °K</u>	<u>Fraction of Molecular Species</u>
BeO	2200	0.2
MgO	2000	negligible
CaO	1700	small
SrO	1600	0.4
BaO	1400	approx. 1

It should be noted that the above listing is for sublimation "in vacuo". Although almost no experiments have been undertaken for oxidizing conditions it is stated (3) that "under oxidizing conditions the concentrations of gaseous monoxide, monomer, and polymer, and perhaps of

higher oxides may be sufficiently large to be significant in several cases".

Beryllium Oxide

Vaporization data for beryllium oxide is based on mass-spectrometric observations by Chupka, Berkowitz and Giese (82) and Theard and Hildenbrand (83). Be and O atoms and $(\text{BeO})_3$ and $(\text{BeO})_4$ molecules were the predominant species observed with smaller amounts of O_2 , BeO, $(\text{BeO})_2$, $(\text{BeO})_5$, $(\text{BeO})_6$ and various tungsten oxides (82). The total pressure of the polymeric species is approximately one-third the pressure of the beryllium atoms.

Chupka et al (82) explain the large quantity of polymeric species for beryllium oxide (in comparison with the absence of these species for all of the other alkaline-earth oxides except BaO) by the much greater tendency of beryllium to covalency.

Magnesium Oxide

The work of Porter, Chupka and Inghram (84) which indicated that vaporization "in vacuo" at 1950°K occurs to the gaseous elements, must be questioned because of the presence of tantalum in the experiment. For "neutral conditions", there appears to be no reliable measurements (3).

Calcium Oxide

Schofield (24) reports that no absolute mass spectrometric determination of CaO partial pressures have been performed.

Under neutral conditions, calcium oxide sublimes to gaseous calcium and a small fraction of CaO (3).

Strontium Oxide

Ackermann and Thorn's calculations (3) suggest that approximately 30% of the vaporized species of strontium oxide is gaseous strontium and the other species is probably SrO as indicated by mass-spectrometric observations (84-88).

Barium Oxide

Although small amounts of other species, e.g. Ba₂O, (BaO)₂ and Ba₂O₃ have been observed mass-spectrometrically, barium oxide vaporizes predominantly to the normal diatomic oxide BaO (89). However, it was concluded (3) that reducing conditions were present in the experiments of Inghram et al (89). Since the total amounts of gaseous oxides other than BaO amounted to less than 0.7%, one can neglect all species other than BaO under neutral conditions (3).

It is suggested (3, 89) that under oxidizing conditions Ba₂O₃ (or BaO₂) may be an important specie in the vapor.

Summary

Under neutral or reducing conditions, only barium oxide vaporizes to the simple diatomic oxide BaO without undergoing extensive dissociation. In the case of magnesium and calcium the dissociation upon vaporization is almost complete. In the case of beryllium and strontium the amount

of dissociation is significant.

Under oxidizing conditions this significant amount of dissociation may change and in fact certain other species may be significant such as the suboxides and polymeric oxides (which have been observed in mass spectrometric studies).

ABSTRACT

An experimental investigation was undertaken to determine the flame structure of metal vapor-phase diffusion flames, in particular the low-pressure flames of the alkaline-earth metals Mg, Ca and Sr. In these studies the flames were generated in two types of experiments. In the first type, metal samples in the form of wires or strands were mounted between electrodes and heated to ignition by passing an electric current through the sample. The resulting "wire flame" was studied by space-resolved spectroscopy which defined the location of emitters in the cylindrically-symmetric flames. In the second type of experiment, a two-dimensional diffusion flame burner was adapted to low-pressure metal combustion studies. The burner provided a flame with a geometry particularly suited for space-resolved spectroscopic observations. The longer exposure times available for obtaining spectra in the burner experiments permitted the observation of oxide band systems which had not been observed in the wire experiments. The observation of these additional band systems aided in the interpretation of the spectral results obtained from the wire experiments.

A new model for the flame structure which accounts for the observations of this investigation and for the results of other investigators is presented. The model is characterized by a broad reaction zone in the inner region of the

luminous envelope. Arguments are made to illustrate that the radiation from the metal and metal oxide vapor in the reaction zone is due mainly to a thermal excitation mechanism. As a result of the reaction (which is thought to be predominantly homogeneous), a large supersaturation of oxide vapor is generated in the inner zone and this leads to rapid nucleation of oxide particles. The nature of the oxide particles and the factors which affect their movement in the flame are discussed. Finally, the various possible kinetic steps for the production of oxide vapor by homogeneous reaction are compared and it is concluded that the three body reaction of a metal atom and an oxygen atom with a third body is more important than other postulated reaction steps involving either the metal dimer or the peroxide.